REGIONAL NORPHLET FACIES CORRELATION, ANALYSIS AND IMPLICATIONS FOR PALEOSTRUCTURE AND PROVENANCE, EASTERN GULF OF MEXICO

by

BRYAN WALLACE HUNT

DELORES M. ROBINSON, COMMITTEE CHAIR
ANDREW M. GOODLIFFE
IBRAHIM ÇEMEN
AMY WEISLOGEL

A THESIS

Submitted in partial fulfillment of the requirements
for the degree of Master of Science in the
Department of Geological Sciences
in the Graduate School of
The University of Alabama

TUSCALOOSA, ALABAMA

2013

ABSTRACT

Norphlet Formation paleotransport is controlled by wind and structure. Facies analysis of the Norphlet Formation shows that structurally routed wadis and alluvial fans are the primary methods for introducing sediment into the Norphlet system. Structural highs provided sediment sources and grabens and basins focused the wadi systems into distinct Norphlet sediment transport systems. Eolian transport directions, calculated from dipmeter analyses, are consistent with the transit directions necessary to redistribute wadi derived sediment into the patterns previously determined from zircon analysis; the primary directions of Norphlet transport are southward from the Appalachian Mountains and westward/northwestward from Florida. Haynesville zircon detrital analysis implies that the sediment transport paths were persistent through Late Jurassic time.

Interpretations of regional 2D prestack depth migrated seismic shows that the Norphlet reflector is persistent through the Eastern Gulf of Mexico. The Middle Ground Arch paleohigh shows erosion during the time of Norphlet deposition and was likely a sediment source for the Norphlet Formation. Integration of the seismic data with the transport model indicates the Norphlet should be present in the Tampa Embayment as well as areas adjacent to the Middle Ground Arch. The eolian facies is extensive with erg migration to the north or northeast in the present offshore and migration generally to the south in onshore Alabama and Florida. The down dip limit of the Norphlet was likely controlled by sediment availability and there may not be a regional, standing water, downdip Norphlet facies.

LIST OF ABBREVIATIONS AND SYMBOLS

BOEM	Bureau of Ocean Energy Management
BSE	Base of salt or equivalent
DC	Desoto Canyon protraction area
DCSB	Desoto Canyon Salt Basin
DD	Destin Dome protraction area
EGOM	Eastern Gulf of Mexico
GOM	Gulf of Mexico
GR	Gamma ray
LL	Lloyd Ridge protraction area
MC	Mississippi Canyon protraction area
MGA	Middle Ground Arch
MMBOE	Million barrels of oil
MO	Mobile protraction area
OCS	Outer continental shelf
PE	Pensacola protraction area
SP	Spontaneous potential
TE	Tampa Embayment
VK	Viosca Knoll protraction area

ACKNOWLEDGEMENTS

I would like to acknowledge the aid of my advisor Dr. Delores Robinson for securing funding for the research group, her guidance through the research, as well as her assistance through the process of writing the thesis. Her aid, support, and expertise were crucial to my success. I would also like to thank my other committee members Drs. Amy Weislogel, Andrew Goodliffe, and Ibrahim Çemen.

I am very grateful for the support of Murphy Exploration and Production Company for making this project possible through their financial support. I would especially like to thank Adam Seitchik, Alex Blacque, Eddy Luhurbudi, and Gary Coburn from Murphy. I would also like to thank Spectrum Geo Inc. for providing the seismic data. I am grateful to TGS, the Alabama Oil and Gas Board, the Mississippi Oil and Gas Board, and the Bureau of Ocean Energy Management for well data.

I extend my thanks to my fellow researchers Tommy Lovell and Lance Wilson for their ideas and help with this project. I also want to acknowledge Subodha Khanal, and Subhadip Mandel, Dr. Joshua Schwartz and the staff at the University of Arizona LaserChron Center for their aid in the preparation and analysis of the detrital zircon samples.

Finally I would like to thank all of my UARFC teammates, my friends and my family who supported me and kept me sane through the process of researching and writing this thesis.

CONTENTS

LIST OF FIGURES

1. INTRODUCTION

To determine the tectonic evolution of the Gulf of Mexico (GOM), the geological history of the understudied Eastern Gulf of Mexico (EGOM) must be unraveled (Figure 1). Little is known about this area due in large part to drilling moratoriums initiated by President George H. W. Bush in 1990 that continue through 2012 (Bureau of Ocean Energy Management, Regulation and Enforcement, 2010). These moratoriums, combined with limited success of early EGOM exploration and sparse subsurface data, created an environment with little motivation to research this region. Discoveries on leases from sales 181 and 197 in the westernmost portion of the EGOM, including Shell's Norphlet Formation deepwater discoveries, Shiloh, Vicksburg and Appomattox, renewed interest in Norphlet prospects in the EGOM.

The Norphlet Formation (Figure 2) has been an important oil and gas reservoir in the onshore since the 1960's and the offshore since the late 1970's (Mancini et al., 1985; Tew et al., 1991). Shell and Nexen had discoveries in the Desoto Canyon (DC) prospects Shiloh (DC 269) and Vicksburg (DC 353) and Mississippi Canyon (MC) prospect Appomattox (MC 392) (Figure 3) with approximately 250 MMBOE for Appomattox (Odum, 2010). The discoveries changed the paradigm of Norphlet facies distributions establishing Norphlet eolian deposits much farther in the offshore than previously assumed. The Norphlet Formation is the first siliciclastic deposit following the deposition of the synrift evaporites of the Louann Salt and Pine Hill Anhydrite. Its temporal relationship with the formation of the EGOM makes it useful in understanding the paleogeography, climate, late rifting and possibly the transition from extended continental crust to oceanic crust. The EGOM remains one of the few frontier exploration areas in the United

States. Improving our understanding of the geological history of this region and its reservoirs is vital to continued efforts meet domestic energy demands.

The purpose of this study is to show the relationship between the paleotopography and the Norphlet Formation deposition. Depositional facies and eolian transport vectors of the Norphlet Formation are integrated with previous provenance studies to develop a sediment transport model. The transport models are used to relate the transport directions and the paleostructures to determine if the topographic highs and lows governed Norphlet distribution. The model is then used, along with 2-D reflection seismic (Figure 4), to extend the facies interpretations through the EGOM and determine the extent of this hydrocarbon reservoir.

Figure 1: The southern United States and offshore EGOM. This is the region where Norphlet Formation is likely to be of economical interest.

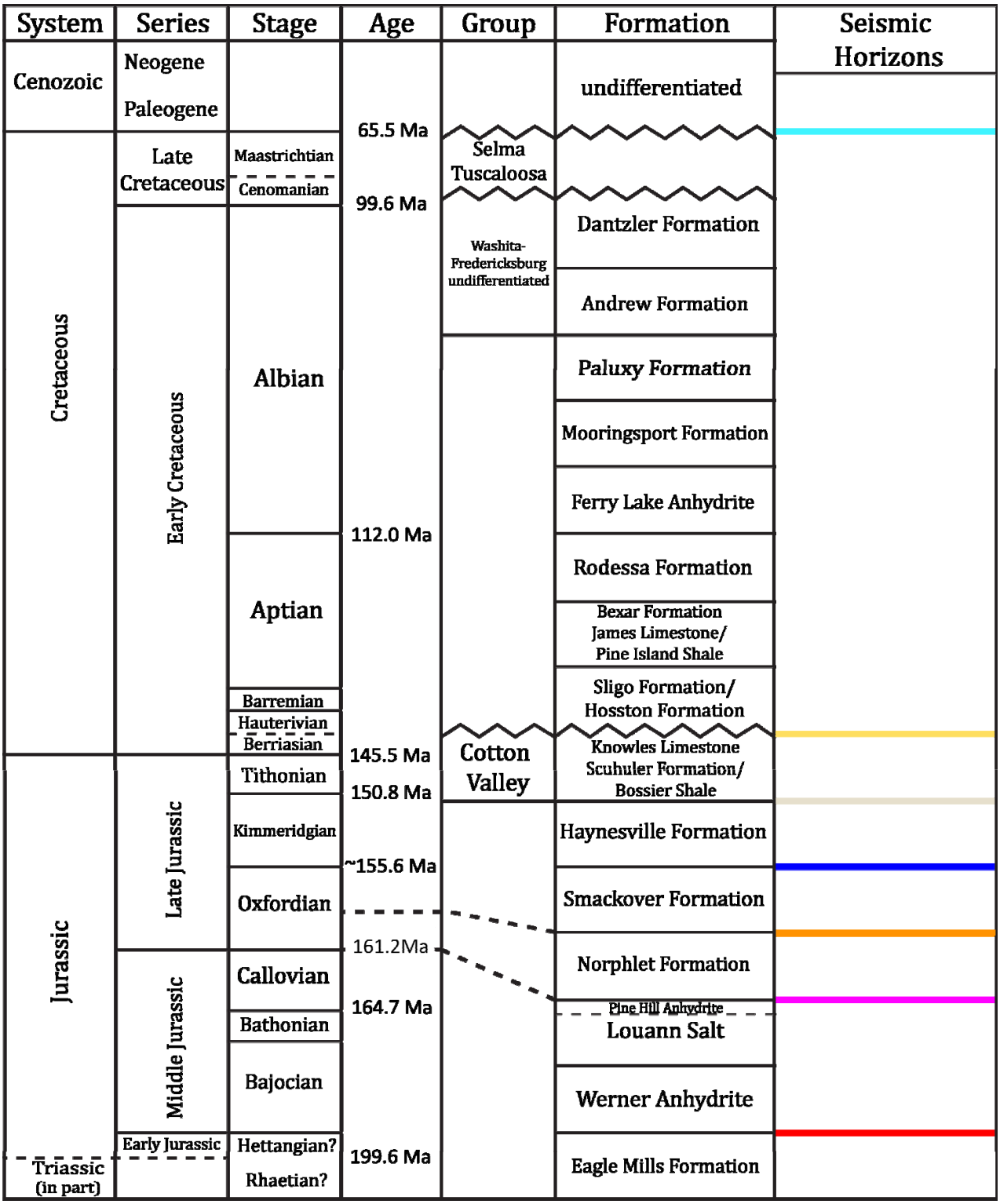

Figure 2: Stratigraphic Column of the Gulf of Mexico (modified from Mancini et al., 2001; Wilson, 2011; geologic time scale from Ogg, 2010). Seismic horizons indicate the colors for the tops of the units used to interpret the seismic lines.

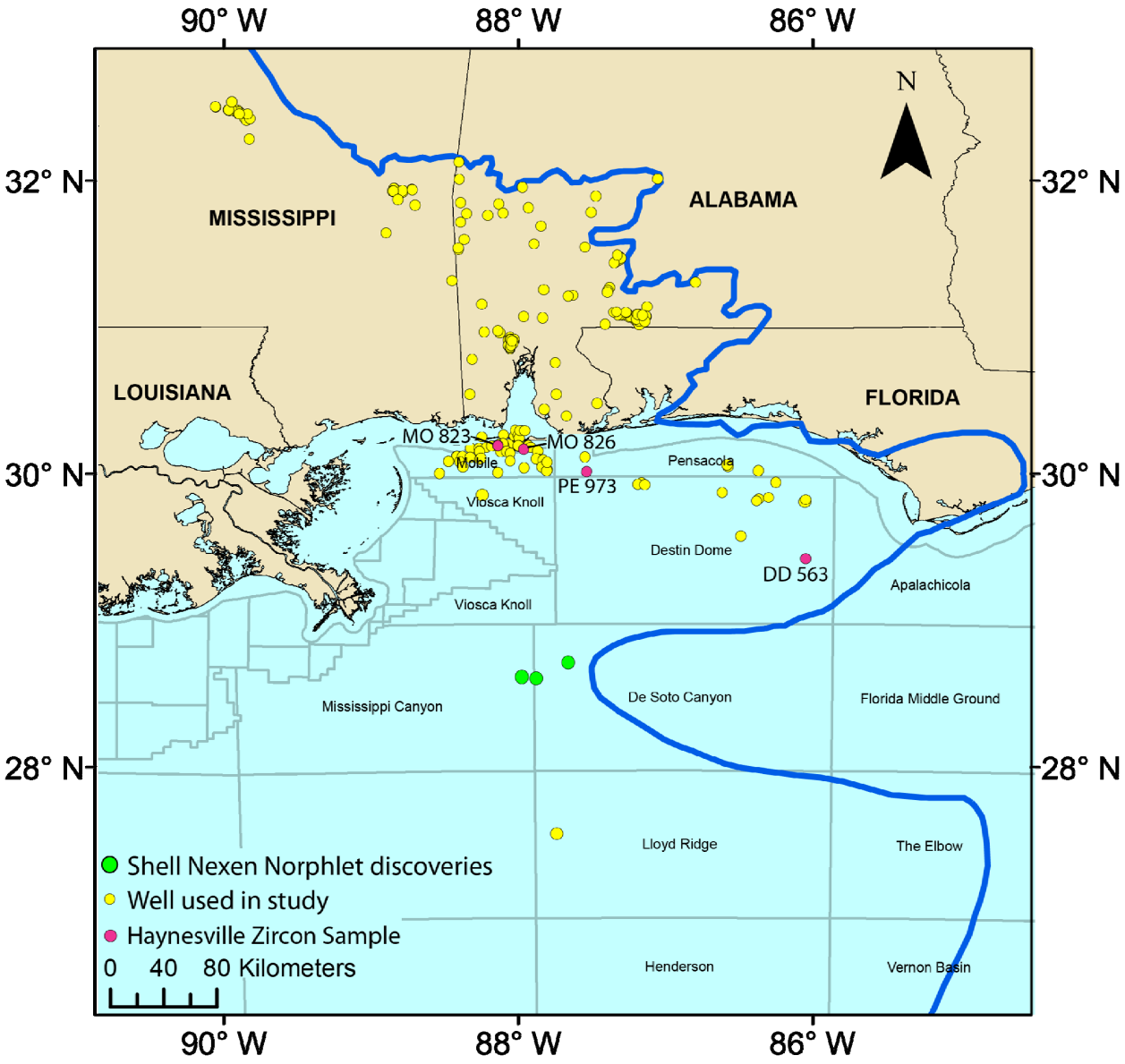

Figure 3: Location of wells analyzed for facies interpretations (all colors) and sampled for detrital zircon analysis (red).

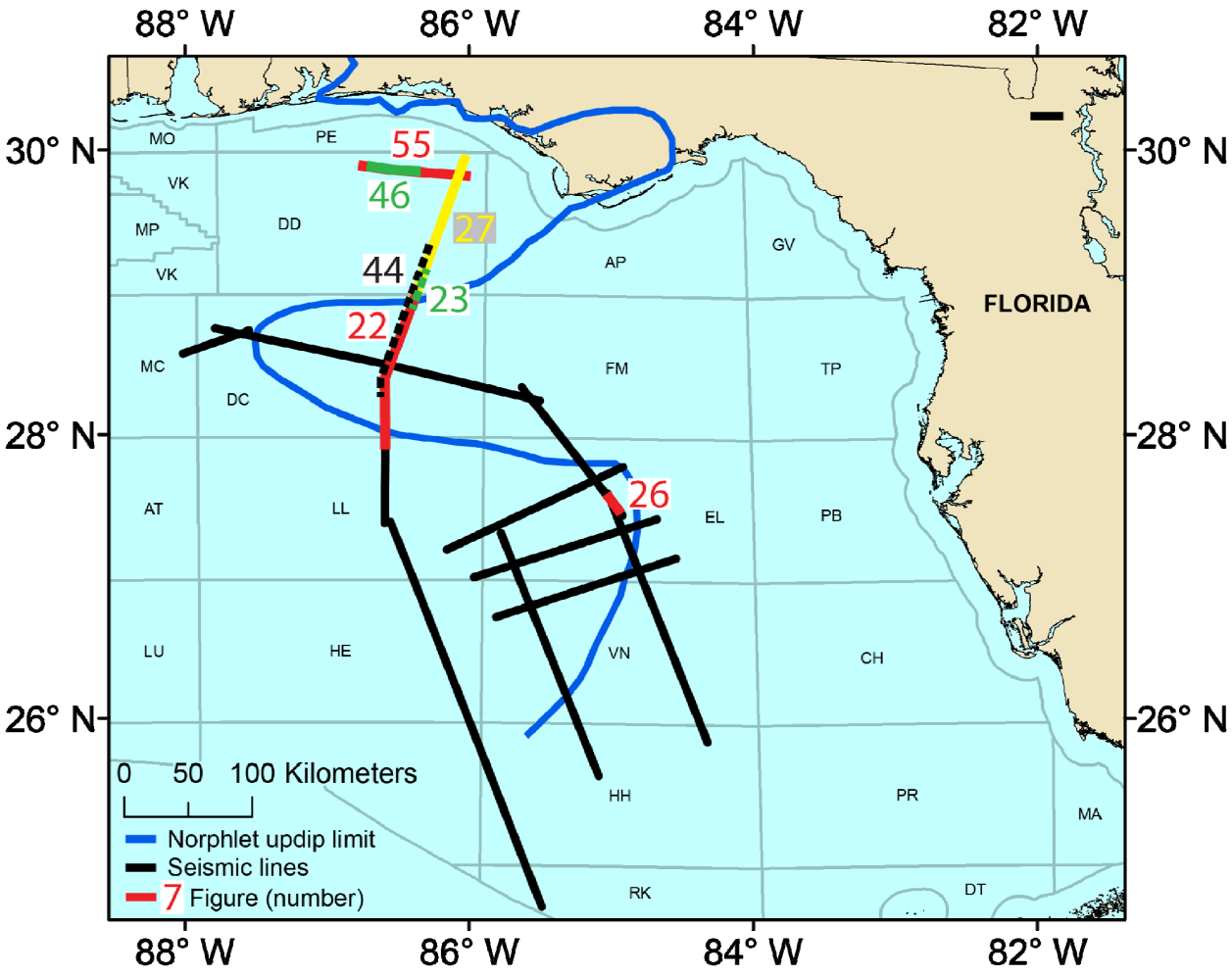

Figure 4: Seismic grid and approximate locations of seismic based figures.

2. GEOLOGIC BACKGROUND

2.1 The Norphlet Formation

The Norphlet Formation was deposited during the Late Jurassic (Oxfordian) time with the evaporitic Louann Salt below and carbonate Smackover Formation above (Mancini et al., 1985; Figure 2). The Norphlet Formation does not crop out and was first discovered in 1922 in Arkansas (Douglas, 2010). The full extent of the Norphlet Formation is not known, but it exists in the subsurface from Texas through Western Florida and into the offshore (Welch, 2003). The formation is an important oil and gas reservoir in the onshore with oil first found in the Norphlet Formation in Mississippi in 1967, Alabama in 1968 and Florida in 1970 (Mancini et al., 1985; Tew et al., 1991). Hydrocarbons were first found in the offshore in the lower Mobile Bay Mary Ann field in 1979 (Mancini et al., 1985), and theoretically economical quantities are present in Destin Dome (DD) blocks 56 and 111 offshore of Florida but are under moratoria (Scott, 1991**)**. The first Norphlet Formation discovery in the deep water was drilled by Shell and Nexen in 2003, and a 250 MMBOE field was found in MC block 391 by Shell in 2010 (Odum, 2010).

The Norphlet Formation was deposited in an arid continental setting, which is supported by the rarity of fossils and red, oxidized deposits (Tew et al., 1991) as well as the underlying evaporites (Mancini et al., 1985). The paleo-Appalachian Mountains restricted the circulation of winds preventing rains from reaching location of Norphlet deposition (Marzano, 1988; Welch, 2003). Peterson (1988) places southern Alabama at 20° latitude at the time of Norphlet deposition putting it within the range of the modern desert belts, though Jurassic atmospheric circulation may have led to different distribution of deserts than modern Hadley cells. Any standing water

within the proto-GOM was likely restricted from normal marine circulation until the time of late Smackover deposition (Badon, 1975). The Norphlet Formation's contact with the underlying Louann Salt may be conformable (Tew et al., 1991) indicated by the interpretation that the Norphlet basal dark shales are intertidal deposits from the regression of the Louann sea (Baden, 1975). The discontinuous nature of the shale and alternate interpretations of the shale's deposition environment imply that the Norphlet-Louann contact is at least in some areas unconformable. The contact of the Norphlet Formation with the overlying Smackover Formation is sharp (Mancini et al., 1985; Mink et al., 1988). Maximum Norphlet thickness varies from 1000 ft (305 m) in Mississippi (McBride et al., 1987a), 800 ft (244 m) in Alabama (Tew et al., 1991), 1350 ft (411m) in the offshore (Martens, 1993), and 410 ft (125 m) in the Panhandle of Florida (Scott, 1991). Oxfordian aged eolian sands that are likely Norphlet equivalent are reported in the southern GOM offshore from the Yucatan Peninsula (Guzman-Vega and Mello, 1999; Rosenfeld, 2002).

The primary lithofacies of the Norphlet Formation are conglomerate, redbeds, quartzose sandstone, and a discontinuous, basal dark shale (Badon, 1975; Mancini et al., 1985). The conglomeratic facies is limited to alluvial fans proximal to the paleohighs. The conglomerate is composed of matrix-supported granule to cobble conglomerate composed of angular clasts of chert, shale, quartzite, granite and rhyolite (Mancini et al., 1985; Rhodes and Maxwell, 1993; Ridgway, 2010). The range of thicknesses is unknown. The other facies have a wider range of occurrence and are found in parts of Mississippi, Alabama, Florida and the offshore (Badon, 1975; Mancini et al., 1985; Scott, 1991; Martens, 1993). The Norphlet in Arkansas, Louisiana and Texas includes conglomerate, sandstone and shale (Bishop, 1967), which are red to grey and are likely fluvial and eolian in origin (Bishop, 1967; Ewing, 2001).

The Norphlet redbed facies ranges from 30-185 ft (9-56 m) thick (Badon, 1975; Martens, 1993), is varied texturally from sandstone to siltstone, and can have scour surfaces, sandstone lenses, or can grade to mudstone and thin shale (Tyrell, 1972; Badon, 1975; Mancini et al., 1985). Mancini et al. (1985) interpret these deposits to be alluvial plain deposits containing predominantly wadi (ephemeral braided streams) deposits interbedded with well-sorted eolian sands. Playa lake deposits may be present within the redbeds in the form of sandstone, siltstone, shale or evaporites. Flow occurs infrequently through the wadi that subsequently dries out and allows winds to rework the wadi deposits into dunes (Glennie, 1972). Wadis also have varied lithologies because of variable periods of high flow leaving coarse deposits with low energy flows depositing mud drapes (Glennie, 1972).

The quartzose sandstone facies is typically grey or brown, with a high quartz content, lamina dipping up to ~30° and can exceed 1000 ft (305 m) in thickness (Badon, 1975; Mancini et al., 1985; Martens, 1993; Adjukiewicz et al., 2010). The grains tend to be frosted, rounded, and become more feldspathic closer to the source terranes (Mancini et al., 1985). The composition varies with quartz content ranging from as low as 35% with 49% lithics in some parts of Florida (Scott, 1991) to 80-90% quartz in parts of Mississippi (Badon, 1975). The sandstone tends to be finer and more lithic in Florida than southern Alabama (Scott, 1991). The depositional environment of these deposits is interpreted to be eolian (Tyrell 1972; Baden, 1975; Mancini et al., 1985).

Dark or black shale that is occasionally present at the base of the Norphlet Formation is thin <40 ft (12 m), devoid of structure, inorganic (Badon, 1975; Pepper, 1982; Mancini et al., 1985) and in places may be micaceous (Badon, 1975). The shale either deposited as the Louann

Sea regressed (Badon, 1975; Mancini et al., 1985) or as distal alluvial fan deposits (Pepper, 1982).

Using detrital zircons as provenance indicators, Lovell and Weislogel (2010) show that the Norphlet Formation through most of Alabama has a predominantly Appalachian (Laurentian) source (Figure 5), and that the DD area of the outer continental shelf (OCS) was predominantly sourced from the Gondwanan Suwannee terrane with a mixing zone in SE Alabama/W Florida. Badon (1975) states that the mineralogy in Mississippi points toward a single provenance, with the Appalachian Mountains as the most likely source. Norphlet deposits become very thin south of Mobile Bay as shown on isochores from Story (1998) and possibly non-existent ~8.6 miles (14 km) south of the Mobile OCS protraction (MO) in Viosca Knoll (VK) 117. The Shell and Nexen Norphlet discoveries in deepwater wells in DC and MC (Figure 3) are >80 mi (130 km) further south and are likely too distal to terranes that source the Norphlet 180 miles (290 km) to the north in offshore and southern onshore Alabama (Mancini et al., 1985; Lovell and Weislogel, 2010) and require a different provenance. Douglas (2010) suggests Middle Ground Arch (MGA) as a source.

Investigating the Norphlet will improve the understanding of the early EGOM tectonic history because Norphlet deposition was synchronous with rifting. Norphlet deposits preserve information about the location of the paleohighs and mechanisms and routes by which sediment was shed into the offshore. The distribution of the formation in the offshore has implications for the timing of structures such as the Tampa Embayment, the extent of seafloor spreading in the EGOM, and paleocirculation patterns in the GOM. If the Yucatan Peninsula is identified as a source of Norphlet sediment in the present day deepwater or the SE GOM, it would constrain the position of the Yucatan and the relative wetness of the gulf basin during Norphlet deposition.

The updip limit displayed on figures in this work (e.g. Figure 1) is based on comparisons with previous publications published interpretations of the updip limit of the Norphlet Formation (e.g. Mancini et al., 1985; Marzano, 1988; Scott, 1991; Tew et al., 1991) as well as log interpretations from this study. In the offshore the line is primarily based on analysis of seismic reflection data and to a lesser extent gravity and magnetic data. The updip limit is primarily a result of increased topography or paleohighs. The updip limit is a controlled by different highlands across the Norphlet depositional trend. In Alabama, it is primarily bounded by the paleo-Appalachian Mountains (Figure 6), in Florida against the Pensacola ridge, and the Middle Ground Arch and Southern Platform in the present day offshore.

2.2 Tectonic Setting

The GOM formed during Late Jurassic time as the North American and African plates began to rift. Hypotheses regarding how the GOM formed mainly include the crustal block that now composes the Yucatan Peninsula rotating away from the northern GOM (Salvador, 1991; Marton and Buffler, 1999; Bird et al., 2005; Pindell and Kennan 2009). Most researchers interpret this rotation to have been ~45-60˚ counter clockwise (e.g. Marton and Buffler, 1999; Pindell and Kennan, 2009).

One hypothesis suggests that the EGOM opened through wrench faulting between a series of parallel shear faults or transforms that trended from the SE to the NW (MacRae and Watkins 1996; Pindell and Kennan, 2001). MacRae and Watkins (1996) explained the existence of a series of basement highs and lows in the EGOM using this model. While any rotational shear must be accommodated within the attenuated and rifted EGOM, there is little to no actual evidence of these faults on regional seismic lines (Wilson, 2011) and recent reconstructions have

abandoned this idea (Pindell and Kennan, 2009). Because the northern and southern margins of the GOM are not symmetrical, Marton and Buffler (1993) interpret the GOM opening by simple shear with the Yucatan as the hanging wall (Marton and Buffler, 1993).

Interpretations of the continental-oceanic boundary are complicated by as much as 10-12 km of sedimentary overburden in the GOM, roughly twice the typical amount in major ocean basins (Hall and Najmuddin, 1994). Nagihara and Jones (2005) used heat flow to model the location of oceanic crust within the GOM assuming that after accounting for the sedimentary overburden, the oceanic crust should have lower heat flow measurements (Figure 7, black line). Their continental-oceanic boundary is similar to reconstructions by Hall and Najmuddin (1994) (Figure 7, green line) and Marton and Buffler (1994) (Figure 7, red line). The location of the continental-oceanic boundary has implications for the style of rifting, the distribution of the Norphlet Formation as it was deposited during hypothesized early seafloor spreading (Pindell and Kennan, 2009), and it can also influence provenance models. If a wide zone of oceanic crust is present, then restoration of the Yucatan to its Jurassic position may bring it close enough to be a potential source for the southernmost Norphlet deposits, although it would require a dry central GOM and winds to the north.

The EGOM contains numerous structural highs and lows (Figure 6). The highs are potential sediment sources for the Norphlet Formation and the lows are potential locations of Norphlet deposition (Miller, 1982; Mancini et al., 1985; Halverson 1988; Mink et al, 1988; Scott, 1991; Tew et al., 1991; Rhodes and Maxwell, 1993). The highs are, however, also barriers for sediment transportation and potentially affect wind circulation patterns. The intervening lows are depocenters for Jurassic sediment. The areal distribution of Norphlet facies is primarily dependent on paleohighs to provide sediment though climatic factors, such as winds, also

contribute to sediment dispersal (Budd and Louck, 1981; Miller, 1982; Mancini et al., 1985; Halverson 1988; Mink et al, 1988; Scott, 1991; Tew et al., 1991; Rhodes and Maxwell, 1993; Douglas, 2010; Godo, 2011). The distribution of the facies indicates potential sediment input pathways that control Norphlet provenance. If rifting in the EGOM was later than the rest of the gulf (Wilson, 2011), and seafloor spreading was not until the Oxfordian time (Pindell and Kennan, 2009) or even later during Kimmeridgian time (Bird et al., 2005), then seafloor emplacement would postdate Norphlet deposition and the downdip limit of the Norphlet Formation would coincide with the continental-oceanic transition in areas south of the MGA.

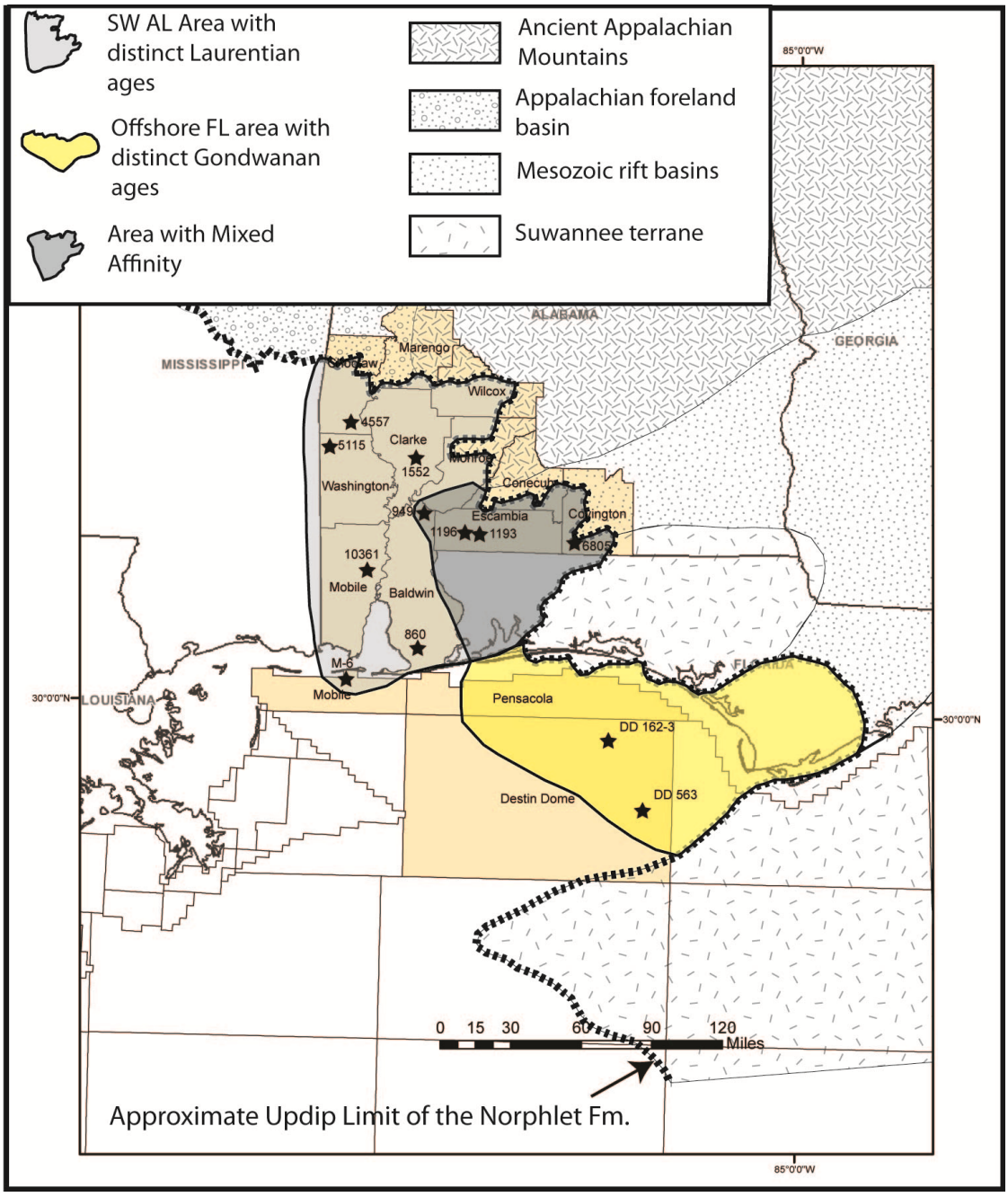

Figure 5: Norphlet provenance in Alabama and the offshore (from Lovell and Weislogel, 2010). The light grey shows the area of strong Laurentian (Appalachian) zircon signature while the yellow represents the area with a strong Gondwanan (Suwannee) zircon signature. Dark grey represents the area of mixed provenance. In order to have these areas of distinct terranes the Norphlet sediment transit system must be segmented.

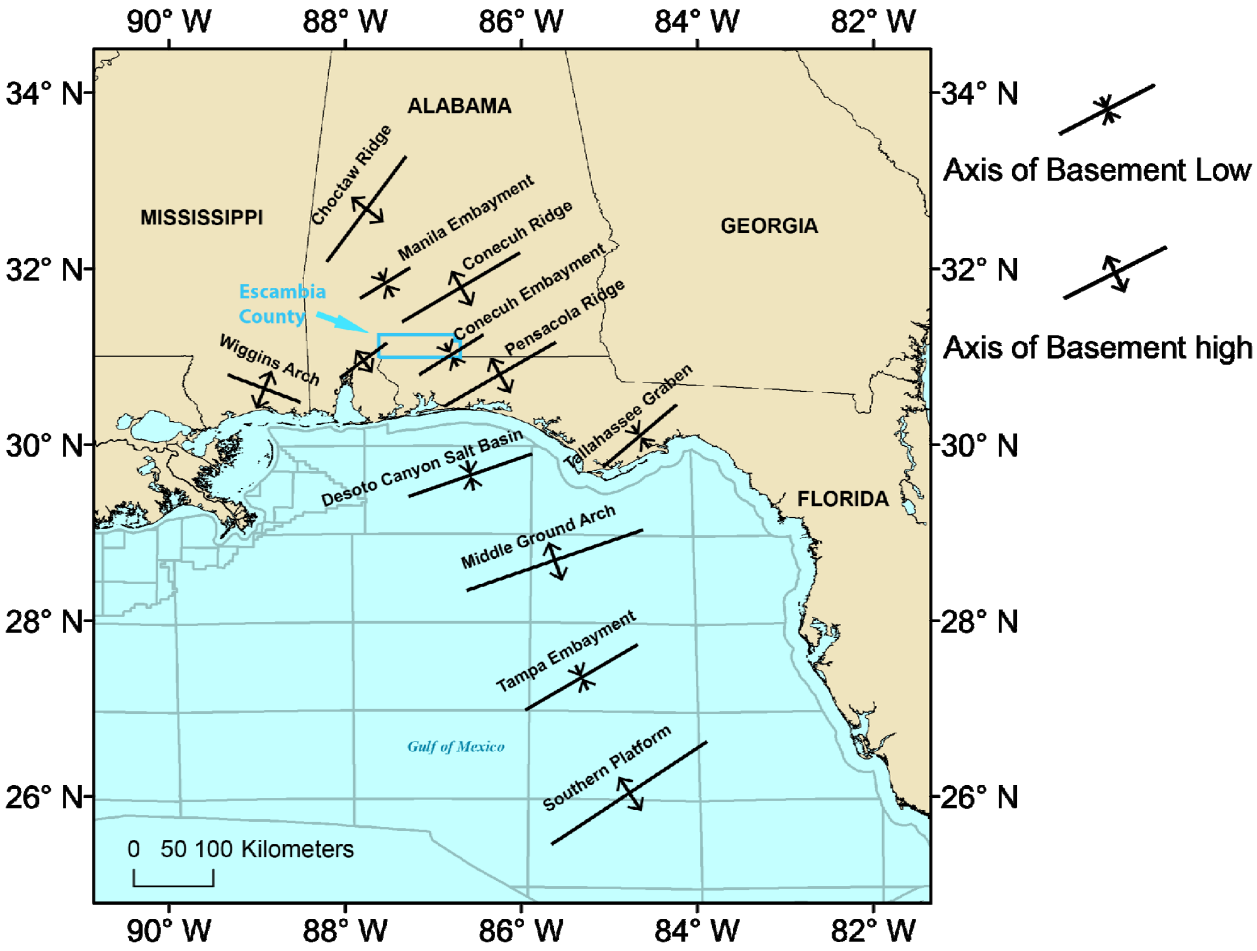

Figure 6: Major structures in the EGOM (after MacRae and Watkins, 1996; Obid, 2006). These structures provide source terranes and depocenters for the Norphlet Formation.

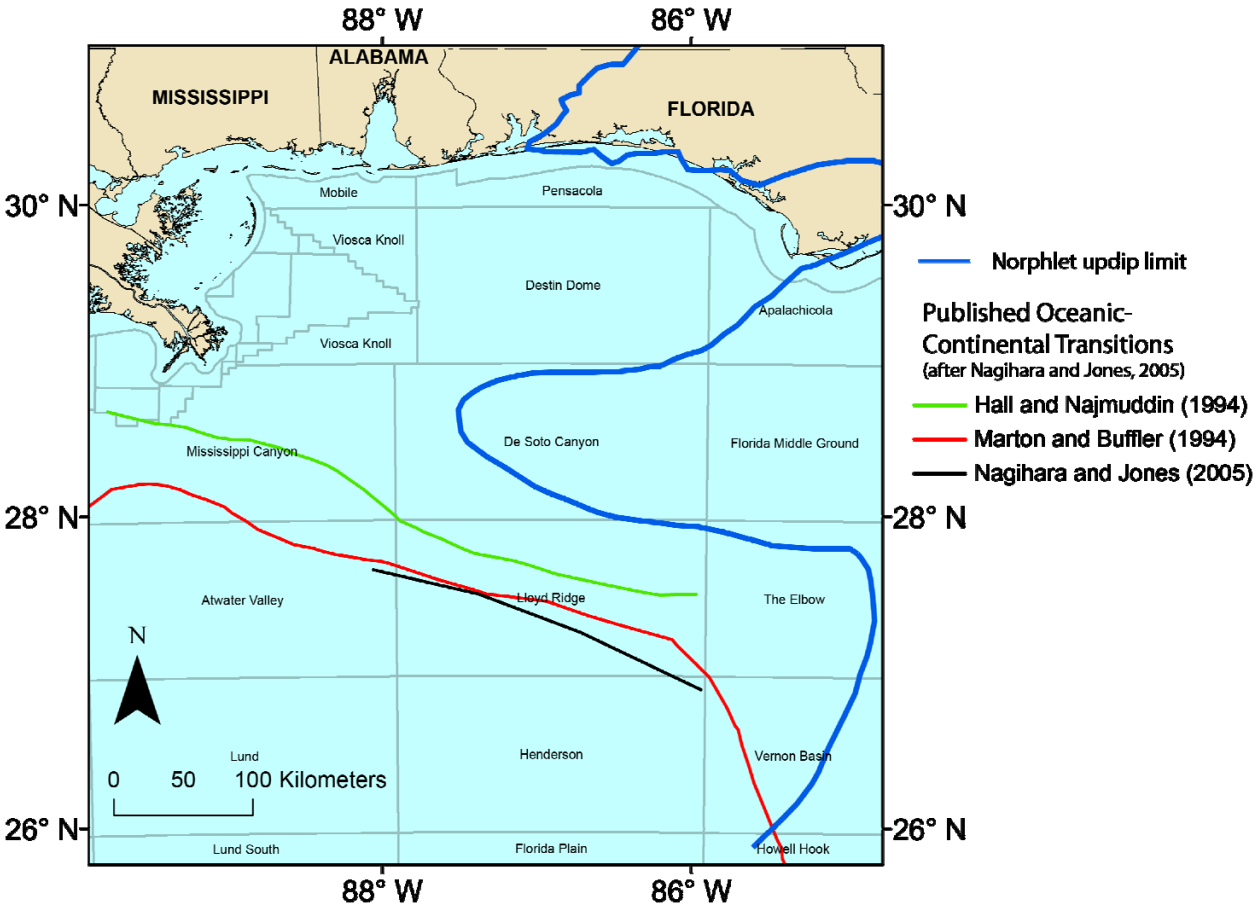

Figure 7: Possible limits of continental crust (after Nagihara and Jones, 2005). The black line is based on heat flow data while the green is based on magnetic anomalies. If the Norphlet Formation was not deposited on oceanic crust then the downdip limit of the Norphlet Formation is in this region.

3. METHODOLOGY

3.1 Log Analysis

In order to understand the regional facies extent and relationships in the Norphlet Formation, 275 wells were analyzed. Logs from 45 wells were acquired from the Mississippi Oil and Gas Board, 169 from the Alabama Oil and Gas Board and 61 from the Bureau of Ocean Energy Management (BOEM) (Figure 3). Published cutting and core descriptions from 51 wells were also considered in the interpretations of regional facies extents (Wilkerson, 1981; Scott, 1991; Markham, 1991; Welch, 2003; Ridgway, 2010). Select wells were compared to facies interpretations from core analysis (e.g. Gupta and Johnson, 2001; Stromback and Howell, 2002; Stinco 2006). A correlation between log and core facies was determined and interpretations were extended to wells with published core descriptions (Wilkerson, 1981; Markham, 1991; Welch, 2003) to refine the picking parameters. The picking techniques were further improved by referring to studies of similar formations (Hocker et al., 1990; Sweet, 1999; Stromback and Howell, 2002), modern desert deposits (Glennie, 1972), and other Norphlet studies (Scott, 1991; Martens, 1993). An analysis of the Norphlet facies was then extended across the region using primarily gamma ray (GR), spontaneous potential (SP), resistivity, density, sonic, dipmeter, and mud logs in addition to some cutting descriptions derived from Tolson et al. (1983).

After each well was interpreted for facies present, those trends were plotted in ArcGIS to determine their spatial relationships. Facies maps were constructed with consideration to the scales seen in analog environments on aerial and satellite photography. The facies maps also

relied on published paleogeographical interpretations (Miller, 1982; Mancini et al., 1985; McBride et al., 1987a; Mink et al., 1988) and seismic analysis to help guide the placement of facies in areas of poor well control (Figure 4). Interpretations of possible maximum extent were then made using paleogeography, modern analogs, existing well control and interpretations of the extent of oceanic crust in the GOM (Salvador, 1991; Hall and Najmuddin, 1994; Nagihara and Jones, 2005; Pindell and Kennan, 2009).

3.2 Dipmeter Analysis

Dipmeter logs are an effective proxy for the various dipping eolian surfaces (Hocker et al., 1990; Nurmi, 1985; Hartwick, 2010). The logs provide the direction and magnitude of dip of dipping beds by correlating resistivity patterns across a well (Goetz, 1966) and can have a resolution as fine as 10 cm (Hocker et al., 1990). Eolian bedding plane dips are useful in determination of paleowinds (Opdyke, 1960; Parrish and Peterson, 1988; Martens, 1993; Hartwick, 2010), dune morphology (Nurmi, 1985; Martens, 1993), and the identification of eolian deposits and their facies (Hocker et al., 1990). The wind directions determined from eolian deposits tend to reflect the regional wind patterns (Parrish and Peterson, 1988), although ground winds may be represented as well (Peterson, 1988).

Dipmeters were used in three ways: 1) to interpret Norphlet facies; 2) to establish sediment transport directions; and 3) to understand dune morphology. The interpretation of facies relied on a comparison of dip patterns on the logs with expected dip patterns within a given facies (Kocurek 1981; Nurmi 1985; Hocker et al., 1990; Strömbäck and Howell, 2002). The other dipmeter analyses required digitized dips. Raster logs were converted to digital logs using Neuralog excluding obviously erroneous and non-eolian dips. The digitized data were then

filtered to remove dips less than 5° that are more likely to be erroneously calculated (Goetz, 1966) and less likely to be eolian in nature. Wells with greater than 5° structural dip were corrected to restore their original dip, which was determined from the next consistently dipping mud rich interval, typically the lower Smackover mudstone. While some low angle eolian data were lost in this filtering process, the non-eolian dips were removed. The dip directions were plotted in rose diagrams and compared with established dip patterns (Nurmi, 1985; Figure 8) to determine general wind directions and to infer dune morphology. To understand how sand moved in a dune field, dune morphology must be determined because dune form is partially a response to the wind regimes (Fryberger and Dean, 1979). Certain dunes form under multiple wind directions and data are lost if one only calculates the net transport direction of the sands (Figure 9).

Once the dune type was determined, net transport direction was calculated. Visual estimates were based on the interpreted morphology of the dunes (Figure 9), but more precise predictions require statistical analysis. Following the methodology in Curray (1956) and Reiche (1938), vector additions were performed on the dipping eolian beds. The dip direction taken from the dipmeter becomes the θ value with the vector magnitude, n, being set to unity for all vectors. In other words, the angle is the dip direction and all surfaces are weighted evenly. The resulting vector angle, $\bar{\theta}$, is calculated by taking the arctangent of sums of the vertical component vectors divided by the sums of the horizontal component vectors (Equation 1). The magnitude of the resultant vector, R', is determined by using the Pythagorean Theorem with the sums of the component vectors (Equation 2). In order to get a sense of variation, or the dispersion of the data, the resultant magnitude is divided by sum of the magnitude of the measurements (Equation 3). Reiche (1938) refers to this as the "consistency ratio", where a

value of zero represents a random distribution and a value of 1 is a perfect statistical fit. Peterson (1988) discards all values below 0.20, but for this study all values were retained due to the complexity of some dunes, and were plotted in a different color to indicate the lower consistency ratio. The filtered dip directions from the digitized logs were put into files and Matlab routines were written to read these files and calculate the resultant angles, magnitudes and consistency ratio for each well. These data were output and plotted in ArcGIS.

$$\bar{\theta} = \arctan \frac{\sum nsin(\theta)}{\sum ncos(\theta)} \quad (1)$$

$$R' = \sqrt{(\Sigma n \cdot \cos\theta)^2 + (\Sigma n \cdot \sin\theta)^2} \quad (2)$$

$$L = \frac{R'}{\Sigma n} \quad (3)$$

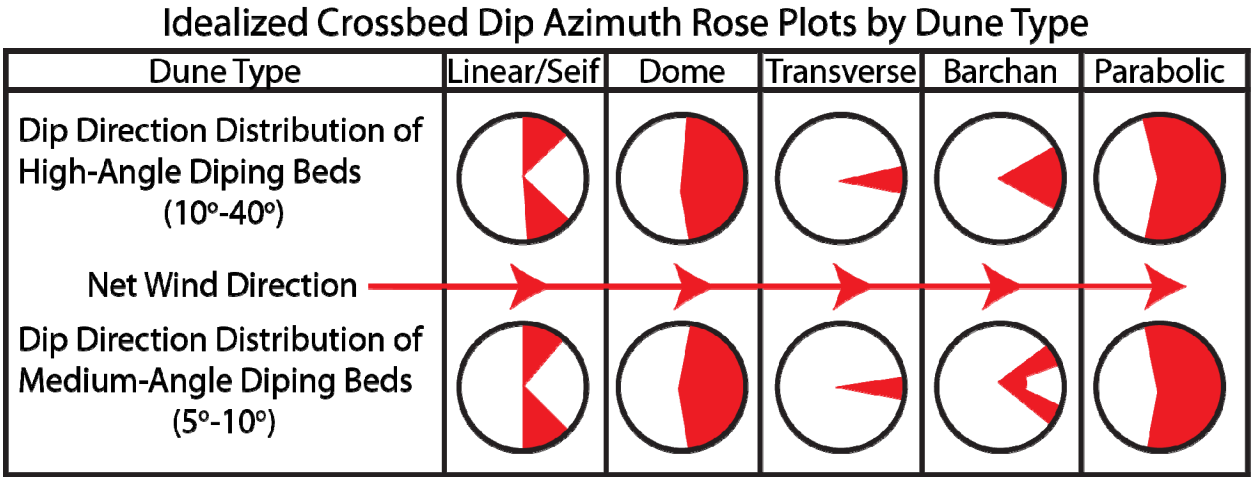

Figure 8: Idealized rose plots for eolian dipping strata (after Nurmi 1985). Rose plots can be useful for inferring dune morphology. Net transport direction is to the right.

3.3 Seismic Analysis

To determine the distribution of the Norphlet Formation and to analyze the potential for source terranes exposed in the EGOM during Norphlet deposition, 1150 mi (1850 km) of prestack depth migrated seismic data provided by Spectrum were analyzed (Figure 4). The data were processed using Kirchhoff PSDM down to 16 km subsea depth. The interpretations were focused primarily on the determination of the distribution of Norphlet deposits in the EGOM and the up dip pinch outs of the Norphlet Formation. Primary surfaces picked include: base of the Louann Salt or equivalent surface (BSE), top of the Louann Salt, the top of the Norphlet Formation, top of the Cotton Valley Group, and top of the Cretaceous sediments (Figure 2).

The Norphlet Formation's extreme depths in the offshore, 16,000 to 25,000 ft (4877-7620 m) complicate seismic interpretation. In many places, the Norphlet is not thicker than the resolution of the seismic (Martens, 1993; Story, 1998) of approximately 170 ft (52 m). In Mobile Bay, the Norphlet appears in the seismic data as a high amplitude trough and the next peak underneath is the Louann Salt (Bearden, 1987). Obid (2006) also picks the Norphlet on a trough in the offshore. The Norphlet Formation is observed to pinch out across the Wiggins Arch and thus, should pinch out on other paleohighs if the paleohighs had similar origin and evolution (Halverson, 1988). When the Norphlet Formation is thicker than the resolution of the seismic, the top of the salt is typically a strong peak after the strong trough that represents the Norphlet Formation (Bearden, 1987; Story, 1998). Interpretations are complicated by the variable thickness and "pods" of sand (Figure 10) created by preserved eolian topography and large dunes subsiding into the salt (Marten, 1993; Story, 1998; Ajdukiewicz et al., 2010).

3.4 Haynesville Detrital Zircons

Detrital zircon geochronology is a common technique used to determine provenance of sedimentary deposits (e.g. Dickinson and Gehrels, 2008). Lovell and Weislogel (2010) used detrital zircons from the Norphlet Formation derived from well samples in southern Alabama and the shallow offshore to establish the provenance of the Norphlet Formation.

In order to determine whether the provenance patterns found in the Norphlet zircons persisted through Late Jurassic time, samples were taken from Haynesville cuttings in five offshore wells (Figure 3). The selection of the wells to sample was based on the geographic location and the availability of cuttings provided by the former Mineral Management Service (now BOEM). Cuttings were used due to the lack of access to core in the offshore. The cuttings were stored in envelopes containing samples from different depth intervals for each well. An amount approximately equal to a teaspoon was taken from each envelope that had cuttings from clastic facies and transferred into a plastic vial. The samples were crushed using a mortar and pestle. Due to the small sample size, and to limit the loss of zircons, the separation steps were minimized. Samples were passed through a sieve (#40) to remove remaining large fragments. Next, the magnetic minerals were removed using a Frantz magnetic separator. Heavy liquids (methylene iodide, 3.2 g/cm^3) were used to float grains of lesser density out of the samples. The final separation step was the manual removal of pyrite and most non-zircon minerals under a microscope. The zircons were mounted on double sided tape and suspended in epoxy along with two zircon standards, or zircons with known ages, used for calibrating calculations. The standards used were Sri Lanka zircons with an age of 563.5 ± 2.3 Ma and R33 zircons with an age of 419.3 ± 0.4 Ma (Black et al., 2004; Gehrels et al., 2008; Gehrels, 2010b). The mounted samples were polished until the zircons were exposed within the epoxy.

The samples were analyzed using a laser ablation inductively coupled plasma mass spectrometer (LA-ICPMS) at the University of Arizona LaserChron Center. Ideally, 100 or more grains are analyzed to obtain a good statistical representation of the zircon population (Fedo et al., 2003). Ages were determined using U-Pb dating. Isotopic values were determined by ablating the zircons with a New Wave 193 nm ArF laser and then measured with Nu HR ICPMS (Gehrels, 2010a). Ages were determined using isotopic ratios of $^{206}Pb/^{238}U$, $^{207}Pb/^{235}U$, and $^{208}Pb/^{232}Th$. In instances of disconcordance between $^{238}U/^{206}Pb$ and $^{235}U/^{207}Pb$ the grains were excluded from the analysis. Relative age probability was calculated and plotted using Isoplot 3 software (Ludwig, 2008). Age probabilities were compared with zircon age distributions from potential source formations to determine provenance (Lovell and Weislogel, 2010).

3.5 Core-Log Correlations

Logs must be compared with core data to determine how various borehole logs responded to the different Norphlet facies. This process highlighted the most appropriate logs for determining individual facies and enabled the creation of a framework for picking the facies by logs alone. Establishing correlations between core and logs allowed interpretations in areas without core and enabled facies determination without time intensive core analysis.

Scott (1991) correlates logs and core throughout western Florida to determine the facies relationships of the Norphlet Formation. Figure 11 shows an example of his interpretation of the more fluvially (wadi) influenced redbed facies within the Norphlet Formation. This log exhibits a serrate SP log response to shale layers within sandy wadi deposits. Wilkerson (1981) describes the Norphlet deposits in 30 wells using core and cuttings. His descriptions lack facies interpretations but facies were inferred (Appendix 1) based on the characteristics described by Glennie (1972) and Mancini et al. (1985). Comparison of the facies inferred from Wilkerson

(1981) with logs aided in establishing the log pattern for the lithofacies. Key aspects used to infer wadi facies include shale lamina, incision, fluvial structures, and pebble lags. To minimize the complexity of facies interpretations, significant buildups of playa and lacustrine deposits were combined with the wadi deposits because all three imply water transportation of sediment. Playa lakes require ephemeral inflow, and fluvial influx is required in the proto-GOM for a lacustrine system to live long enough to leave measureable deposits. Playa lake deposits are similar on logs to the wadi facies with preserved mud layers and are unlikely to have a regional footprint or significant thickness.

The wadi facies is arkosic sand with lithic content as well as a clay matrix (Mancini et al., 1985), which contributes to a high GR response. In Mississippi, the eolian facies has 7.4% feldspar and only 0.6% lithic content while the red sandstone has an average of 9.4% feldspar and 4.4% lithic content with the most common lithics being dolomite fragments, red shale and "argillaceous rock fragments" (Badon, 1975). Point counts by Lovell and Weislogel (2010) show eolian facies in Alabama permit #4183 to have 13.3% feldspar and 16.3% lithic content while the wadi facies in permit #4543 had 16.1% feldspar and 26.4% lithic content. The majority of the lithics are potentially radiogenic volcanic rock fragments and metamorphic rock fragments (McBride et al., 1987a; Dixon et al., 1989). The wadi and eolian sandstone in west Florida do not have a large variation between combined feldspar and lithic content, 26.3% feldspar and 12.2% lithic content for the eolian facies and 15.6% feldspar and 23.1% lithic content for the wadi facies, because of the proximity to the sources areas (Scott, 1991). Grain type abundances are similar in Escambia County, Alabama, north of west Florida. The lithology shift toward a high lithic and feldspar, including potassium feldspar, content as seen in west

Florida is enough to cause an increase in radioactive response in areas near source terranes, such as, west Florida and Escambia County, Alabama, and thus leads to a higher GR reading.

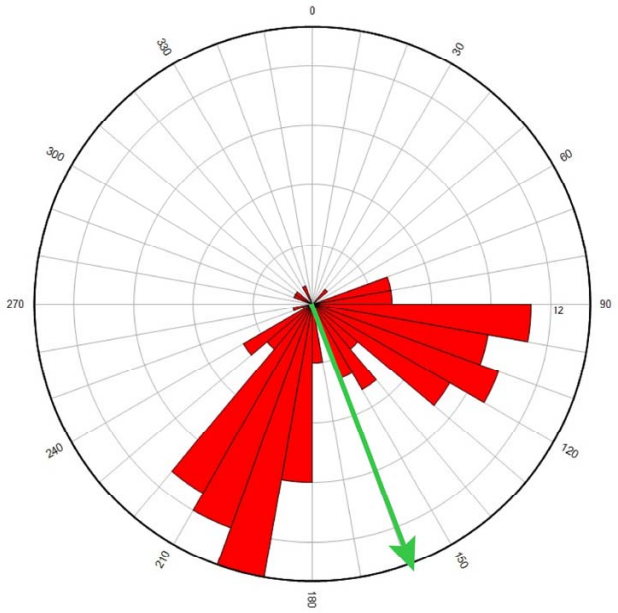

Figure 9: Typical rose plot of dipping beds in a linear dune (MO 867). The green arrow shows net transit calculated from a vector resultant. The diverging pattern of dipping surfaces approaching a 180 degree spread is typical of a linear dune. Norphlet dunes near Mobile Bay commonly exhibit this pattern.

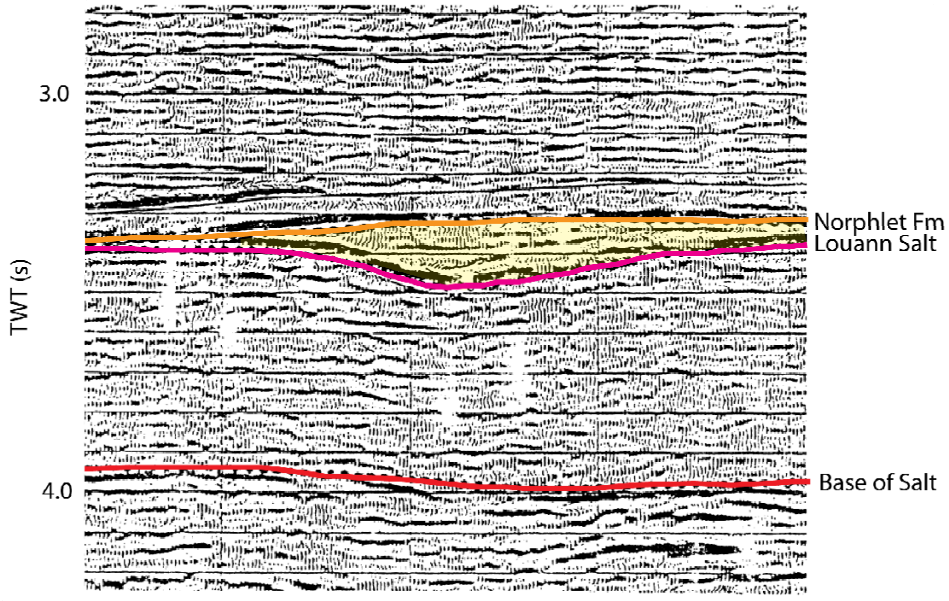

Figure 10: Example of a Norphlet pod (Martens, 1993). Large Norphlet dunes cause the underlying Louann Salt to deform allowing the dunes to partially sink into the salt and leave a thickened Norphlet section.

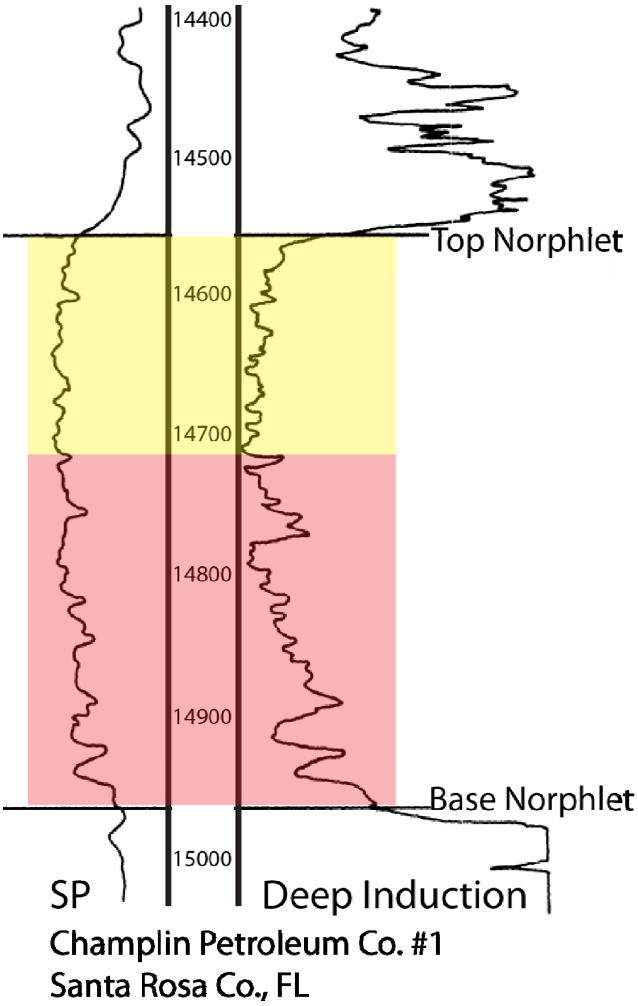

Figure 11: Log example of eolian and redbed/wadi facies (after Scott, 1991). The red area shows the extent of wadi deposits. The SP curve on the left is highly serrate and both the SP and resistivity curve (right) exhibit more variation than the overlying yellow eolian section.

4. DATA

4.1 Core Analysis and Comparisons

Core from the Mosbacher Powell Gas Unit 19-1 #1 core was analyzed over a 78 ft (23.8 m) interval. Three different Norphlet facies were identified in this well: Eolian, interbedded wadi and eolian, and thin shale at the base (Figure 12). The underlying Smackover formation and underlying Louann Salt were also identified. The eolian facies was present between 15,438-15,448 ft (4705.5-4708.6 m) and 15474-15,496 ft (4716.5-4723.2 m). The interbedded wadi and eolian facies were indentified between 15,448-15,474 ft (4708.6-4716.5 m). The shale was identified between 15,448-15502 ft (4723.2-4725.0 m).

Because access to core in the offshore is limited, facies were inferred from core lithology descriptions released by the BOEM in the Shell DD 160 well #2. The Norphlet interval in this well is between 16,560 (5,047.5 m) and the bottom logged interval at 16,864 ft (5,140.1 m). Eolian, wadi, interbedded wadi and eolian and shale facies were indentified in this well (Figure 13).

Facies were inferred from cutting and core lithology descriptions from Wilkerson (1981) in 29 wells (Appendix 1). The eolian facies was interpreted in 22 wells, the wadi facies in 6 wells, conglomeratic facies in 3 wells, and shale was identified in 4 wells. In the AL permit #1902 well, eolian, interbedded eolian and wadi deposits and shale facies were inferred from Wilkerson's (1981) descriptions of core lithology. Wireline logs analyzed in this well yielded interpretations of indistinguishable wadi and eolian facies, shale facies and the Louann Salt underlying the Norphlet Formation (Figure 14).

4.2 Log Facies Interpretations

In Alabama, Norphlet facies were identified in 169 wells (Figure 15). Eolian facies were identified in 142 of these wells, 46 contained wadi facies, 13 had shale facies present and 8 encountered conglomerate facies (Appendix 1).

Facies were identified in 45 wells in Mississippi by analyzing well logs (Figure 16). Eolian facies were identified in 42 wells, wadi facies in 11 wells, shale facies in 1 well (Appendix 1). The conglomerate facies were not identified within these wells.

Norphlet log facies were identified 58 wells in OCS (Figure 17). Within DD, 11 wells contained Norphlet facies, 4 in wells in PE, 2 wells in DC, 39 wells in MO and 1 well in MC (Appendix 1). One well in each of LL, DD and VK which reached presumed Norphlet depths were analyzed without encountering any definitive Norphlet deposits. Within DD 10 wells had eolian facies, 7 had wadi facies, 3 shale facies and a 12th well in DD appeared to have the Norphlet section faulted out. In PE, all 4 wells contained eolian facies while only 3 contained wadi facies and 1 contained shale facies. The eolian facies was identified in all of the MO wells except possibly MO 999, the wadi facies were present in 8 wells and the shale facies in 1 well. Both of the DC wells contained eolian facies while only DC 353 contained the wadi and shale facies. The eolian facies is present in MC 392. LL 399 had evaporites of the Louann Salt directly below the lower Smackover carbonate mudstones and the VK 117 did not log any Norphlet sands beneath the lower Smackover Formation.

The Norphlet deposits are variable (Figure 18). Deposits in Alabama ranged from less than 100 ft (30.5 m) to greater than 1000 ft (305 m) in Alabama. In Mississippi Norphlet deposits ranged from less than 100 ft (30.5 m) to greater than 1100 ft (335 m). The OCS had deposits ranged between less than 100 ft (30.5 m) to ~1000 ft (305 m).

4.3 Detrital Zircons

MO 826 Haynesville detrital zircons showed age peaks between 250-400 Ma, 550-600 Ma, and 1000-1200 Ma (Figures 3 and 19). The age peaks in MO 823 where between 250-400 Ma and 950-1300 Ma. PE 973 has a major peak between 250-600 Ma and minor peaks between 1000-1250 Ma and 2050-2200 Ma. DD 563 strong peak at ~550 Ma and ~2650 Ma with minor peaks 1250 Ma and 1750 Ma.

4.4 Dune Dip Patterns

The majority of the 30 vector resultants (Appendix 2) of the dipping beds taken from wells in Alabama had an azimuth within approximately 45° of south though there are 8 wells are within ~90° of north (Figure 20). In MO, the azimuth of the vector resultants were between 101 and 211 while all but two wells between DD and PE were within 60° of north. DD 563 has a vector resultant of 265, and PE 973 has a vector resultant of 94. The wells in Mississippi ranged from 173 to 305 azimuth. The distribution of the dipping beds (Figure 21) varies from nearly random in Escambia County, Alabama, with an approximate 180° spread in Mississippi and offshore Alabama and MO, to a very tight cluster in the northern extent of the Norphlet in Alabama and parts of DD.

4.5 Seismic Data

Several important structures were identified on seismic (Figure 4). The MGA showed erosion and possible faulting on its crest (Figures 22-25). The Tampa Embayment was a location of deposition during Norphlet deposition (Wilson, 2011) and showed possible evidence of eolian deposition (Figure 26). The DCSB was a major location of Norphlet deposition and significant pre-salt extensional tectonics (Figure 27). Reflectors interpreted to be Norphlet are found throughout the area south and west of the MGA (Figure 28).

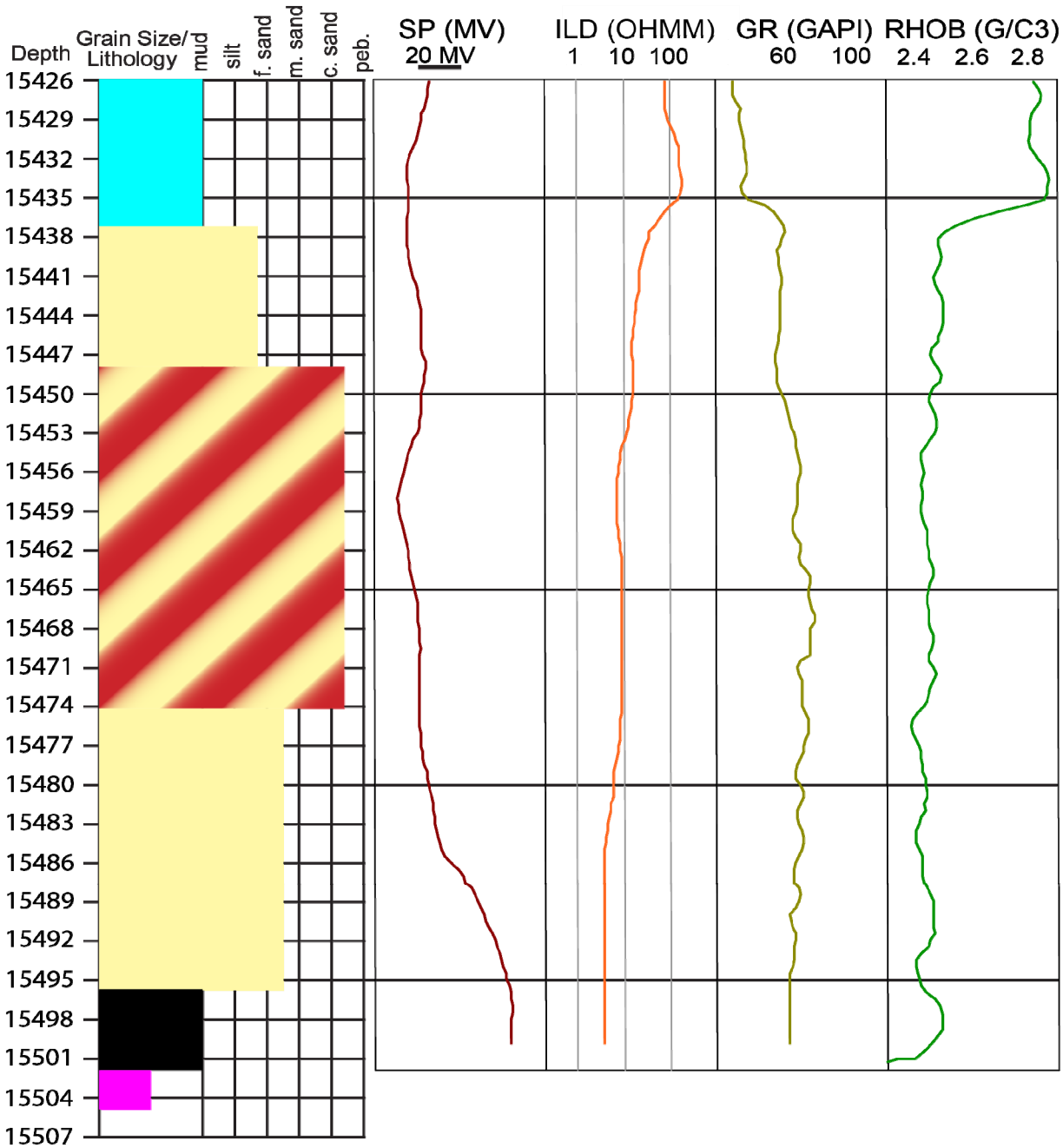

Figure 12: AL permit #2991 well core facies and logs. The core lithologies are highlighted by the colored rectangles: Louann Salt (pink), lower Norphlet dark shale (black), eolian deposits (yellow), alternating eolian and wadi deposits (red and yellow), and the Smackover Formation (blue). The SP and density logs have strong reactions to the lower shale, but other than a minor increase in GR counts, there are no significant log responses to the wadi section. This is likely because the wadi and eolian sections are mineralogically similar.

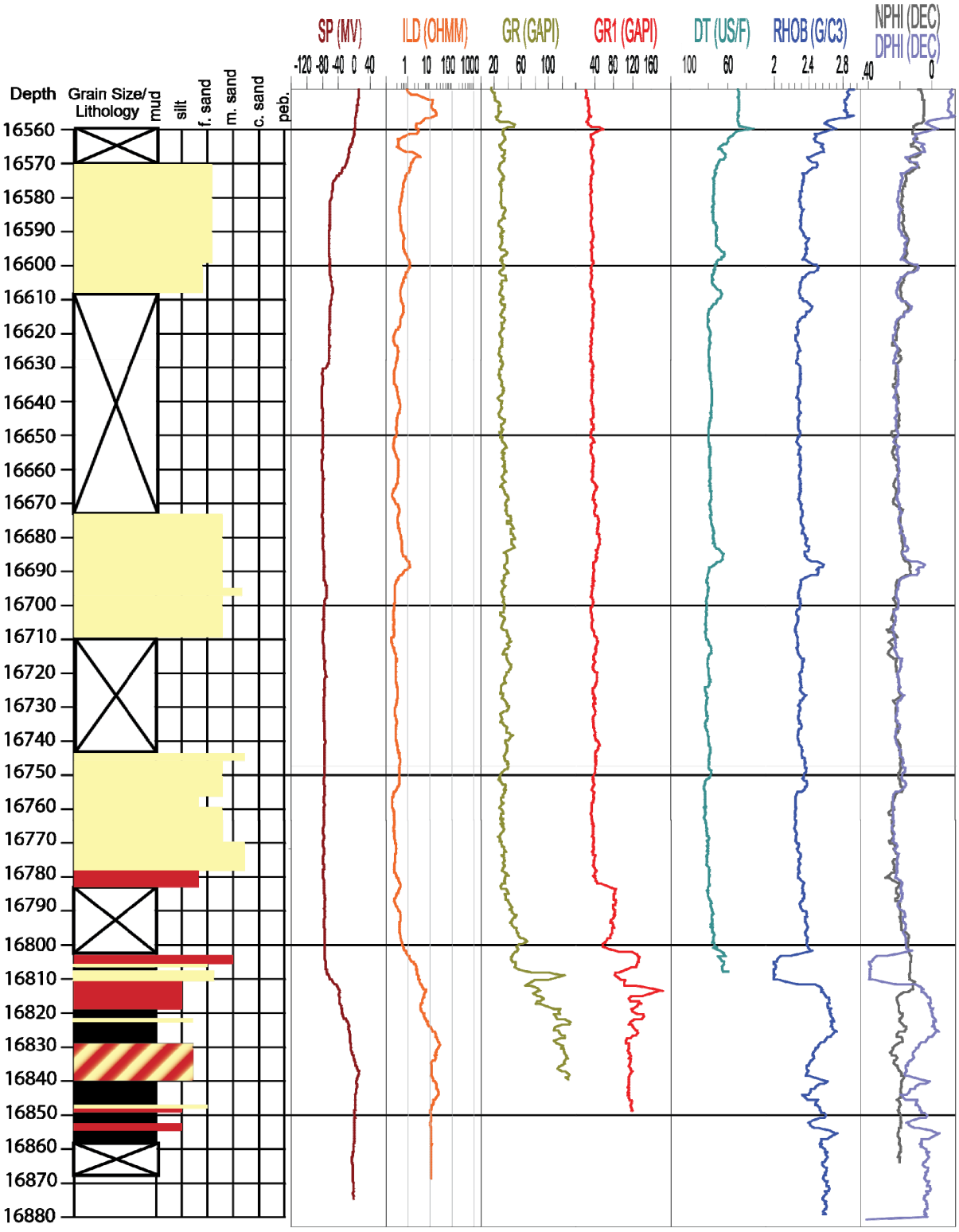

Figure 13: Inferred facies from core description and log correlations in the Shell DD 160 #2. The wadi facies have a higher GR, SP and more variation within the logs. The shale facies show an increased SP and a slight density increase. The lithofacies are eolian (yellow), wadi (red) and shale (black).

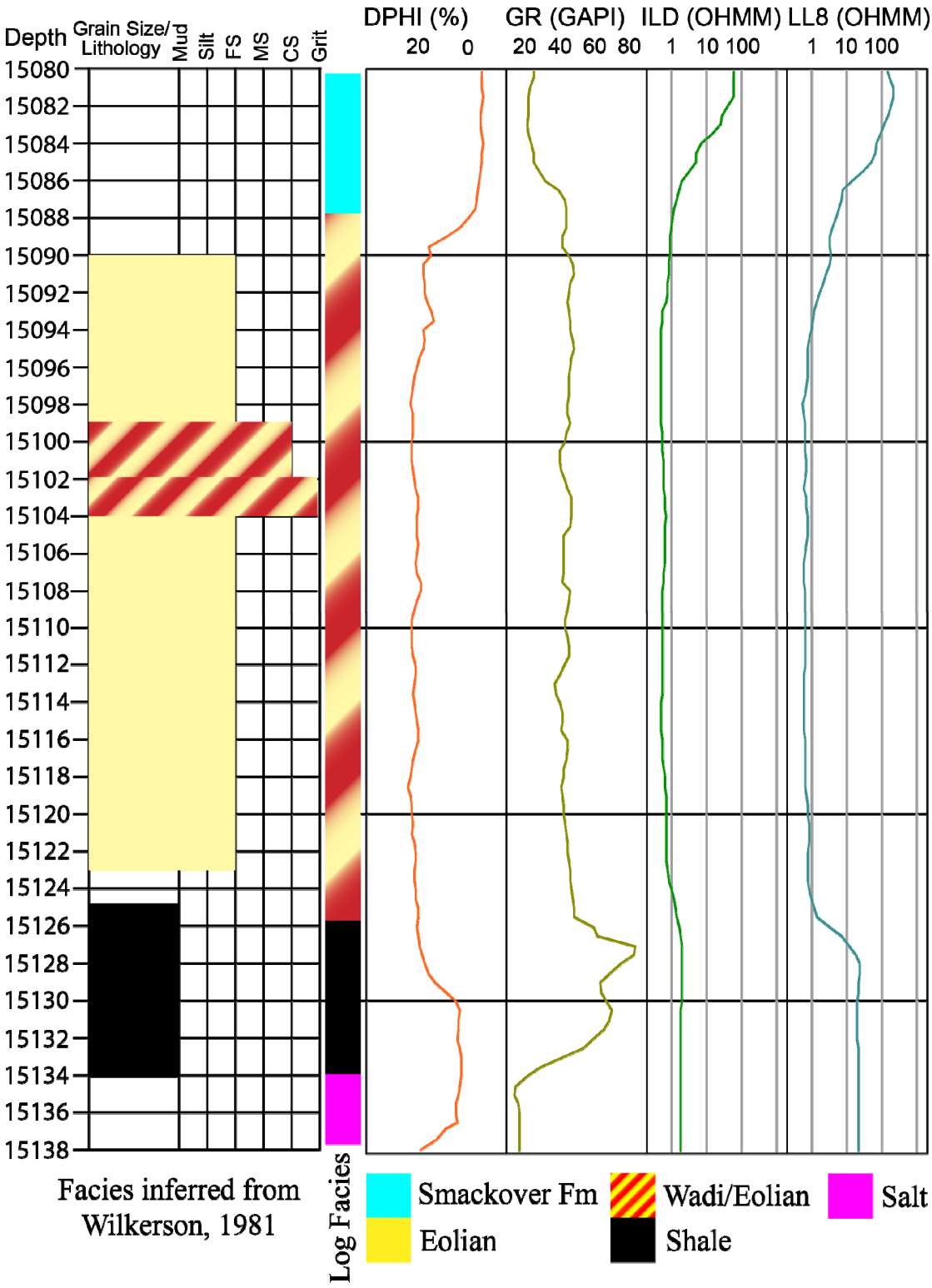

Figure 14: Correlation between logs, facies interpreted from logs and facies inferred from Wilkerson (1981) core and cutting descriptions. The shale interpretations are consistent with those from Wilkerson (1981), while the logs facies were picked as indeterminate eolian/wadi deposits.

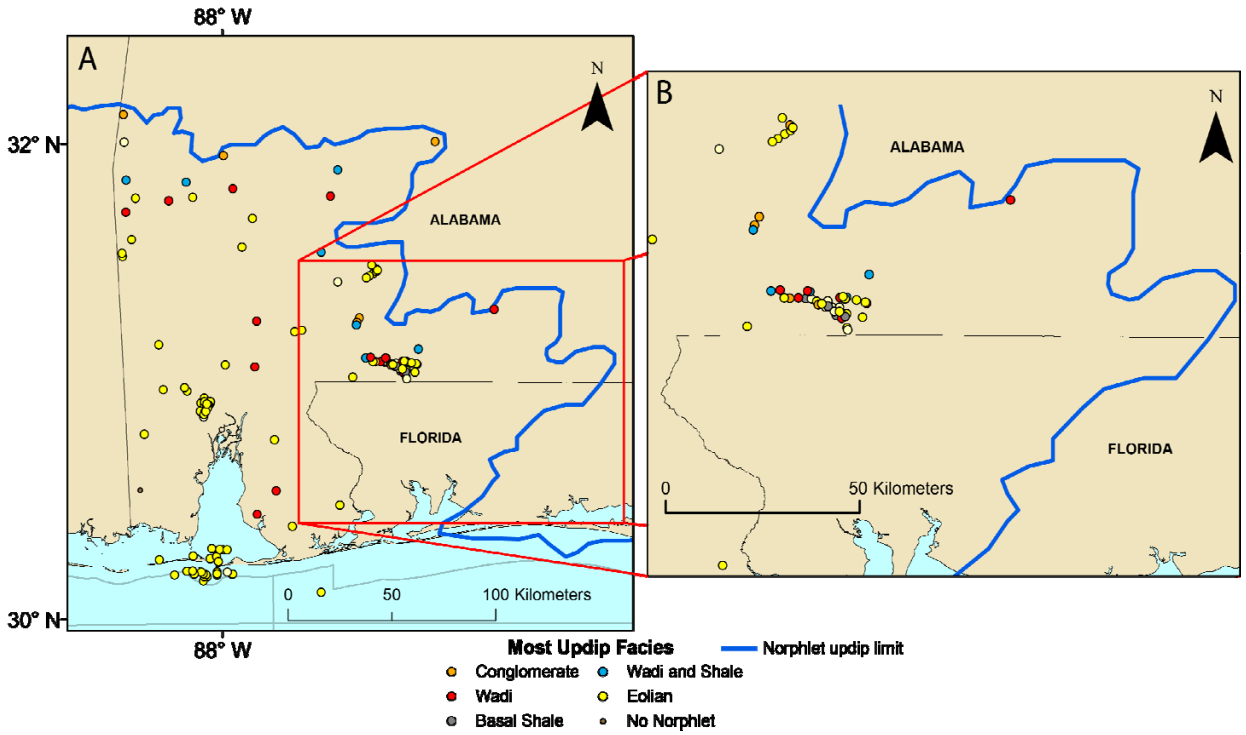

Figure 15: Facies interpreted in Alabama. A: The most updip facies present in each well are displayed. The distal facies are almost exclusively eolian in nature, and the updip regions have deposits with a greater degree of water transport (alluvial or wadi deposits). Red box is location of B. B: Shale and wadi facies are common in Escambia County because of their proximity to the Conecuh Arch. The difficulty of distinguishing between eolian and wadi deposits in this area explains the variation between neighboring wells.

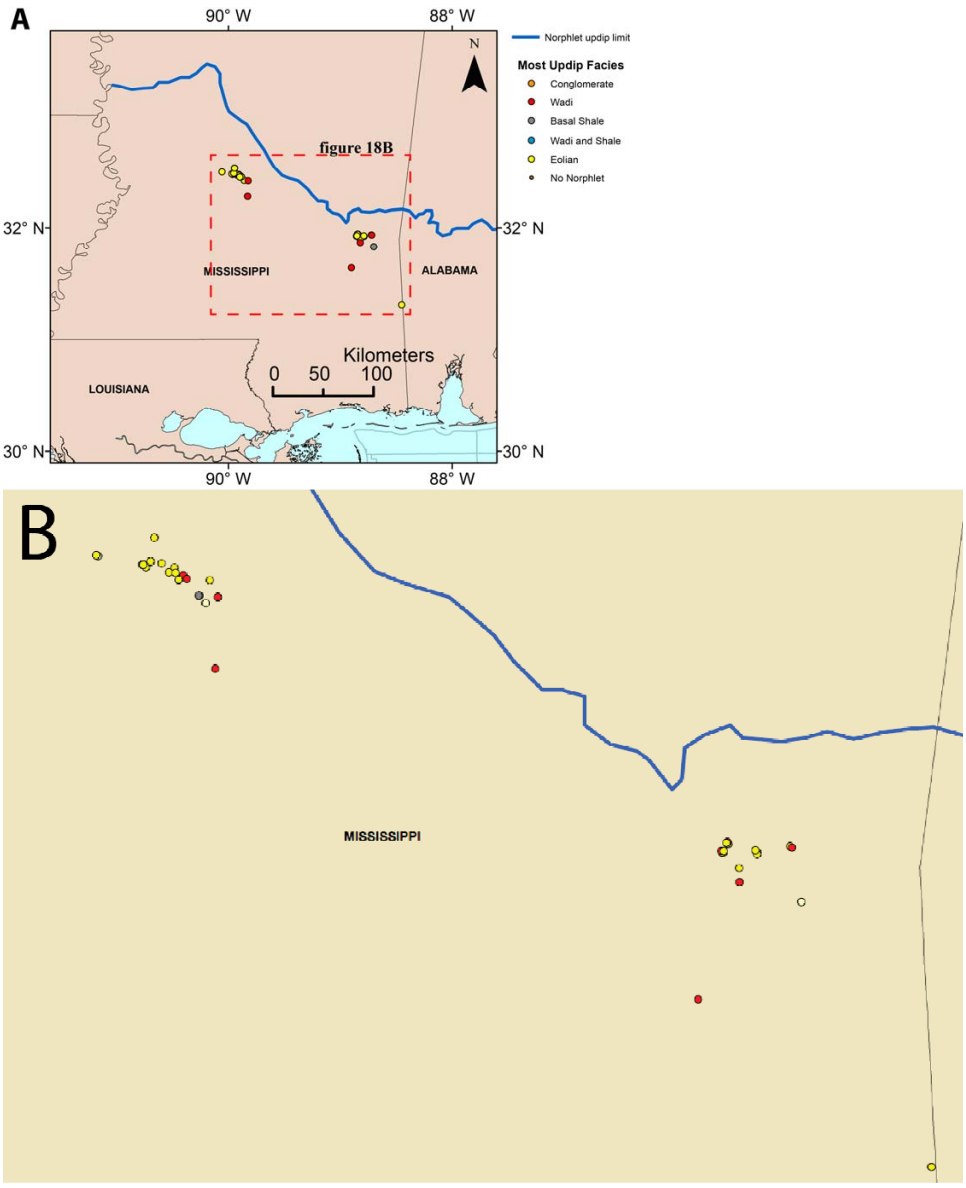

Figure 16: Facies interpretations in Mississippi wells. A: Location of Mississippi wells with the most updip facies is displayed for each well. Red dashed outline is the location of B. B: No wells contained the conglomeratic facies but some were interpreted to have wadi facies showing a similar depositional pattern to that of Alabama with eolian sands most common away from the highlands.

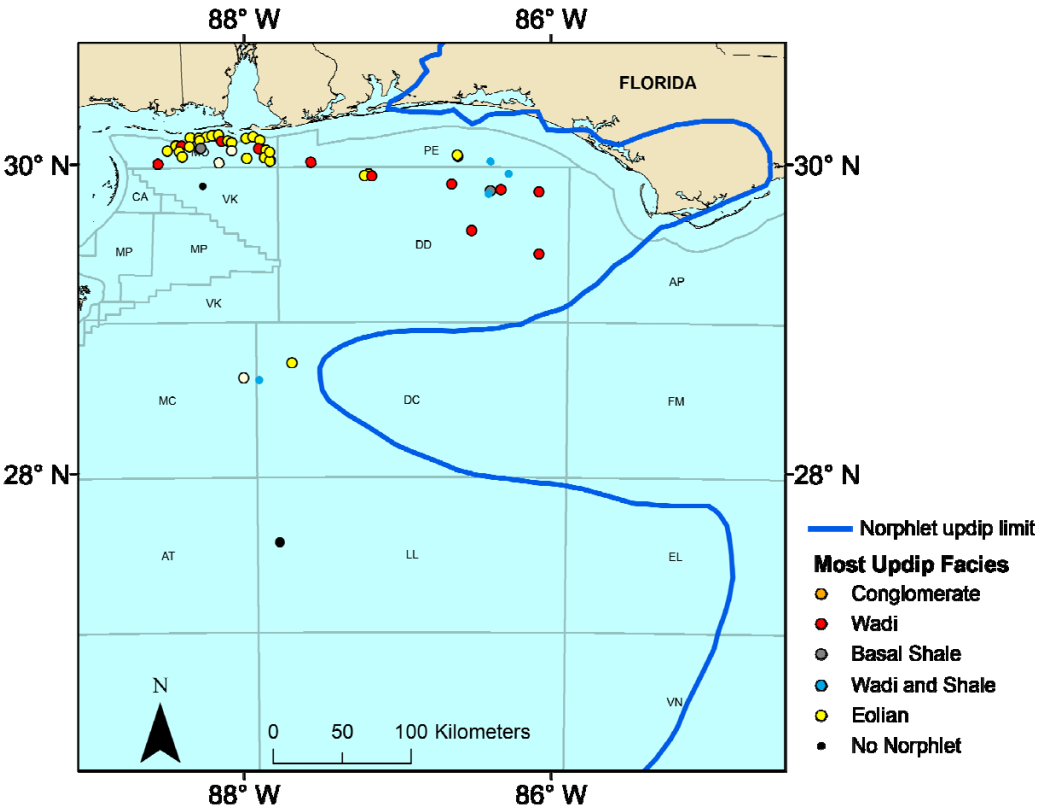

Figure 17: Gulf of Mexico most updip facies interpretations. Near Mobile Bay, the most updip facies is predominantly eolian with minor wadi deposits. In DD, the wells have thick eolian deposits in addition to some basal shale or wadi deposits, which indicate a strong, laterally extensive wadi influence.

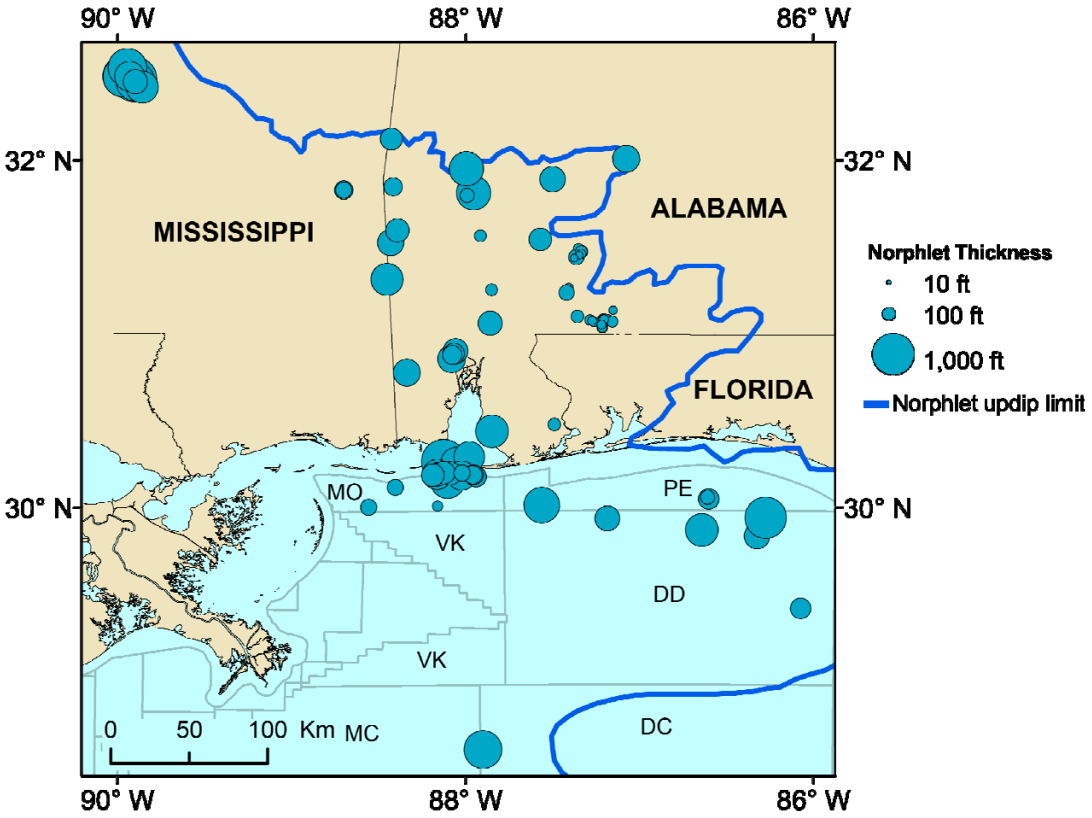

Figure 18: Isochore map of Norphlet deposits. The Norphlet formation is highly variable in thickness both locally, as seen in MO, an regionally as seen by the transition from thin deposits near the Alabama-Florida border to thick deposits in other parts of Alabama.

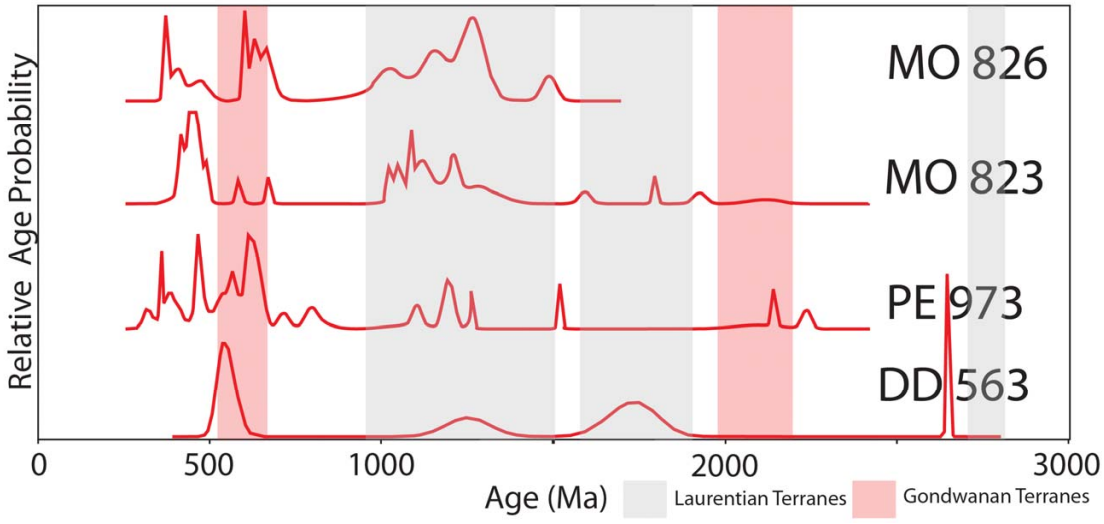

Figure 19: Haynesville Formation detrital zircon relative probabilities. Haynesville zircons probabilities are similarities to the Norphlet zircons. The zircon recovery from these samples was poor and results are speculative; however, the results suggest that the same sediment delivery systems were active during both Norphlet and Haynesville deposition.

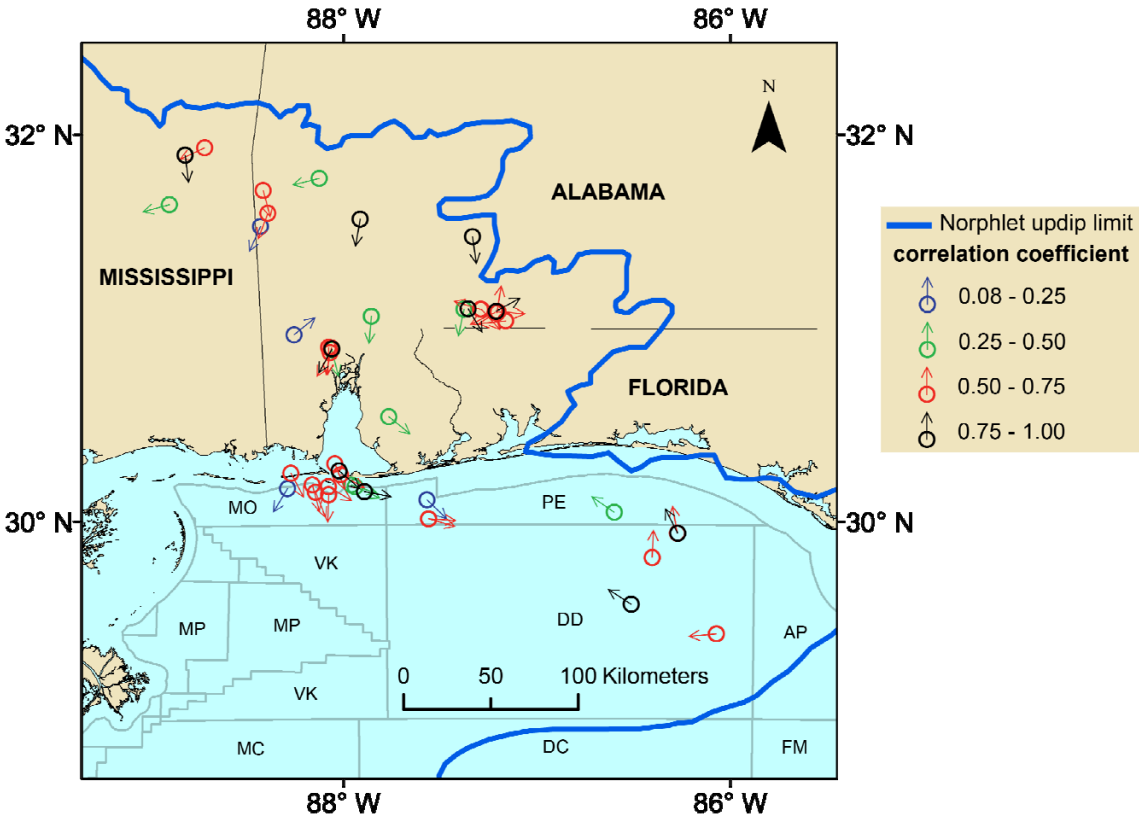

Figure 20: Vector resultants of dipping eolian surfaces in Norphlet wells. There is a general southern transport direction in Alabama that shifts slightly east in the deposits just outside of MO. DD and western PE have a general NW transport trend.

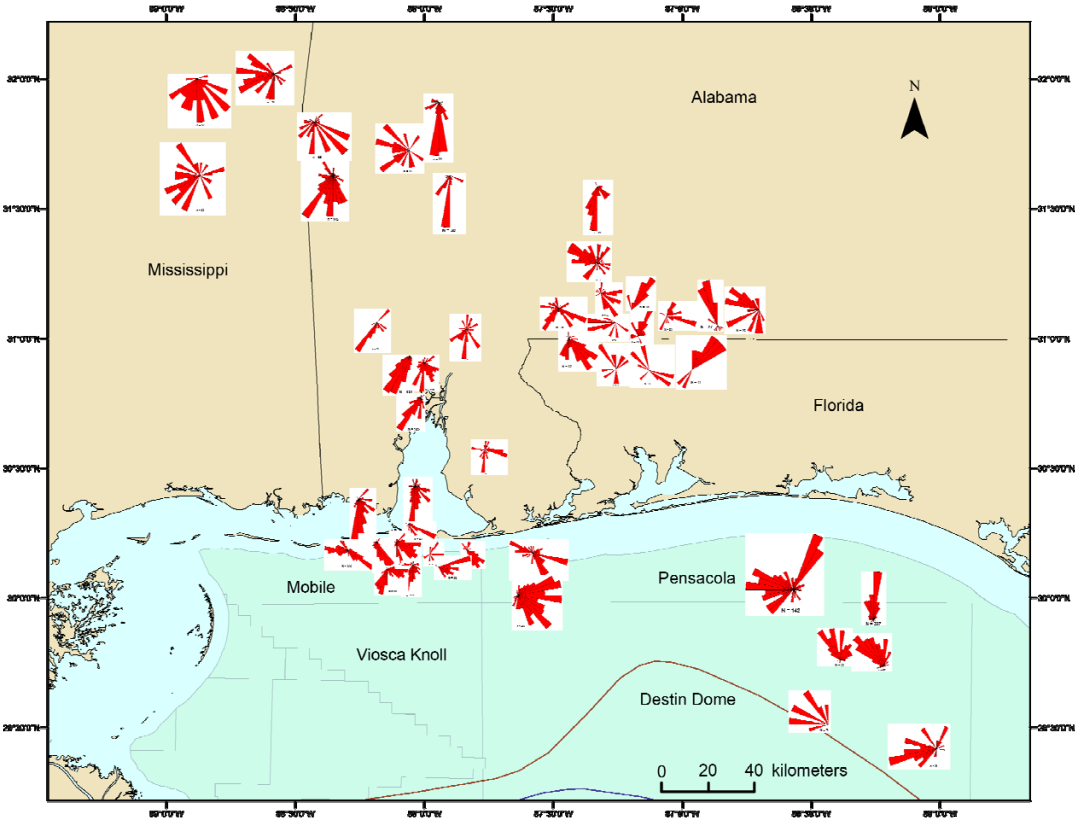

Figure 21: Dipmeter rose plots of dipping eolian beds. The plots show that the Norphlet dunes had varied morphologies, and transit to the south in Alabama and to the west or northwest in DD.

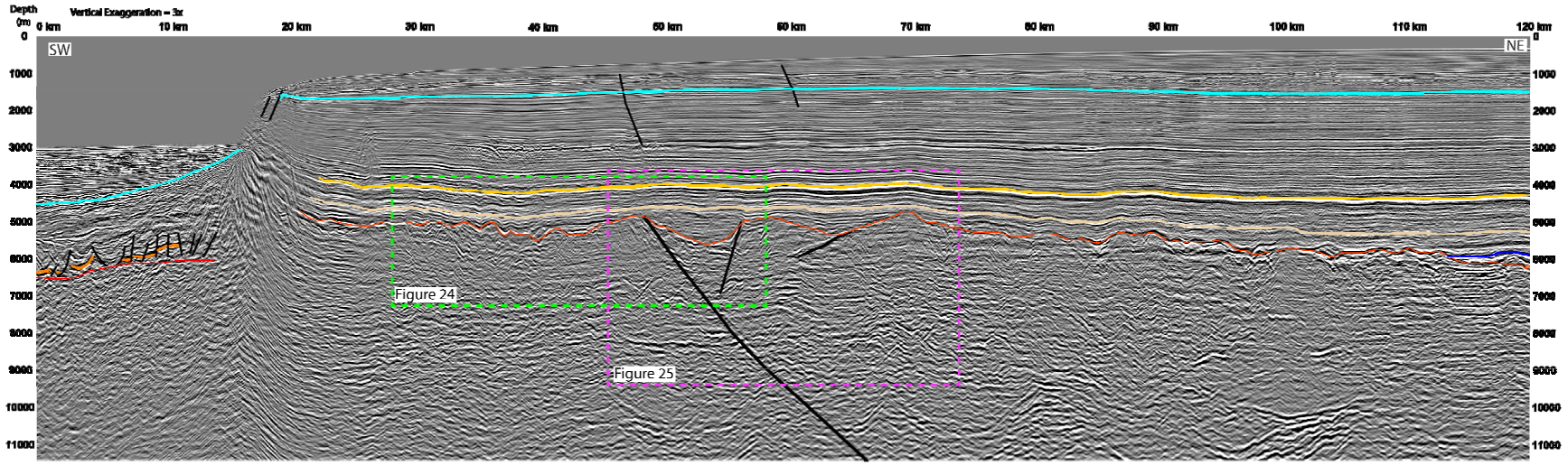

Figure 22: SW (left side) to NE (right side) seismic line through the Middle Ground Arch (Figure 4). The basement of the arch is faulted creating a mini-basin in the middle of the arch, a potential transport pathway at the time of Norphlet deposition. There are also obvious eroded channels on the arch.

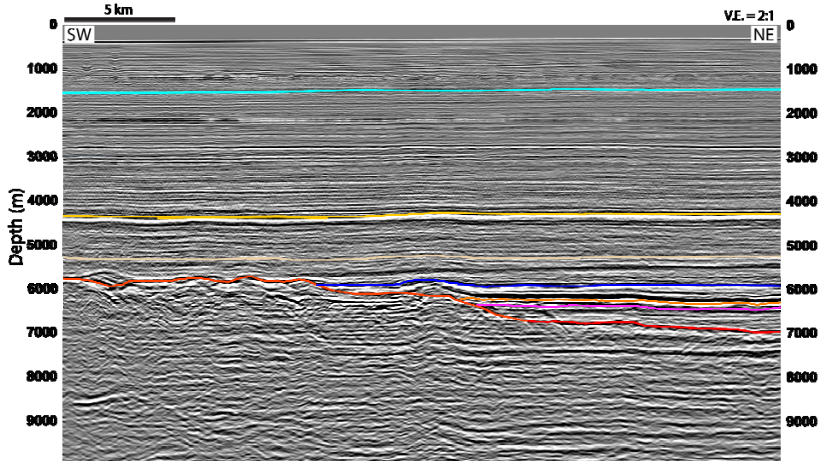

Figure 23: Oxfordian-Kimmeridgian onlap on the Middle Ground Arch (Figure 4). The Louann Salt, Norphlet Formation, and Smackover Formation, all onlap the MGA, which indicates that the MGA was subaerial at the time of Norphlet deposition and could be a source for deep water Norphlet sands.

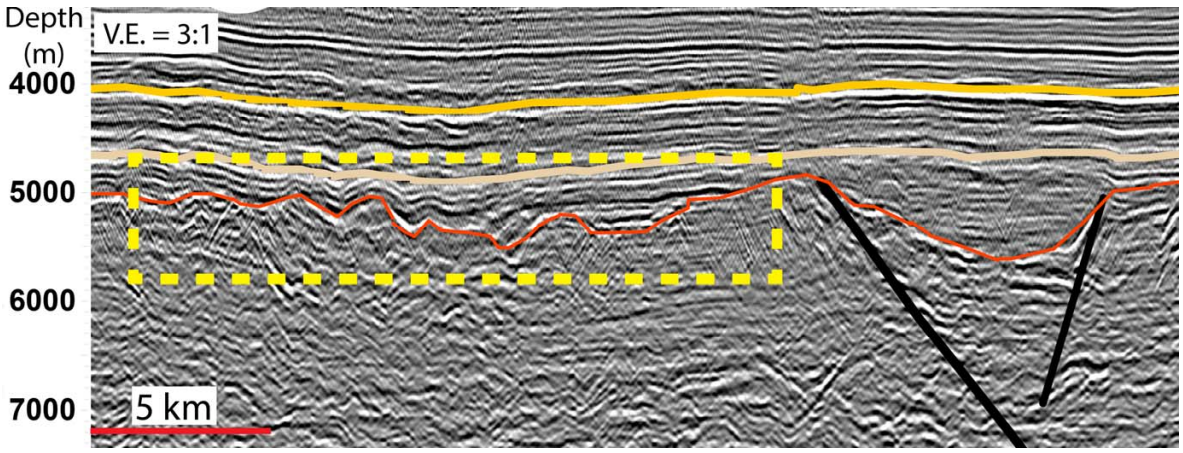

Figure 24: Erosion on the Middle Ground Arch (Figures 4 and 22). The yellow dashed box outlines a series of valleys eroded in the MGA that may have transported sediment into the deep water at the time of Norphlet deposition.

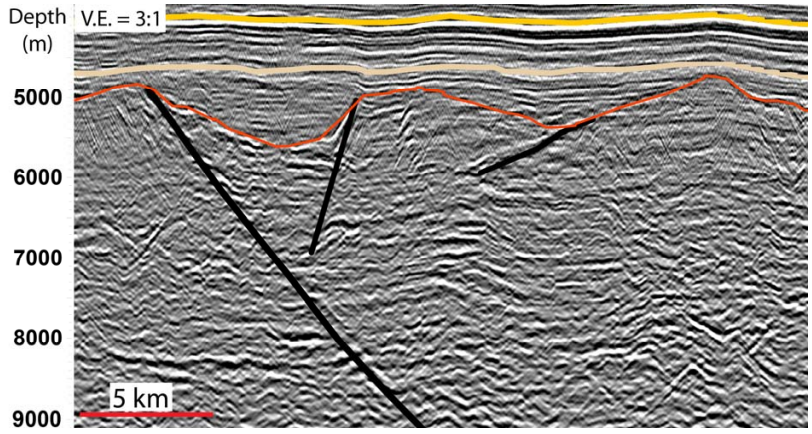

Figure 25: Graben within the Middle Ground Arch (Figures 4 and 22). Basement faults in the MGA opened a graben that filled during the time of Haynesville deposition. This may have created a path for sediment to be transported into the deep water and provide sediment for the Norphlet erg near the MGA.

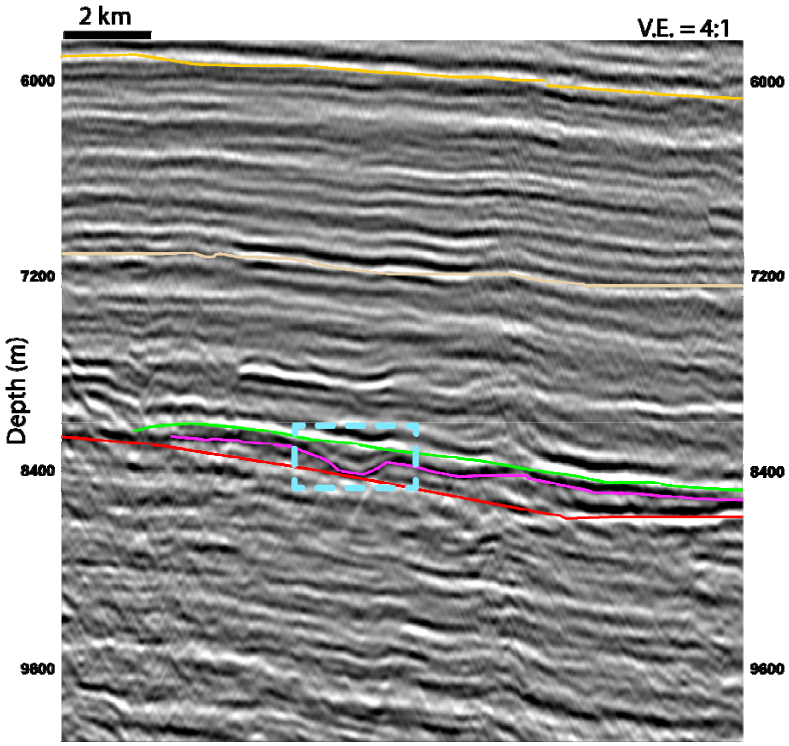

Figure 26: A potential Norphlet dune sunken into the salt in Tampa Embayment (Figure 4). This pod in the blue box provides evidence that the Norphlet has eolian facies within the TE. Red: top of basement, pink: top of salt, green: top of Norphlet.

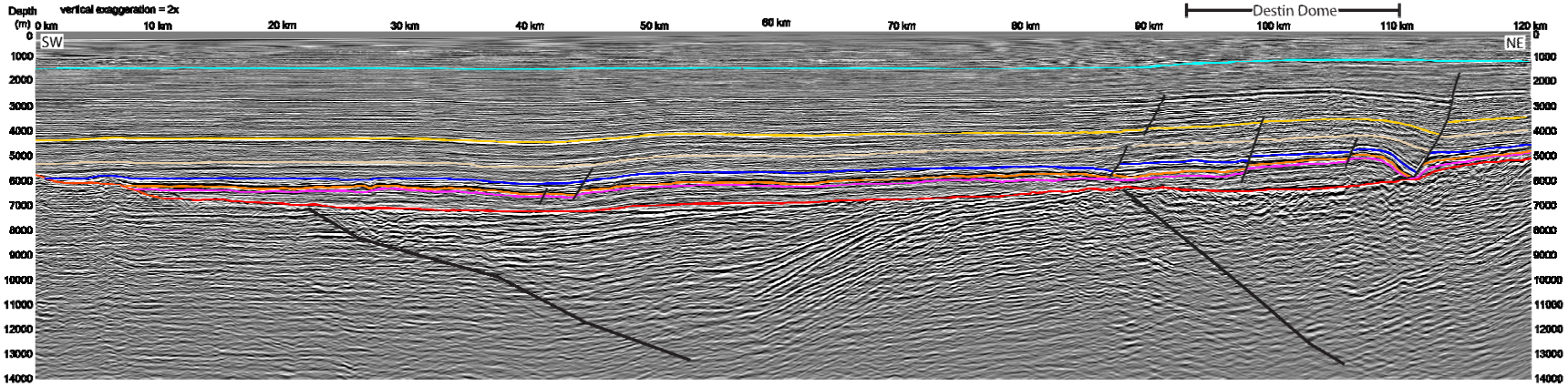

Figure 27: North-south seismic line through the Desoto Canyon Salt Basin (Figure 4). Below the salt, there are high amplitude dipping reflectors. The salt forms a large salt anticline on the right of the line. Above the salt the Norphlet Formation is present in variable thickness throughout the basin.

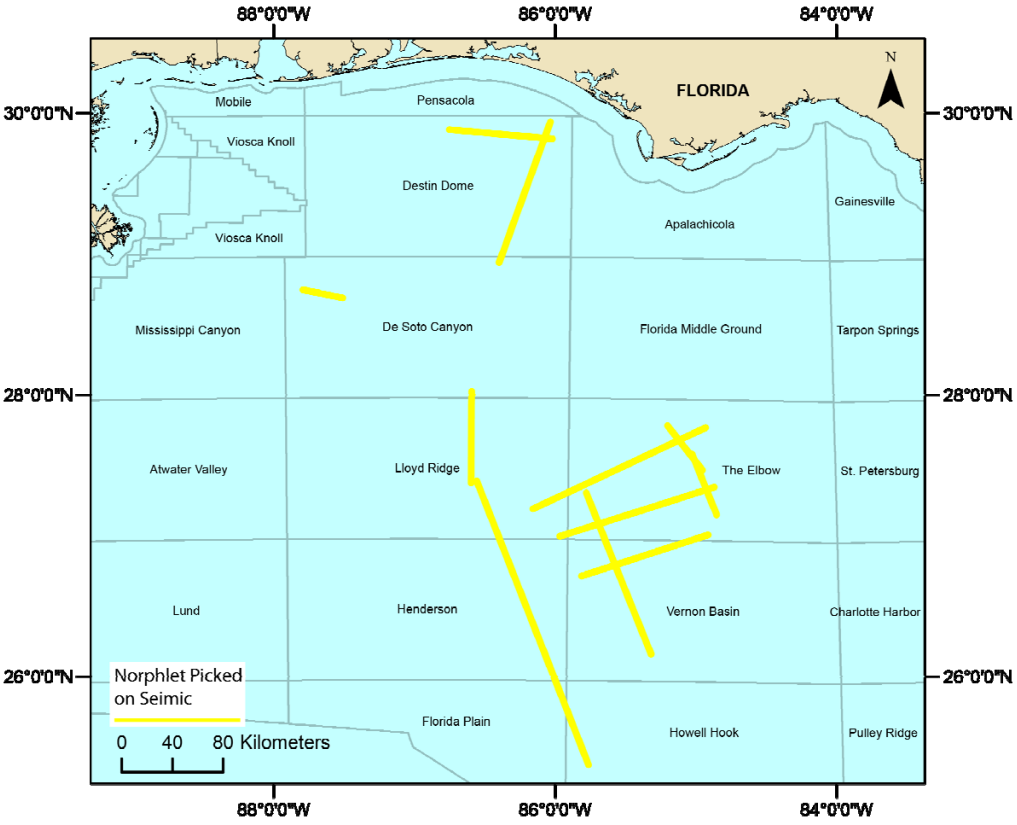

Figure 28: Locations of Norphlet reflectors on seismic. The Norphlet Formation is present in the deep water, DCSB, and the TE, but is absent over the MGA (gap in the De Soto Canyon protraction area).

5. INTERPRETATION OF RESULTS

5.1 Core-Log Correlation

The Mosbacher Powell Gas Unit 19-1 #1 core (Alabama permit number 2991) from Escambia County (Figure 3) has all of the Norphlet facies except the alluvial conglomeratic facies, which is restricted to areas very proximal to the highlands (Figure 12). The basal portion of the well has dark Norphlet shale (18496 ft). The density log shows a slight increase at the top of the shale while the SP log shows a shift to the right; the GR log does not reach this depth. The eolian deposits show little variation in the SP and GR logs as well as a consistent density log pattern (Figure 12, 15438-15448 ft, 15474-15495 ft). Alternating eolian dune, wadi and deflated wadi deposits show little to no variation from the eolian deposits (Figure 12, 15448-15474 ft). However, there is an absence of shale layers or lamina within the wadi deposits as all fines have been removed. The winnowing of fines and the high total feldspar/lithic content in eolian deposits proximal to the source in the West Florida (Scott, 1991) support the possibility that wadi facies exist in a well without a significant log response. The upper portion of the well is eolian and reworked Norphlet shoreface deposits, which exhibit similar log responses to the lower eolian portions of the Norphlet.

In the Shell DD 160 well #2 (Figures 3 and 13), the SP log does not have a noticeable change when entering the wadi facies found in the core unless significant shale layers exist, which may be due to lower eolian and upper wadi deposits possessing similar porosities. The porosity logs agree with this suggestion, though there is no SP response to a relatively thick

eolian section within the basal shale deposits (Figure 13, 16840 ft). The GR logs show an increased response at the top of the wadi facies. A GR response without an SP response suggests a mineralogical change in the sands towards more radiogenic sandstone composition, with a similar self potential to the relatively quartz rich eolian sands. An increase in potassium feldspar sand or possibly volcanic rock fragments could explain the increase in the GR. The density logs react strongly to shale, but not significantly to the wadi deposits that lack thick shale deposits. The GR logs are the most appropriate logs for picking the top of the Norphlet wadi facies as a significant increase in radioactivity occurs at the top of the wadi facies likely due to an increase in mud or feldspar (Figure 13, ~16780 ft). The GR is serrate throughout the deposits before becoming consistently "hot" in the shale interval at the base of the well (Figure 13, ~16820-16860 ft). A slight increase in resistivity occurs at the top of the wadi facies. The eolian facies shows a very consistent pattern on all the logs despite grain size variations. The shale facies is characterized by high density, higher resistivity and pronounced leftward shifts on both the GR and SP logs.

Log trends (Figure 29) correlated with core facies (Figures 12 and 13) are useful in picking the facies in wells with only logs. In the Sohio PE 948 well #1 (Figure 30), the top of the Norphlet Formation is marked by a strong SP response to the pyrite rich basal Smackover Formation (~18670 ft). The well is primarily composed of eolian deposits; thus, the GR is largely featureless until ~ 18900 ft where there is an increase in radioactivity. The SP log gradually shifts to the left through most of the section, likely related to secondary pyrite from the Smackover Formation and not Norphlet depositional traits. The density and velocity logs may also be affected by the secondary pyrite or responding to a lower porosity in the upper Norphlet sands (~18670-18760 ft). The lowermost portion of the Norphlet deposits are wadi deposits

(~18920-TD ft) as indicated by an increase in radioactivity without a density or SP shift implying a shale composition similar to the shallower wadi deposits in AL 2991 and DD 160-2 (Figures 12 and 13).

Figure 14 shows facies inferred from descriptions by Wilkerson (1981) in AL permit #1902 well compared with log-based facies interpretations. The interbedded wadi/eolian facies interpretation is based on a moderate GR, variable density and the frequency of similar deposits in Escambia, County. The shale facies picked on the logs are similar to that from Wilkerson (1981), while the lithology descriptions help determine which portions of the sandy deposits are wadi and which are eolian. Overall the log-based facies interpretation technique presented in this study shows good correlation with the facies inferred from Wilkerson (1981) (Appendix 1; Figure 14), Welsh (2003) (Appendix 1) and Ridgway (2010) (Appendix 1). Their interpretations show conglomerate restricted to areas within ~5 mi (8 km) of the Norphlet updip limit (Figure 31). The wadi deposits extend further from the highlands (up to ~16 mi. [25.7 km]) but do not frequently reach the distal areas that are dominated by eolian deposits. Markham (1991) describes the Norphlet from wells in Mobile Bay that consist almost entirely of eolian deposits with some basal "detrital sabkha" deposits. The preponderance of eolian facies is consistent with facies interpreted from well logs in the area of Mobile Bay. Wilkerson's (1981) descriptions of the basal shale deposits are limited to three Escambia County wells.

5.2 Alabama Log Facies Interpretations

The Norphlet Formation is extensively drilled in Alabama, providing numerous data points for establishing facies trends. The shale, wadi, and conglomerate Norphlet facies are typically found near the Norphlet updip limit (Figure 15). The conglomeratic facies is limited to a narrow strip adjacent to the paleo highlands within ~6 miles (9.7 km) of the updip limit.

Escambia County has some conglomerate but these are likely fluvial/wadi conglomerate. Escambia County is close to the extension of the Conecuh ridge complex (Figure 6), which helps explain the larger grain size. No conglomeratic facies was identified in the far southern portions of onshore AL. Rhodes and Maxwell (1993) identified conglomerate on the Wiggins Arch; thus, there may be some limited conglomerate or wadi deposits in the extreme SW portion of onshore AL. As discussed by previous authors (e.g. Badon, 1975; Mancini et al., 1984), the basal shale facies is not consistently found in the wells distal from the paleohighlands. Wells drilled in Escambia County consistently have the shale facies but the facies is less frequently penetrated in other updip portions of Alabama. The wadi facies is consistently present near the highlands, but becomes more discontinuous further from the highlands as eolian deposition becomes more common. The furthest areas from the paleohighs, near Mobile Bay, lack obvious wadi deposits though a few wells may have thin wadi deposits. Eolian deposits are present in all wells except a few wells analyzed immediately at the updip limit.

5.3 Mississippi Log Facies Interpretations

The 45 wells used are located in two clusters (Figure 16; Appendix 1). Mancini et al. (1999) established Norphlet presence in Issaquena, Sharkey, Leflore, Smith, Jasper, Wayne, Jones, Perry, and Simpson Counties. Alluvial and fluvial Norphlet deposits are present on and around the Wiggins Arch in southern Mississippi (Rhodes and Maxwell, 1993). Wells in western and central Mississippi contain primarily eolian facies; however, four of these wells in each cluster contain some wadi facies. The distance from the highland to the wadi facies in Mississippi is comparable to the distances in Alabama. All wells are too distal from the updip limit to contain the conglomeratic facies. Only one well penetrates the basal shale facies, exhibiting its discontinuous distribution. The Mississippi interior salt basin (approximate area of

Figure 16B) is characterized by eolian facies with some wadi facies, which brought sediment into the low region.

5.4 Florida Facies

This study did not analyze any wells in Florida; however, Scott (1991) interpreted eolian, wadi and conglomerate facies in west Florida (Figure 31). The wadi and conglomeratic facies are close to the paleohighlands in the east while westernmost Florida has several hundred feet of eolian deposits (Scott, 1991).

5.5 GOM Log Facies Interpretations

The Norphlet has not been tested south of the MGA or in the southern and western portions of DD. Four wells reach the Norphlet west of the MGA (Figure 32). Only LL 399 reaches Norphlet depths to the southwest of MGA; however, the well went directly from the Smackover Formation into salt and anhydrite without penetrating Norphlet deposits. DC 269, also known as Shiloh, penetrated approximately 300' of eolian sands while DC 353 (Vicksburg) to the SW of Shiloh penetrated approximately 1200' of Norphlet. Vicksburg has a thick eolian section as well as a basal section of shale and red sandstone interpreted by Godo et al. (2011) to be lacustrine. The lacustrine section on the Vicksburg well logs is similar in appearance to the wadi facies in other wells. In 2010, Shell and Nexen discovered significant hydrocarbon reserves in their Appomattox prospect at MC 392 in Norphlet deposits (Odum, 2010). While the logs have not been released for this well, nor the appraisal sidetrack, many speculate that they contain eolian sands.

The northern portion of DD and portions of PE have 15 wells with Norphlet sediments (Figure 33). Four wells have between 10 and 50 ft (3-15 m) of basal shale (DD 160-1, DD 160-

2, DD 31, and PE 996). These wells are clustered on the eastern side of PE and DD (Figure 33). Though typically thin, several of the DD wells have either the wadi facies or lacustrine deposits at their base (DD 111, DD 160-2, DD 162-3, DD 167, DD 31, DD 422 and DD 57). Most of the Norphlet penetrations in PE exhibit potential wadi facies deposits near the base including PE 918-1, PE 973, and PE 996. Because these blocks are close to paleohighs in west Florida or are near the mouth of the Tallahassee Graben (Figure 3), the presence of the wadi facies is consistent with the depositional pattern.

Large natural gas discoveries in the Norphlet Formation in MO has led to extensive drilling in comparison to the rest of the EGOM. The Norphlet Formation in MO has preserved eolian dunes with a linear form (Figure 34; Story, 1998; Ajdukiewicz et al., 2010) that are a minimum of 5.6-9 mi (9-14.5 km) long and have a wavelength of ~1.2 mi (2 km; Story, 1998), similar to the wavelength of linear dunes in the Namib desert of SW Africa (Figure 35; Ajdukiewicz et al., 2010). The majority of the wells drilled are near the crests of these preserved dunes.

Most MO wells only penetrate eolian sands either because there is only the eolian facies present or the wells were not drilled to the salt (Appendix 1; Figure 36). MO is 12+ mi (20+ km) from the Wiggins Arch, the nearest paleohigh, and in other areas, the conglomerate facies is within about 6 mi (9.7 km) of the highlands; thus, the lack of conglomerate is expected. MO 909 is the only well that penetrated/contains the basal shale facies. MO 916-B3, MO 867, MO 862, and MO 991-2 contain wadi facies; however, these wadi deposits do not correlate from well to well. Markham (1991) interprets portions of wells MO 823-1 and Alabama 76-2 to contain "detrital sabkha" deposits that may represent wet interdune deposits similar to sabkha deposits as described by Kocurek (1981) and Kocurek et al. (2001). No Norphlet penetrations exist in the

western part of the MO block; however, the Norphlet is present in the southern, central and eastern parts. To the south in Viosca Knoll (VK), the VK117 well was drilled 24000'+ without finding any Norphlet sands.

Log / Facies	GR	SP	Density	Dipmeter	Resivity	Sonic
Eolian	Low little variation	Low little variation	Low	Low to high angle	Variable	Lowest velocity
Wadi	Low-moderate Serrate/ variable	Low-moderate Serrate/ variable	May be variable	Likely random	May show an increase over eolian	Low velocity
Standing Water	Highest	Highest	Slightly higher	Nearly flat lying dips	Moderate to high	Low velocity
Evaporite	Low	Low	Lowest	Random	Highest	High (Anhydrite) to medium velocity

Figure 29: Table of log responses to Norphlet Facies.

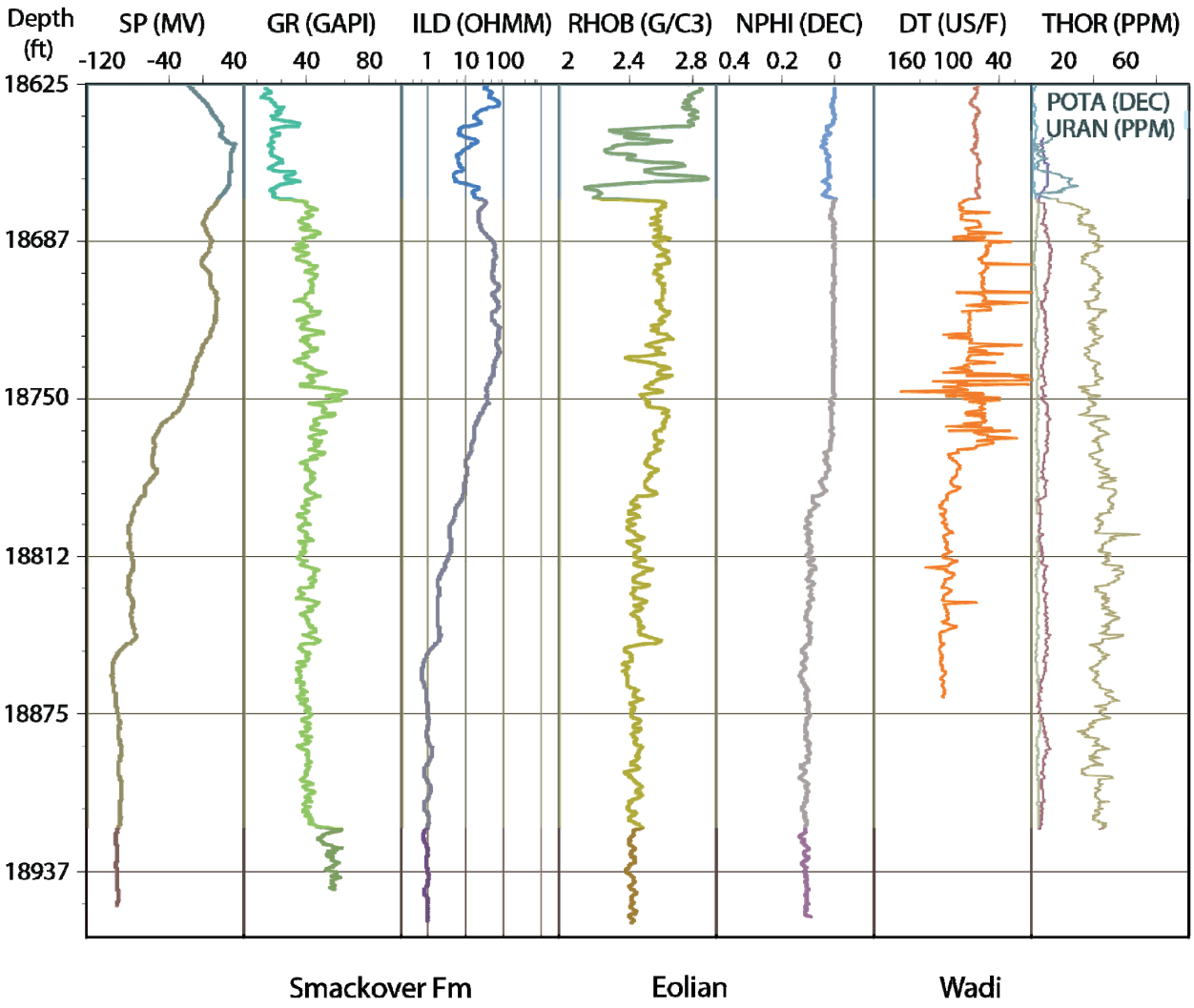

Figure 30: Application of facies picking methodology to Sohio PE 948 well #1. Top Norphlet is picked on a SP anomaly at the base of the Smackover Formation. The eolian facies have a relatively consistent low GR while the wadi deposits are picked by a significant increase in GR.

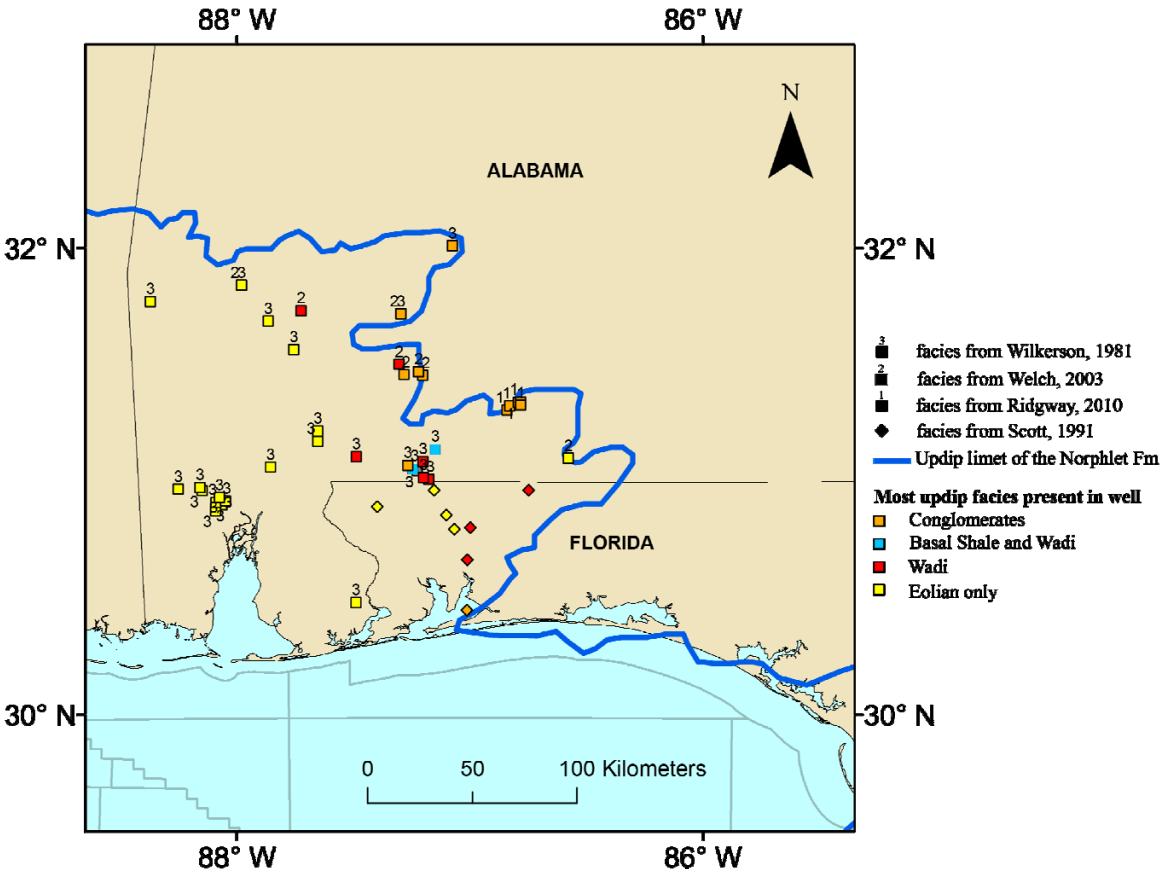

Figure 31: Map with facies from published core descriptions. The updip regions have a more fluvial influence while more distal areas are almost exclusively eolian.

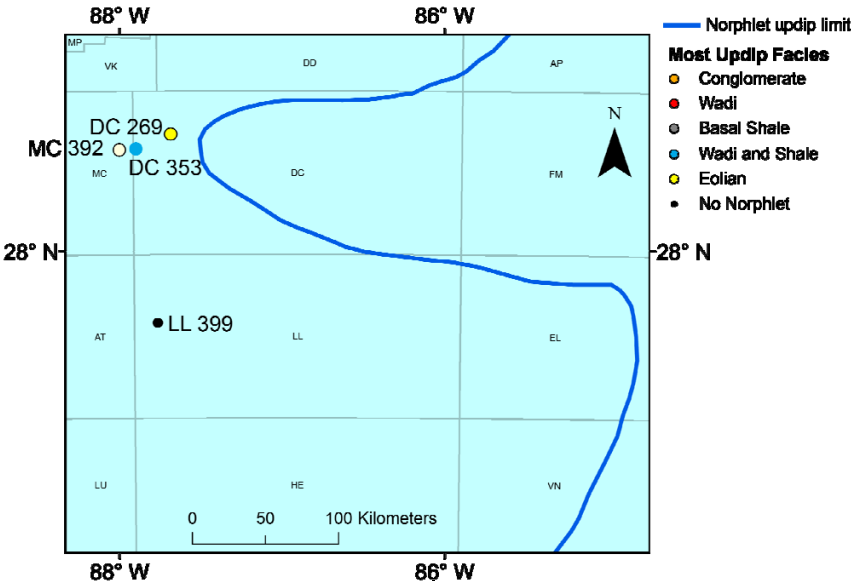

Figure 32: Most updip facies in the SE GOM. West of the MGA in DC and MC, there are thick eolian sands in the recent deep water Shell wells indicating an extensive deep water Norphlet erg. LL 399 penetrated the evaporites without encountering Norphlet sands and may represent the down dip limit of the Norphlet Formation.

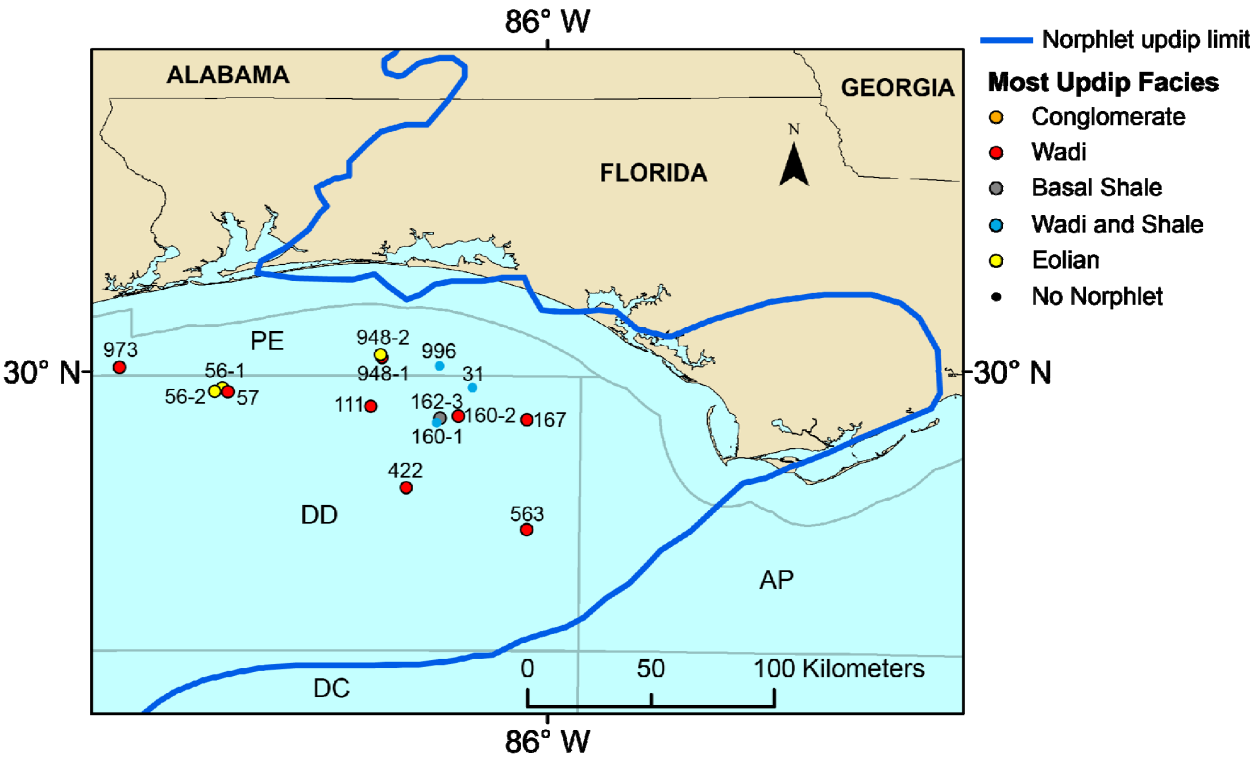

Figure 33: Most updip facies in DD and PE OCS protractions. While Norphlet eolian deposits are upwards of 1000 ft (305 m) in parts of DD, most of the wells in DD and PE have at least a thin non-eolian section. Nearby paleohighs likely contributed to the frequency of non-eolian deposits as well as the potential for wadi systems focused by the nearby Tallahassee Graben draining into DD.

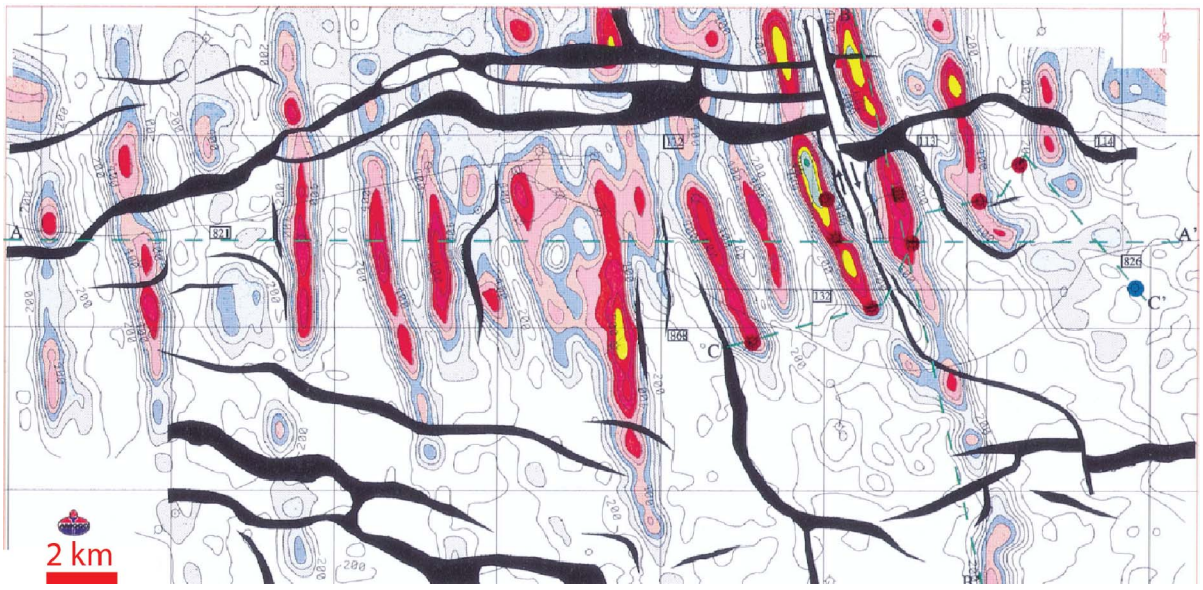

Figure 34: Isocore map of the Norphlet Formation in MO (Story, 1998). Linear dune topography is apparent from isocores made with 3D seismic data (See Figure 1 for location).

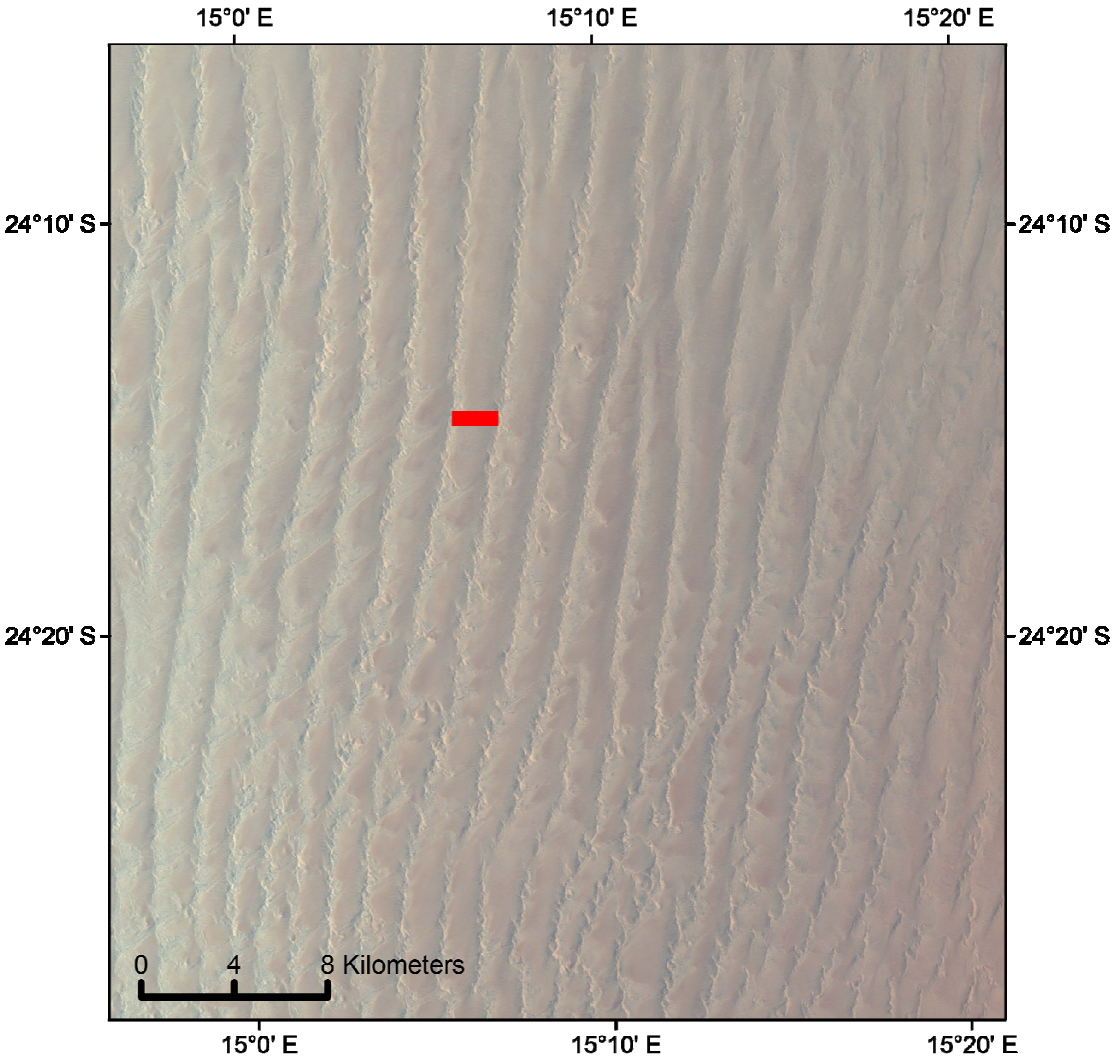

Figure 35: Linear dunes in Namib Desert, Namibia (NASA Landsat 7). The red bar is 2 km long showing the approximate wavelength of large linear dunes in Namibia. These dunes are similar in size to the Norphlet dunes near Mobile Bay (Ajdukiewicz et al., 2010)

5.6 Norphlet Facies Outside of the Study Area

Outside of the EGOM, the Norphlet is present as thin fluvial and eolian deposits in Louisiana and Texas (Ewing, 2001). In East Texas, thin eolian, fluvial, and possibly marine Norphlet deposits overlie the Louann Salt (Montgomery et al., 1999). Budd and Louck (1981) described South Texas Norphlet deposits as wadi shale, tidal flat shale, dolostone, and fine to medium grained sandstone with a thickness of 19-33 ft (5.8-10.1 m).

In the southern GOM, there are eolian and fluvial sandstones of Oxfordian age in Campeche Sound of Mexico and the paleoenvironment was arid and restricted (Guzman-Vega and Mello, 1999; Rosenfeld, 2002). During Late Oxfordian time, the Yucatan Peninsula was flooded (Rosenfeld, 2002) and Smackover equivalent sand, mudstone and limestone were deposited (Angeles-Aquino and Cantú-Chapa, 2001; Rosenfeld, 2002). The distribution of Oxfordian eolian deposits, including the southern GOM, the EGOM, and Louisiana and Texas shows that the Oxfordian environment was consistently arid during Norphlet deposition.

5.7 Norphlet and Haynesville Detrital Zircon Trends

The Laurentian zircons, derived from Appalachian terranes, are characterized by ages between 950-1900 Ma or 2700-2800 Ma, while zircon ages between 530-680 Ma or 2000-2200 Ma are characteristic of the Gondwanan Suwannee terrane (Figure 37; Lovell and Weislogel, 2010). The zircons analyzed in the Haynesville Formation show similarities to the patterns described in the Norphlet zircons (Figures 3 and 19). The Haynesville samples from wells PE-973 and MO-826 (Figures 3 and 19) have the same mixed source signature that Lovell and Weislogel (2010) found in the Escambia County wells. MO-823 (Figures 3 and 19) has a signature that implies a primarily Laurentian source with a possibility of some mixing from the

Gondwanan terranes. DD-563 (Figures 3 and 19) did not yield enough zircon ages to imply a source; however, it does have zircons with ages expected for both Gondwanan and Laurentian derived zircons. The Haynesville zircons ages are similar to the Norphlet zircons ages, and I suggest that the same sediment pathways remained in place at least through Haynesville deposition.

5.8 Sediment Transport

Lovell and Weislogel (2010) showed that Norphlet transitions from an Appalachian Laurentian source in much of Alabama to a mixed source along the Alabama/Florida border near Escambia County, Alabama to a primarily Gondwanan Suwannee terrane source offshore of west Florida (Figure 5). The Mesozoic grabens present in the EGOM could serve as potential sediment "funnels" (McBride et al., 1987b; Figure 6), which Lovell and Weislogel (2010) hypothesize drive the provenance trends. In the more updip areas of Alabama, paleohighs provided sediment to the wind system that built the dunes (Mancini et al., 1985). Other areas may have been influenced by the Mesozoic grabens, which have highlands on the flanks of the structures that shed sediment and lows in the center capable of channeling both winds and fluid flow south and/or west into the Norphlet system. The DCSB may be the offshore continuation of the Tallahassee Graben (Figure 6). Seismic data show that the DCSB contains a large half graben system (Figure 27) that may have funneled sediments. Any post-salt movement, even minor, on the main faults would have focused wadi systems and sediment input along the southern margin of the basin (Sweet, 1999). Immediately south of the DCSB is a paleohigh known as both the MGA and the Sarasota Arch (Figures 6 and 22). The Norphlet Formation, Smackover Formation, and portions of the Haynesville Formation pinch out onto the MGA (Figure 23), and the MGA shows evidence of erosion contemporaneous with the deposition of

these formations (Figure 24). Figure 25 shows a large fault controlled valley on the MGA that was potentially a sediment transport pathway providing sand to the Norphlet system off the arch. The two seismic lines cut the potential pathway obliquely; thus, determining the direction is difficult. South of the MGA is the TE, a graben (Wilson, 2011) that is both a potential depocenter and, as with the other graben complexes, a potential system to funnel sediment into the present day deepwater.

5.9 Dune Dip Patterns

The dip logs from the Norphlet deposits in Alabama are varied in character (Figure 21). In northern part of the study area (Figure 1), the dip logs have a narrow distribution of southern dips within the dunes. In eastern Mississippi, the wells show a 90°+ spread in the distribution of the dip directions with a possible overall trend to the SW. North of Mobile Bay, the dip rose plots are less consistent than exhibited north of 30.5° N but still show a pattern of southern dips except the dip directions are oriented slightly more to the west. In Mobile Bay, orientations have more variation and show bimodal distributions (Figure 38). The number of surfaces dipping to the SE increases the further to the SE of Mobile Bay a well is located. In Mobile Bay and MO there is some potential for rotation of the dips as the Norphlet subsided into the salt, but the dipmeters do not show evidence significant evidence of rotation (e.g. flattened eolian dips). In Escambia County, most of the dips in the core section fall between about 5-15°, but a few dip as much as ~20-22° (e.g. Figure 39), which complicates the identification of eolian deposits and eolian transport trends. Although some Escambia County wells have a consistent distribution, others have a random distribution of dip orientations and there is no clear trend (Figure 40). Regional rose diagrams (Figure 41) show that the trends are consistent in northern part of the

study area and southern Alabama; however, the Escambia County rose diagram indicates a general predominance of dips to the S or SE.

In offshore Florida, the wells show a significant difference in character (Figure 21). Those in DD have a spread of dipping surfaces greater than or equal to 90° with dips oriented to the N or NW. Wells in PE also exhibit variation in the rose diagrams; however, the apparent average dip direction is nearly 180° different from E/SE to W across the protraction area.

The Norphlet erg shows varied dune morphology (Figure 42). Where the Mississippi and Alabama portions of the erg merge, there is a nearly random distribution of the dipping eolian beds (Figure 21). The majority of dunes in central through southern Alabama appear to be barchan or large barchan ridges with the majority of the dipping eolian beds trending in the same direction. In southeastern Alabama the dips are less consistently dipping in one direction, but are still mostly in similar directions. The thin deposits in this area along with the dip patterns (Figure 38) indicates the dunes are likely isolated barchan dunes, possibly traveling in different direction with changing winds. In MO, the distribution of the dipping eolian beds is primarily bimodal indicating linear dune form. In DD and PE, the nature of the dunes is more difficult to determine, possible complex dunes in PE indicated by the scattered distribution of the dipping beds (Figure 38), and there is evidence for barchanoid ridges or perhaps linear dunes in DD.

The calculated vector resultants from the dipmeter interpretations yield the net transport direction within the dune fields (Figure 20). Through most of Alabama, outside of Escambia County, the primary transit direction is southward. South of Mobile Bay, the trend progressively changes from southward to southeastward (Figure 43). Escambia County wells have vector sums pointing south towards Florida as well as counter regional trends pointing north towards the highlands. In Mississippi, the dip resultants show a southern to southwestern transport direction

(Figure 20). DD wells show vector sums to the west or north/northwest, similar to east PE, which is consistent with the findings of Martens (1993). A northwest moving erg was interpreted by Douglas (2010) from core logs in the Shiloh and Vicksburg wells in western DC.

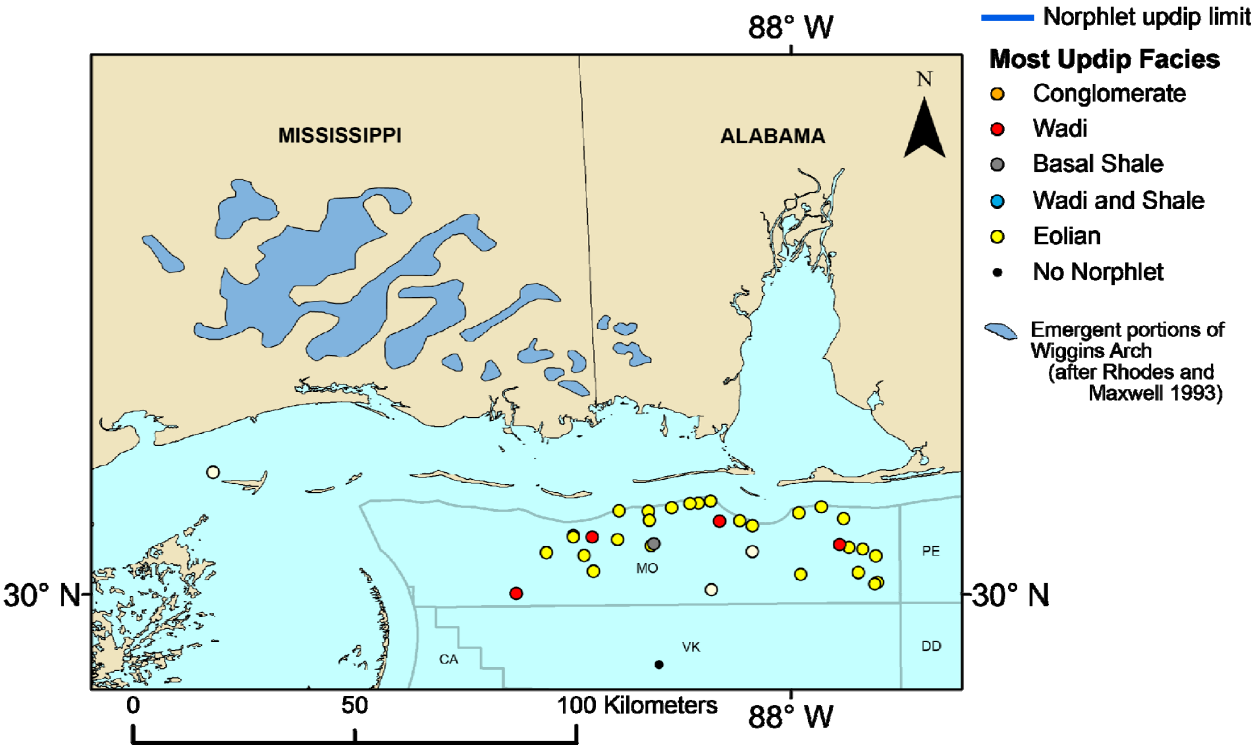

Figure 36: Facies in MO OCS protraction. Most wells in MO only penetrate thick eolian facies with thicknesses up to 1100 ft (335 m) but a few have other facies present. These may be sourced from small wadis flowing from the nearby Wiggins Arch or are potentially long wadis that may have flowed when a flood significant enough to break through the dune fields carried sediment from paleo-Appalachians to MO.

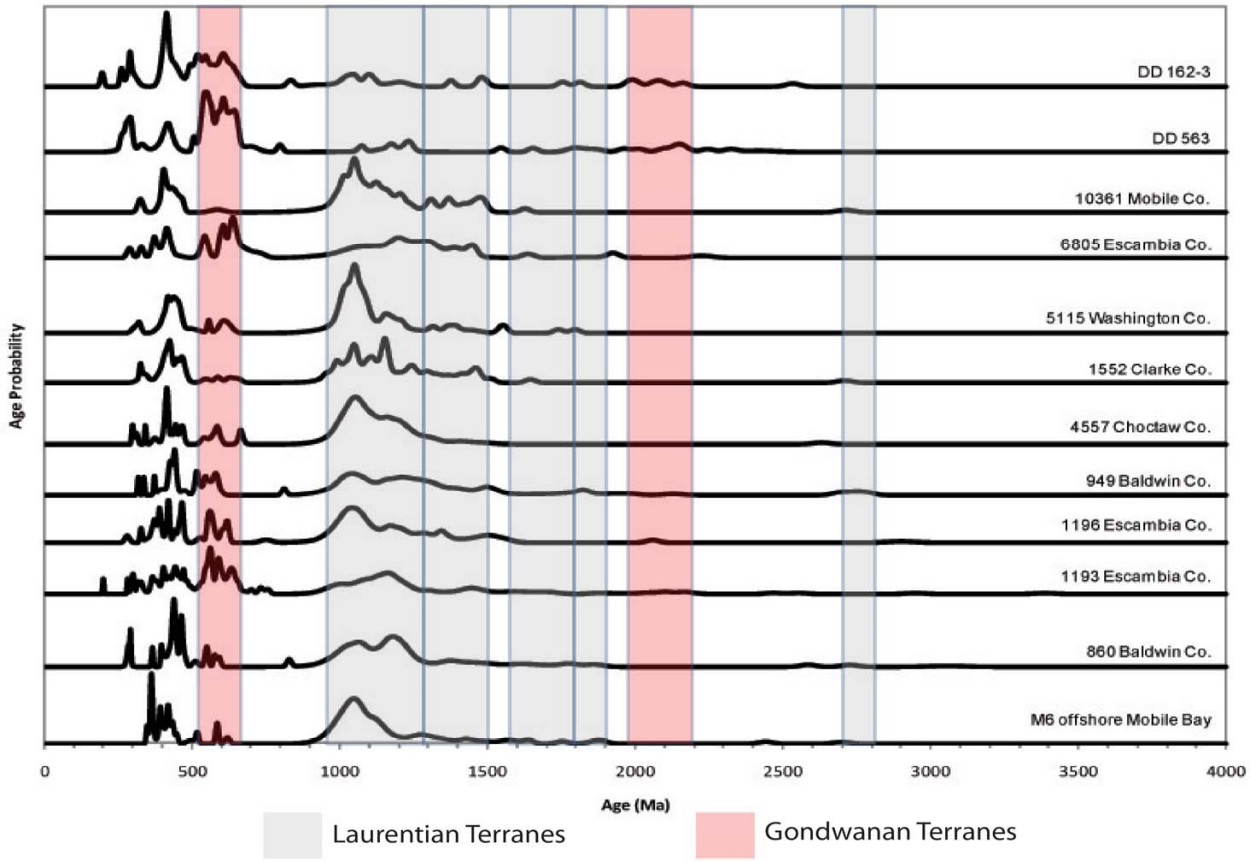

Figure 37: Norphlet Formation detrital zircon relative age probabilities (after Lovell and Weislogel, 2010). The distinct Gondwanan populations are shown in the red and Laurentian in the grey. Those with populations in both are considered to have a mixed provenance.

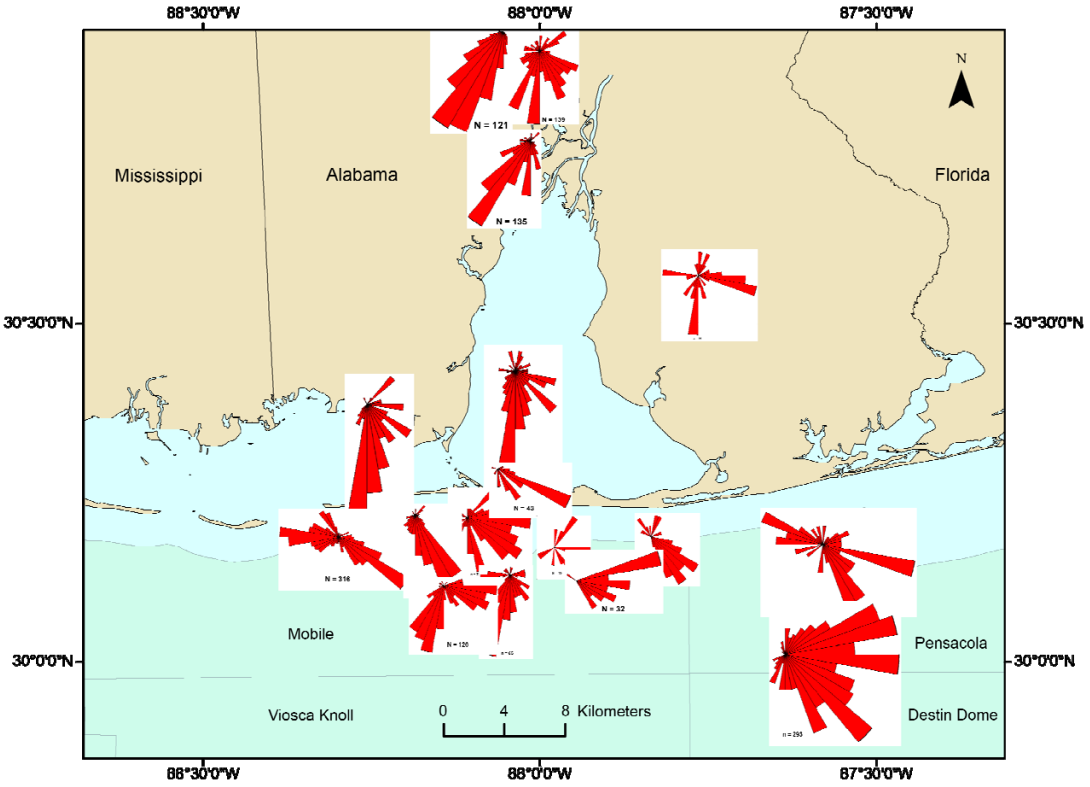

Figure 38: Dipmeter rose plots Mobile Bay. The plots show a distinct bimodal spread in the dip patterns, diagnostic of linear dunes. The transport direction shifts from towards the south to towards the east as they deposits towards PE and DD.

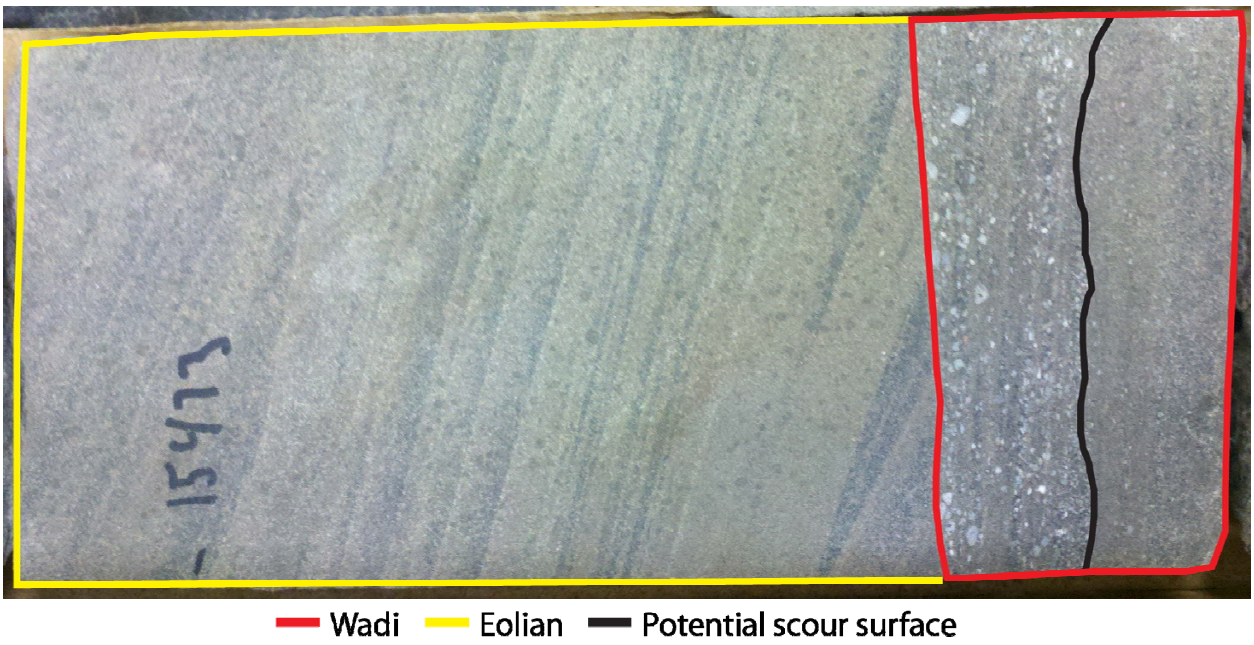

Figure 39: Core photo AL permit #2991. Low angle eolian deposits are interbedded with wadi deposits in Escambia County as seen in this core.

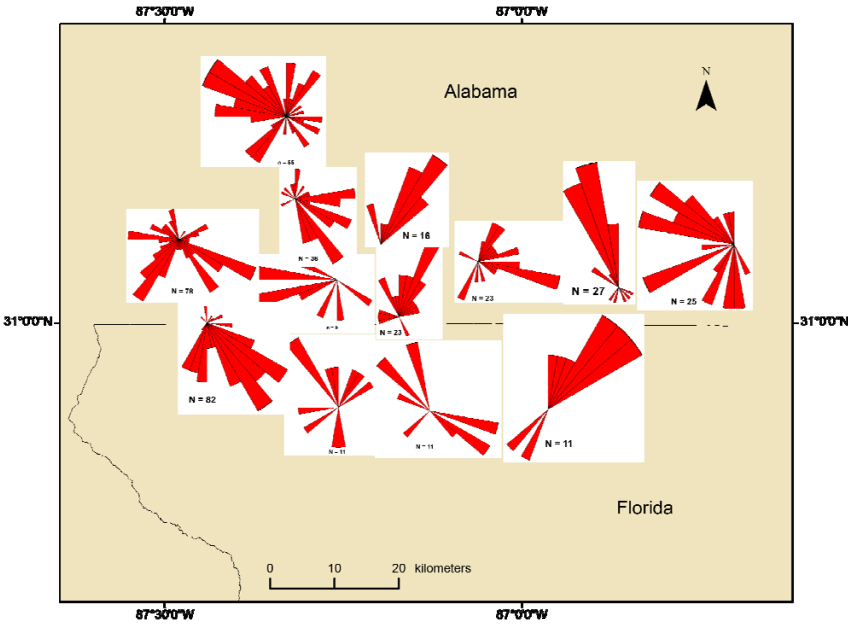

Figure 40: Dipmeter rose plots for Escambia County. The plots show a high degree of complexity within the deposits and may reflect regional and counter regional winds.

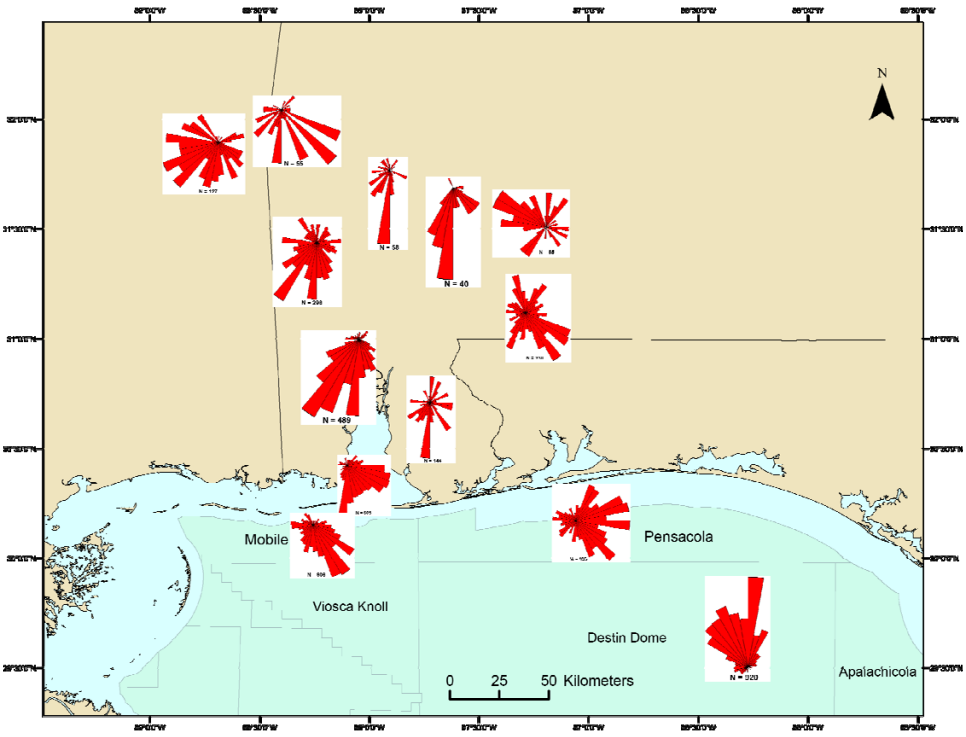

Figure 41: Dipmeter rose plots summed by county or OCS protraction. The dunes are complex in PE and near the Alabama-Mississippi border. while most of the Alabama dunes are barchanoid. MO and Mobile Bay have a clear bimodal distribution. which supports the seismic interpretations of linear dunes. DD dunes are linear or barchanoid but interpretations may be biased by the sample size.

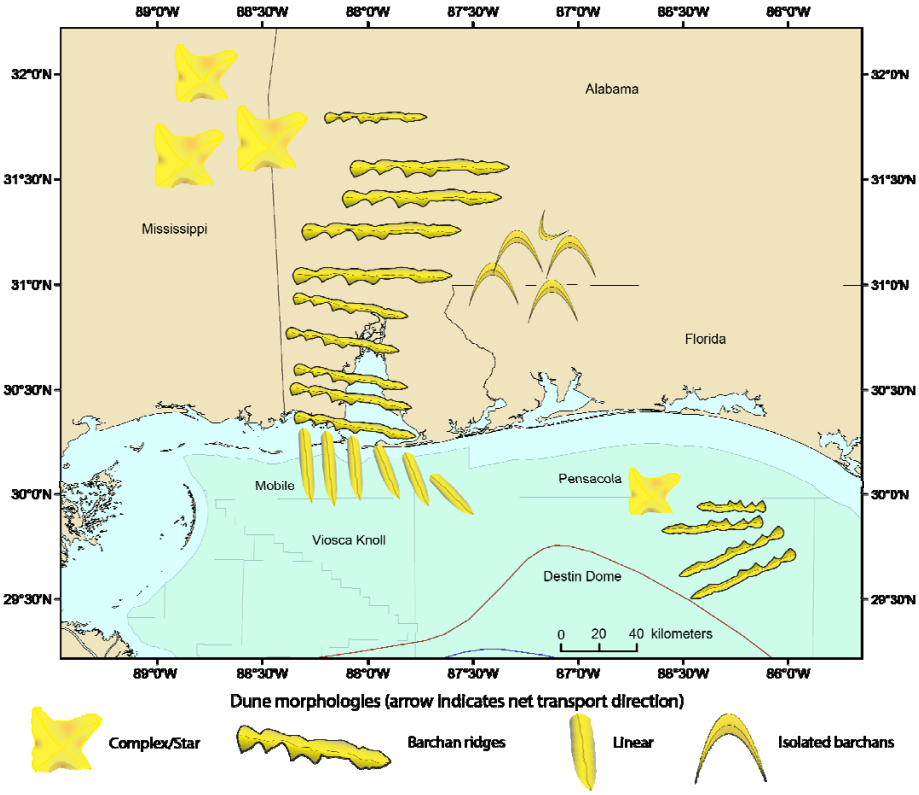

Figure 42: Morphology of Norphlet dunes. The morphology of the dunes is varied throughout the Norphlet deposition trend with dune type reflecting the local sedimentological, structural and wind conditions.

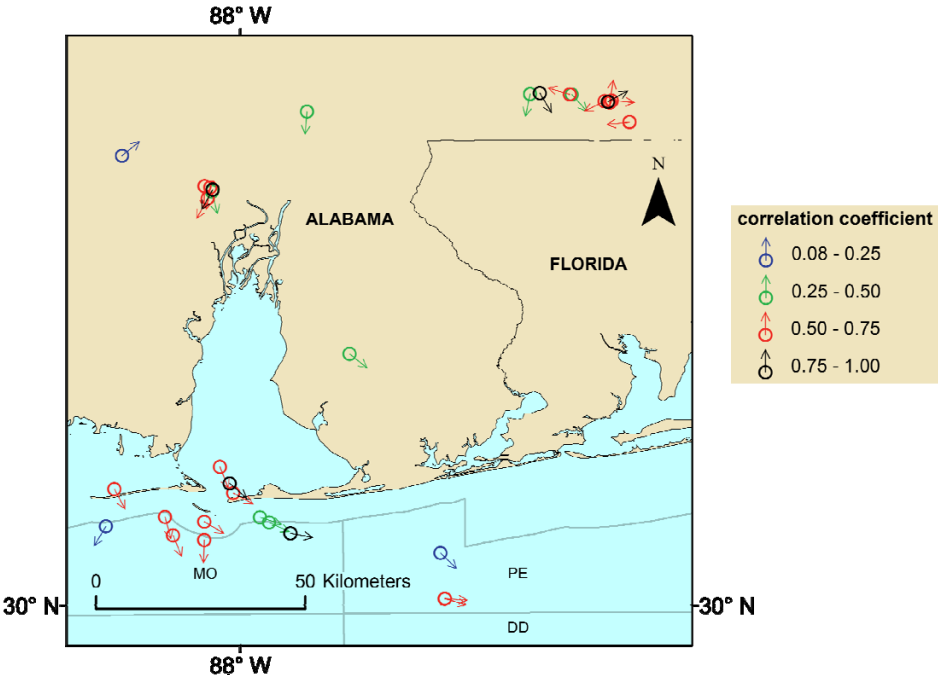

Figure 43: Vector resultants of dipping eolian surfaces in Norphlet wells in south Alabama. The southern portion shows a gradual change from a southern to an eastern transport direction.

5.10 Major Structures

The largest structures (Figure 6) on the seismic data are from north to south the DCSB (low), MGA (high) and the TE (low). In the DCSB, the Norphlet Formation reaches thicknesses in excess of 1300 ft (400 m) (Martens, 1993). Western DC, west of the MGA, contains Norphlet sands (Godo et al., 2011). While the Norphlet Formation has not been drilled immediately south of MGA or in the TE, the timing of the formation of TE is conducive to potential deposition of the unit (Wilson, 2011). Seismic analysis shows a Norphlet/Smackover reflection pattern of a strong Smackover peak followed by a strong Norphlet trough above the salt in and to the west of TE. This pattern is similar to that seen in DCSB and west of MGA, and these reflections are interpreted to be Norphlet sands (Figure 28). The seismic data reveal that Norphlet deposition is extensive south of MGA just west the Florida Escarpment. The Norphlet onlaps the northern edges of MGA and again appears south of MGA (Figure 23).

The MGA was a paleohigh at the time of deposition of the Norphlet Formation because the Louann Salt, Norphlet Formation, Smackover Formation and the lower section of the Haynesville Formation onlap the structure (Figure 23). The first formation to drape MGA is the upper section of the Haynesville Formation (Figure 22). MacRae and Watkins (1993) suggest minor thermal subsidence in DCSB and the edge of MGA during Late Jurassic time, which may be visible in minor thickening of the Cotton Valley Group (Figure 44).

The MGA has significant erosion on the BSE horizon as shown by the irregular character of the horizon and apparent incised channels (Figures 22 and 24). Some of these incised valleys may have carried sand into the present day offshore during storms, or wet periods during the deposition of the Louann, Norphlet, Smackover and lower Haynesville formations (Figure 24). The center of MGA also has a small graben 4.3 mi (7 km) wide and 2,000 ft (610 m) deep

(Figure 25). Haynesville deposits fill the graben, requiring the graben to be at least Kimmeridgian in age; however, because of sediment bypass, the grabens may be older.

Within DCSB, the most obvious structure is the Destin Dome (location on Figure 27), a large salt dome studied by MacRae and Watkins (1992, 1993, 1996). Salt migration formed the Destin Dome during Late Jurassic/Early Cretaceous through Early Cenozoic time (MacRae and Watkins 1992). The northeast margin of the dome is bounded by a large listric normal fault (Figure 27; MacRae and Watkins, 1992; Martens, 1993). The original salt thickness was a minimum of 2,500 ft (760 m) in DCSB (MacRae and Watkins, 1992).

Below the salt, dipping reflectors indicate faults bounding a half graben basin (Figure 27; Appendix 3). The seismic lines show an apparent dip on the subsalt reflectors to the south on the N-S line and to the west on the E-W line (yellow lines, Figure 45). MacRae and Watkins (1993) identified similar pre-salt dipping reflectors and showed a predominance of SW dipping reflectors on SW-NE oriented lines, and reflectors that dip toward each other on NW-SE oriented lines (Figure 45). The extent of the dipping reflectors was 23 miles (37 km) further to the south in this study than identified by MacRae and Watkins (1993). A few faults (Figure 46) offset the base of the salt between ~400-640 ft (120-195 m).

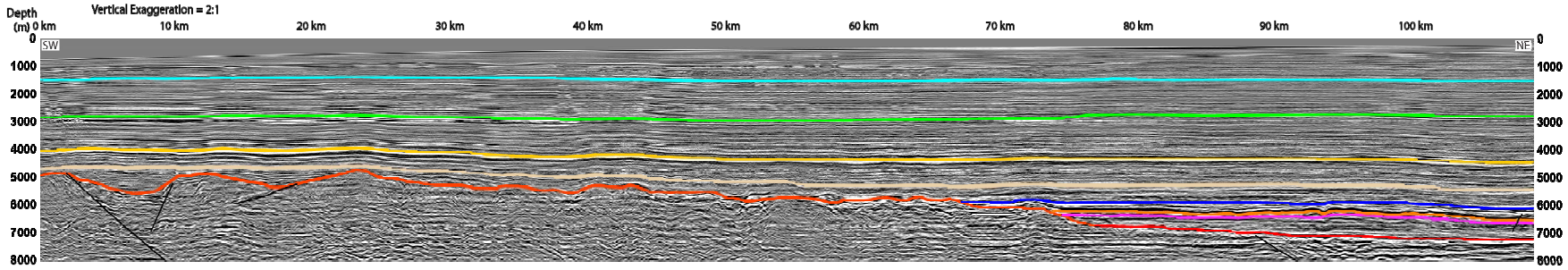

Figure 44: Possible thickening of Cotton Valley Group and Early Cretaceous on seismic (Figure 4). The Cotton Valley (figure 2) appears to be roughly 50% thicker in the middle of the basin than it is on MGA indicating the possibility of minor thermal subsidence in the DCSB on the right side of this line.

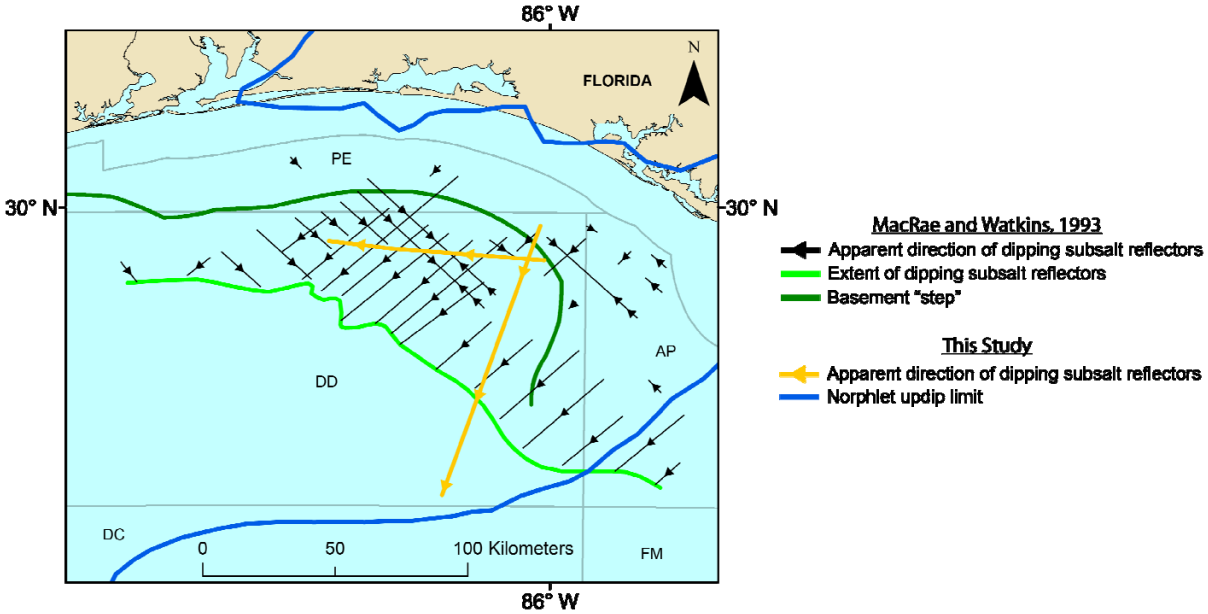

Figure 45: Map of dipping reflectors subsalt (after MacRae and Watkins, 1993). While the DCSB might have a NE-SW trending synclinal axis (MacRae and Watkins, 1993; Dobson and Buffler, 1991), it appears to also have a large NE-SW extensional component indicated by the large number of SW dipping reflectors implying grabens opening parallel to this trend.

6. DISCUSSION

6.1 Facies Distribution

Prediction of the distribution of the facies of the Norphlet Formation is complicated by the sporadic preservation of wadi deposits and other waterborne sediments. Minor environmental changes can shift the depositional style and replace wadi channels with eolian sediments, preventing significant fluvial type buildup (e.g. Simpson Desert, Australia; Craddock et al., 2010). Another potential factor preventing thick fluvial type buildups is winnowing of fine sediment particles after rare flood events (Glennie, 1972), which leads to thin and laterally discontinuous wadi deposits everywhere except areas proximal to the highlands. When fluvial systems break through the dune field, total deposits may only be a few meters thick, are primarily composed of reworked sands from the dunes, and are laterally continuous for tens of meters (Svendsen et al., 2003). On the Skeleton Coast of the Namib, these floods occur once per 9 years in the Uniab River and more infrequently in drier areas (Svendsen et al., 2003). The Uniab River is able to break through the dune field and reach the coast 15.5 mi (25 km) away (Svendsen et al. 2003). 500 km to the south, aerial photography shows evidence of past breakthroughs reclaimed by the dunes at Tsondabvlei and Sossusvlei where the dune field is in excess of 60 miles (97 km) wide (for location see Figure 47a index map). While updip areas may have extensive fluvial deposits, sediment may be carried to the distal part of the system without significant evidence at down dip locations.

In the Norphlet, the wadi facies is easily identified in updip regions (Figure 48) where the facies is laterally consistent and thickness can exceed 100 ft (30 m) thick. However, locating the

wadi facies downdip is challenging due to the low abundance and the frequent partial penetration of the Norphlet section by wells. Wadi deposits are primarily found in the lower portions of the Norphlet section while the upper deposits are primarily eolian in nature. This predominance of dry deposits in the upper section indicates that floods large enough to provide the amount of water needed to break through the Norphlet dune field and transport coarse sediment down dip were likely infrequent (Sneh, 1983; Svendsen et al. 2003). The decrease in wadi abundance may have caused stranding of wadi discharge within the dune field leading to playa or lacustrine deposits (e.g. Sossosuvlei, Namib Desert; Simpson Desert, Australia) (Figure 47). In Mobile Bay, large linear dunes formed (Story, 1998; Ajdukiewicz et al., 2010), leaving continuous interdunes open for wadis to flow through; thus, biasing the distribution of the wadi facies towards the interdunes similar to the manner in which floods are channeled in the interdunes of the Skeleton Coast in Namibia (Svendsen et al, 2003). Wells are drilled in the crests of the dunes with the intent of drilling for hydrocarbons; thus, data are not available for the interdunes. Detrital-dominated sabkha deposits (Markham, 1991) at the base of the Norphlet in Mobile Bay could be related to wetting of this area from floods before the erg migrated into the Mobile Bay area. Where dune morphologies are more complicated, and interdunes do not readily route fluid flow, such as northern DD (Marten, 1993), wadi deposits are more equally distributed and the potential for shale deposited on the margin of the erg is increased (Svendsen et al., 2003). From these data, all areas of the Norphlet adjacent to the paleohighs are expected to have some fluvial influence (Figure 49).

The Shell/Nexen EGOM Norphlet discoveries extended the known limit of the Norphlet eolian facies further south (Godo et al., 2006; 2011). In LL 399, the Smackover Formation lies directly on top of the Louann Salt without Norphlet deposits, setting a potential down dip limit of

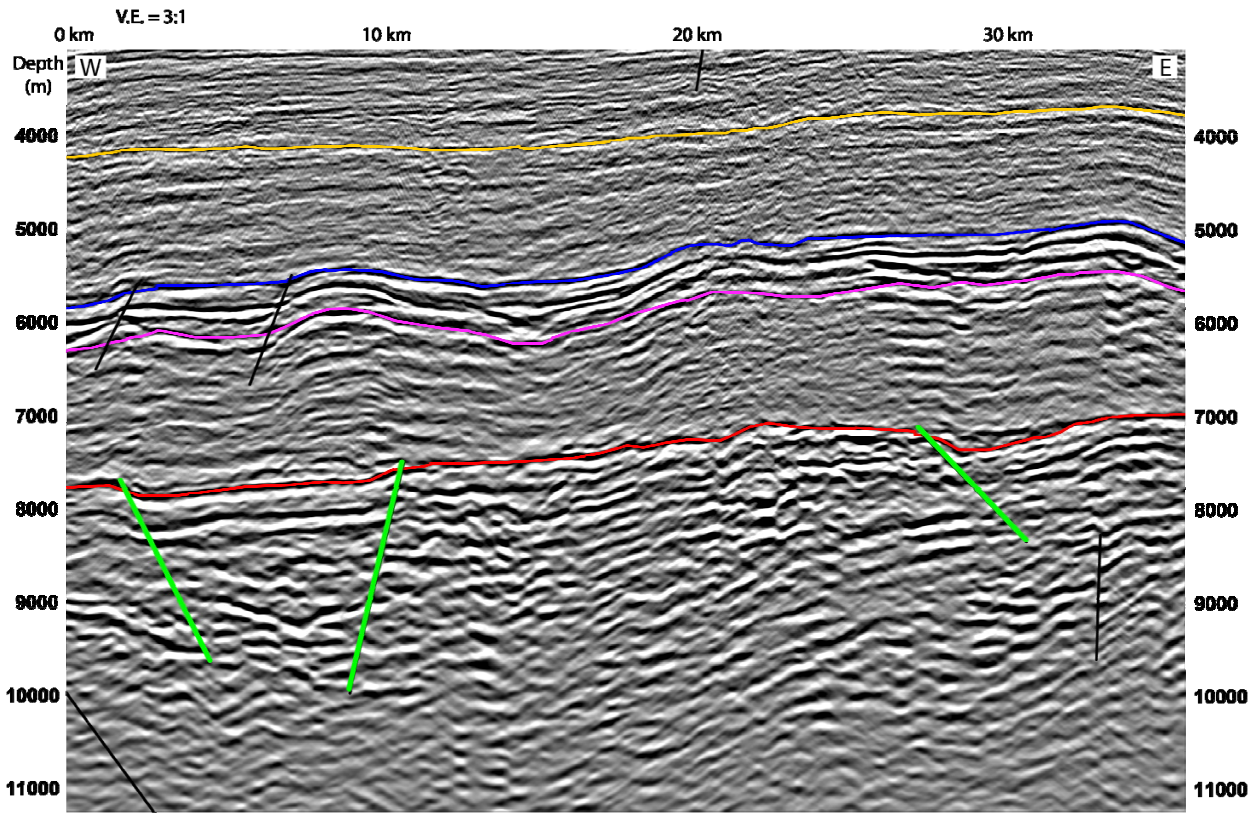

Figure 46: Faults offsetting base of salt (Figure 4). The timing of the faults (green) offsetting the base of salt (red) is difficult to determine due to the overprint of salt migration, which peaked during Cretaceous time (MacRae and Watkins, 1992). There are two minor faults in the Oxfordian section that may be related to late extension, but are likely caused by salt migration placing the faults offsetting the base of salt after the main extension, and probably prior to Oxfordian time and certainly before the unfaulted Cotton Valley Formation was deposited.

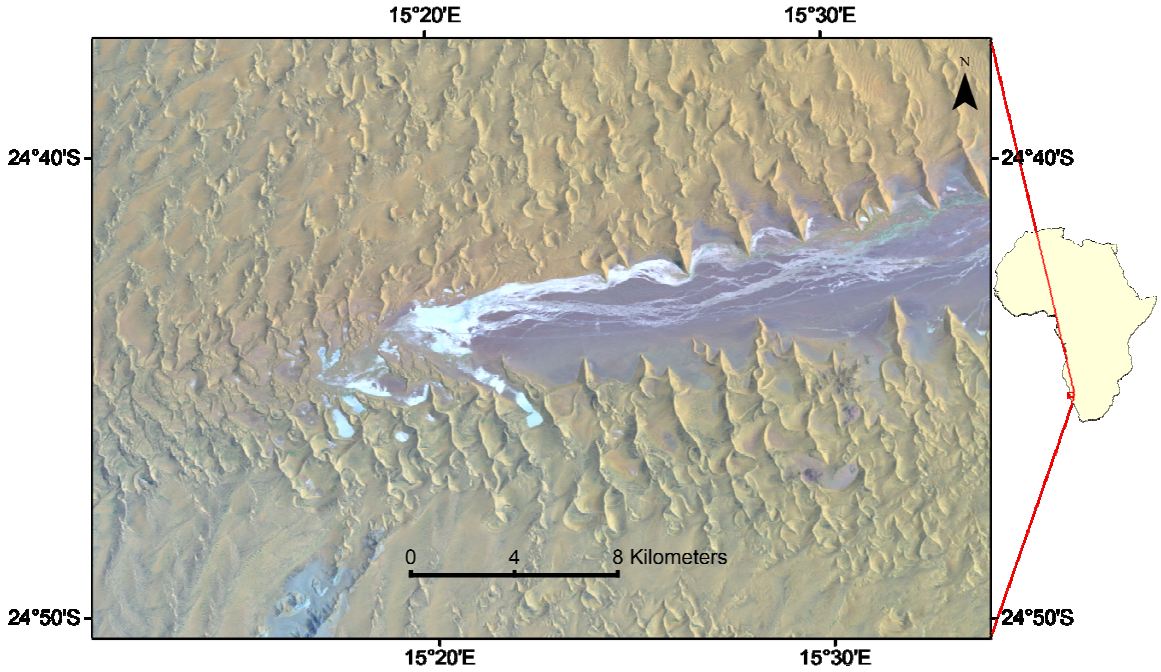

Figure 47a: False color image of Sossuvlei, Namibia. This is a wadi and playa system in the Namib Desert where the green areas indicate vegetation near a fluvial incursion that does not reach the end of the area without dunes. The white areas are playa lake deposits and indicate that water has previously pooled in the western portion of this wadi. (NASA Landsat 7)

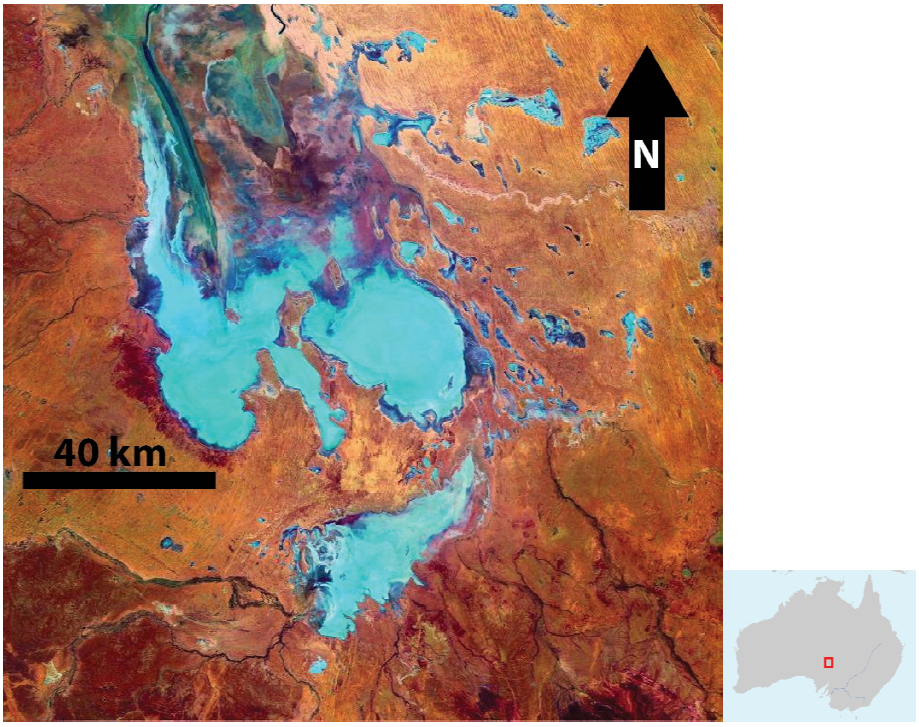

Figure 47b: Landsat 7 image of Lake Eyre, Simpson Desert, Australia (NASA, Landsat 7). A large lake forms during wet periods in the southern Simpson Desert. This lake fills in areas between the dunes as it grows beyond its typical bounds.

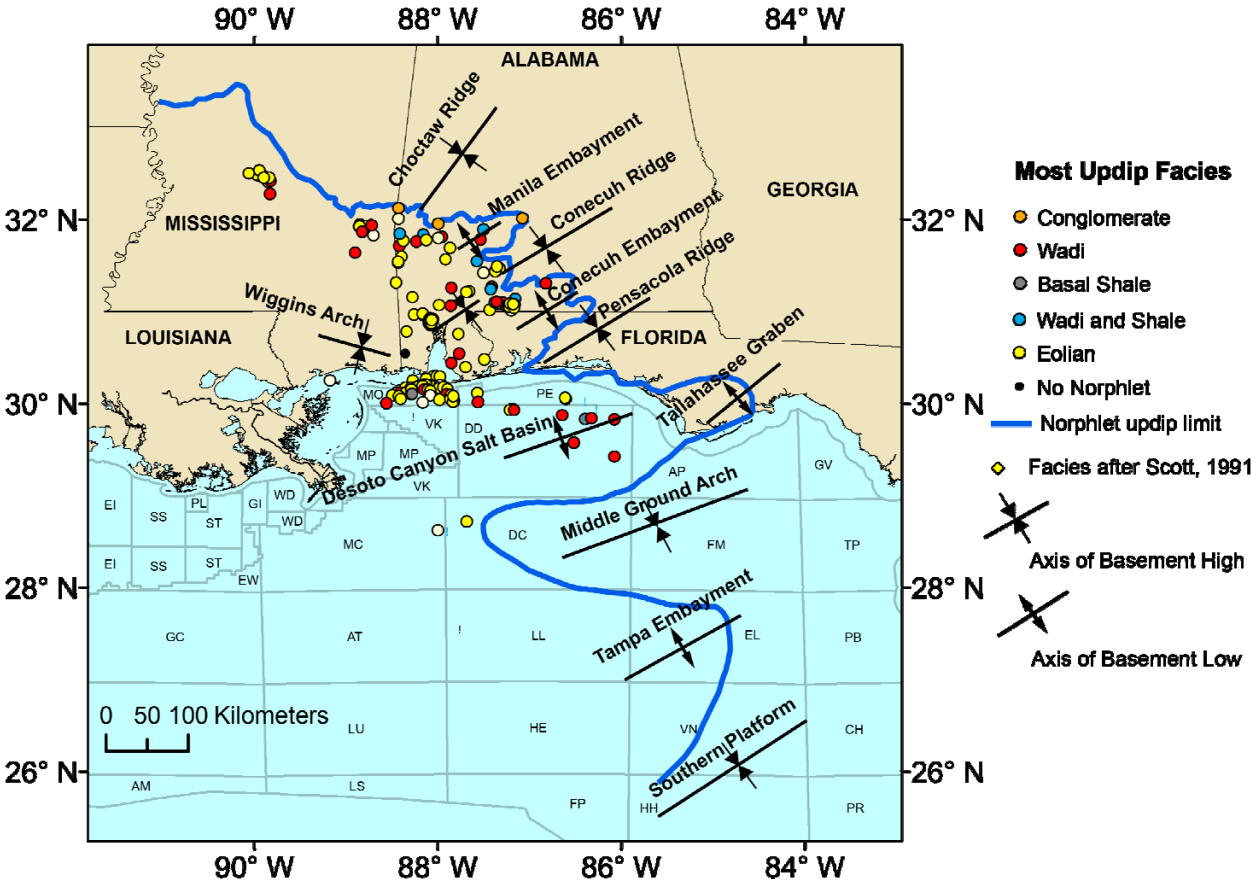

Figure 48: Facies interpretations across the Norphlet trend. Wadi facies influence is more common in the updip regions indicating that each high serves as a local sediment source, which resulted in the Norphlet deposystems being at least partially compartmentalized.

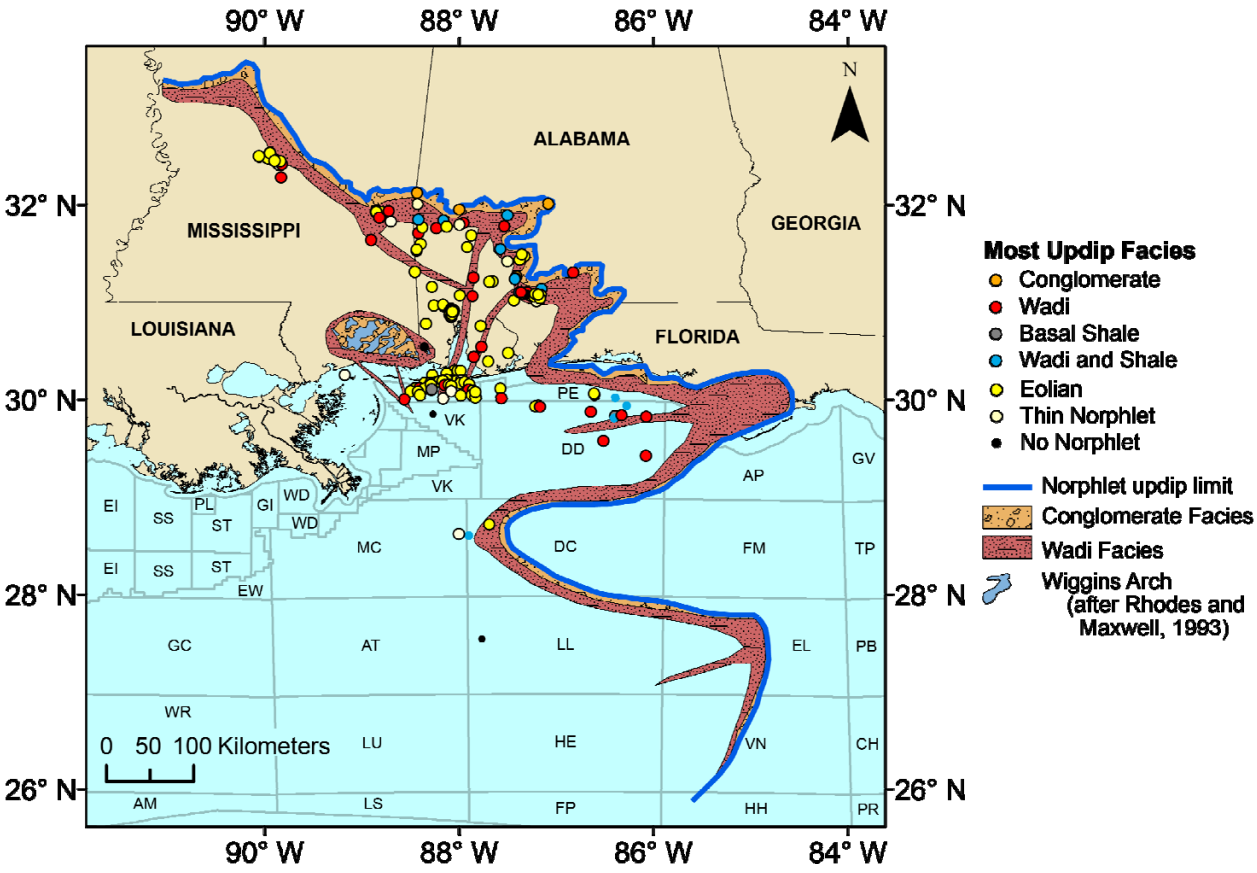

Figure 49: Interpretation of the full extent of Norphlet waterborne facies in the GOM. The down dip extentions are schematic, but represent the well data and the structural elements of the GOM during Norphlet deposition. The wadi systems moved sand from the highs into the Norphlet system after which the sands were reworked into the thick dunes sands in the Norphlet Formation.

the Norphlet Formation. Furthermore, this well was drilled just south of the line where Nagihara and Jones (2005) found a sharp transition in heat flow from 39.9 to 21.4 mW/m^2 suggesting a regional transition from attenuated continental crust to poorly radiogenic oceanic crust (Figure 7). If this is oceanic crust, depending on the timing of emplacement, this crust may be younger than Norphlet deposition. Alternatively, because most interpret seafloor spreading in Callovian to Oxfordian time (Marton and Buffler, 1994; Salvador, 1991; Pindell and Kennan, 2009), the Norphlet erg did not migrate far enough south to reach LL 399. Potential source terranes for the Norphlet in LL are the MGA and Florida with the sediment funneled through the TE. Douglas

(2010) interprets the erg to be migrating to the NW in the western portion of DC (75 mi [120 km] to the north of LL 399) and if migration directions in LL are also to the NW it would lead to a thinner belt of Norphlet along the MGA because instead of moving sediment away from the highs, as in Alabama, the winds would be moving the dunes toward the paleohighs. Another possibility is that this area was topographically low enough that it was too wet for eolian deposition and potentially an area of either evaporitic deposition or early Smackover type carbonates. Regardless of the factors preventing Norphlet deposition, LL 399 marks a point at which more distal Norphlet eolian deposits are unlikely.

Eolian deposits are extensive in southern Alabama, Mississippi as well as the northern EGOM (Figure 50). While the Norphlet has not been drilled in the moratorium area south of MGA or in the TE, the presence of thick Norphlet eolian deposits in MC and DC reveal a working eolian system that should extend along the source terranes to the SE (Figure 50). The presence of an interpreted Norphlet reflector in the TE strengthens this argument. In MO, Mobile Bay and DD, seismic "pods," considered reliable indicators of eolian Norphlet deposits that have subsided into salt, are present (Figure 10; Hoar et al., 1990; Martens, 1993; Story, 1998; Ajdukiewicz et al., 2010), and similar pods are found in the TE (Figure 26) indicating the eolian facies. One of these pods is near the updip pinchout of the Norphlet reflector in the TE (see Figure 4 for location of Figure 26), suggesting that Norphlet eolian facies onlaps the paleohighs. Log interpretations to the north show eolian facies near the updip paleohighs. Aerial photography shows dunes in the Gran Desierto near the Gulf of California also onlap the highlands (Figure 51), and dunes in the Kelso Dune field in the Mojave Desert have also migrated onto the lower slopes of the adjacent mountains (Kocurek and Lancaster, 1999). Eolian deposits are present across the entire Norphlet trend (Figure 52) except on the extreme updip

margin and perhaps some distal areas such as the western Mississippi territorial waters, as identified in the Mississippi Sound Block 57 (Petty et al., 1994).

6.2 Transport Pathways

The primary transport agent of the Norphlet sediment deposition is wind reworking of sediments delivered to the system by fluvial/alluvial processes (Wilkerson, 1981; Mancini et al., 1985; Scott, 1991; Lovell and Weislogel, 2010). Lovell and Weislogel (2010) show varied Norphlet provenance. The facies relationships within Alabama reveal a decreasing influence of fluvial systems as the deposits move away from the paleohighs with the distal areas containing evidence of the wadi facies. In Escambia County, deposits could be derived from either alluvial fans or wadi systems coming south off the paleo-Appalachian Mountains, or from the wadi systems from the east channeled within the Mesozoic grabens. This would explain the mixed Gondwanan/Laurentian affinity described by Lovell and Weislogel (2010).

In DD and PE, 12 wells have at least minor basal deposits indicating waterborne deposition (Figure 33). These deposits are either the wadi facies or basal shale facies, similar to those found in the updip areas (Figure 48) that Pepper (1982) describes as the distal ends of alluvial fans. These facies relationships indicate wadi, or alluvial systems shedding sediment off of Florida, which supports the concept that the sand in this area had a Suwannee terrane (Florida) source, with minor input from alluvial fans on Pensacola Arch to the north and the MGA, while the majority of the sediment was transported from the south through wadi systems channeled by the Tallahassee Graben to the west, which MacRae and Watkins (1993) interpret as an onshore continuation of DCSB (Figure 53). Applying these interpretations to the southern EGOM would

require wadi transport within the TE and alluvial fans on MGA to be the main delivery mechanisms to the southern EGOM.

The waterborne transit system is therefore controlled by structure with highs creating catchments and causing alluvial fans to build up on their flanks (Figure 53). Connectivity of structural elements such as the joining of the Wiggins Arch and the Conecuh Ridge (Figure 6) are enough to divert the path of any wadi facies while grabens, like the Conecuh Embayment and the Tallahassee graben, capture and focus the wadi systems (Figures 6 and 45). These elements are part of the system that partitioned of the provenance described in Lovell and Weislogel (2010). It is likely that the waterborne systems are the primary determinant of the provenance because the similarities between the Norphlet and Haynesville provenance would have been difficult for the noneolian Haynesville Formation to mirror if there were a significant eolian contribution.

Eolian transport directions in the Jurassic EGOM were spatially varied (Figure 20). The models by Parish and Peterson (1988) of Late Jurassic winds show a prevailing eastern wind direction in the GOM with a south directed winter wind (Figure 54). The direction of sediment transport in the dunes is at least partially dependent on the local highs as opposed to a consistent regional wind pattern. In Alabama and Mississippi, the general trend appears to be moving the sediment south to southwest (Figure 20) with an Appalachian (Laurentian) source for Alabama and Mobile Bay sediment (Lovell and Weislogel, 2010). In Escambia County, the thin Norphlet section makes determination of the transit directions difficult but the dominant direction is southerly despite some of the wells showing possible northern transport (Figure 43). In areas near highlands, winds can blow counter to the prevailing winds in wadi channels, which would explain the scatter in the Escambia County data (Glennie, 1972). The predominant southern

direction of transport in Alabama would prevent Suwannee terrane sourced sediment from the Conecuh Embayment from mixing with areas only sourced from the Appalachian Mountains.

In the offshore, the transport directions are broken into two regimes, one to the E-SE and the other to the N-NW (Figure 53). As the dunes in the Mobile Bay area move south of the Wiggins Arch, the transit direction rotates eastward with the Norphlet dip-directions in wells of western PE oriented nearly due east (Figure 43). This may be a reflection of regional winds becoming a dominant factor after the sediment is no longer sheltered by the paleohighs in Alabama and Mississippi (Parrish and Peterson, 1988). In DD and eastern PE, the transport is primarily to the north or the northwest. Without a transport direction to the west or north, DD would have received some Appalachian zircons. Therefore, a transport direction to the north or the northwest is consistent with a Suwannee sourced Norphlet erg in DD (Lovell and Weislogel, 2010). If the erg in DC is migrating to the NW as Douglas (2010) interprets, then the southern EGOM is likely characterized by a similar northern transit direction in DD and DC. Northward or northwestward migration and the presence of Norphlet equivalent eolian deposits to the south in the Yucatan (Guzman-Vega and Mello, 1999; Rosenfeld, 2002) would allow for potential eolian transport from the Yucatan into the southern portions of the EGOM. If the GOM was in fact very dry and LL 399 is a location of oceanic crust (Figures 7 and 32) that is younger than the Norphlet Formation, then sediment in the LL, DC and MC areas may have some Yucatan derived sediment. If there is no Yucatan input, the NW transport direction would limit the extent of the Norphlet to the far south and may cause a narrow band of Norphlet deposition immediately south of MGA as sediment shed migrates toward western DC instead of building southward like in Alabama.

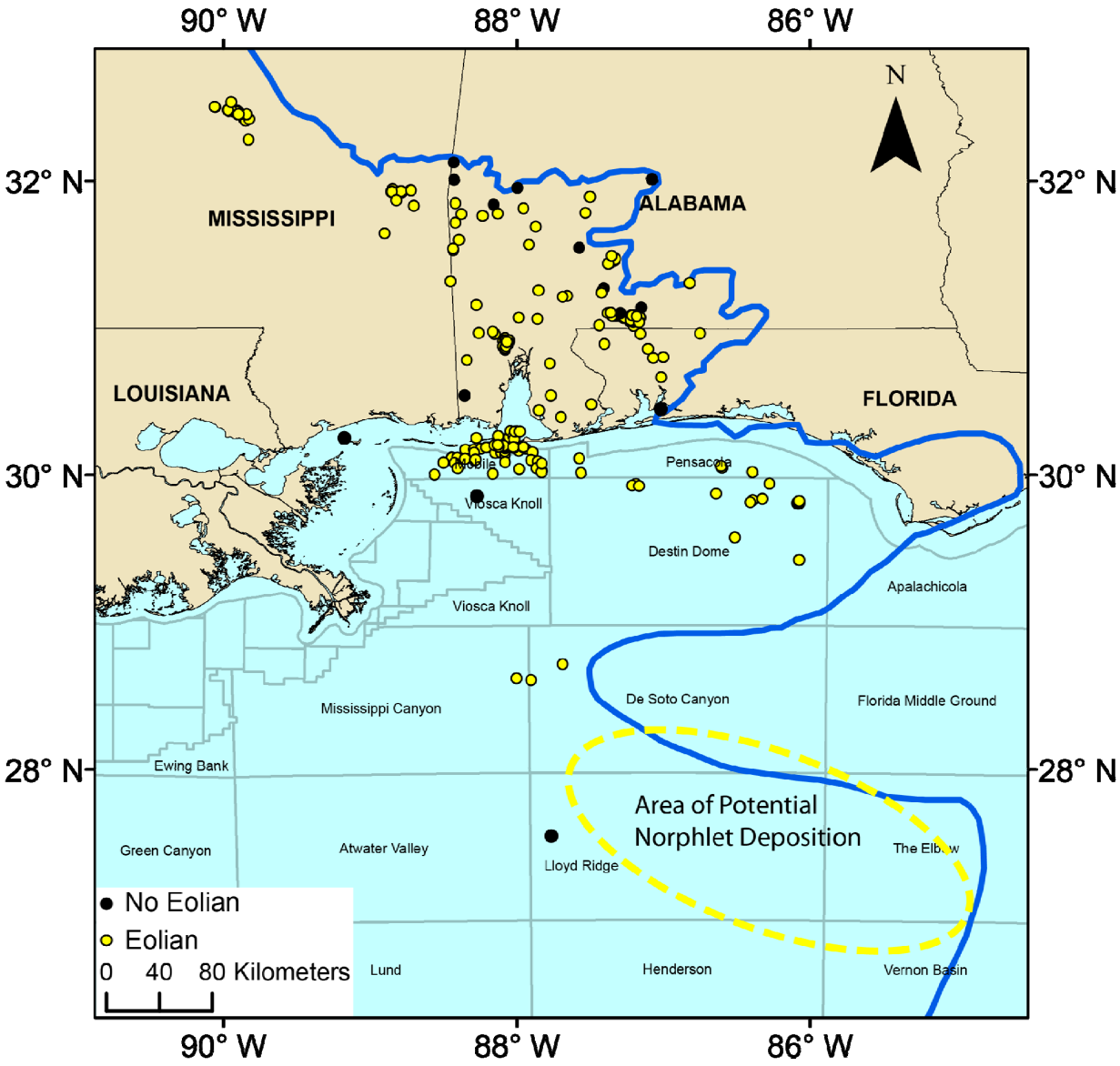

Figure 50: Wells containing eolian deposits. Yellow circle indicates area of potential Norphlet deposition south of the MGA.

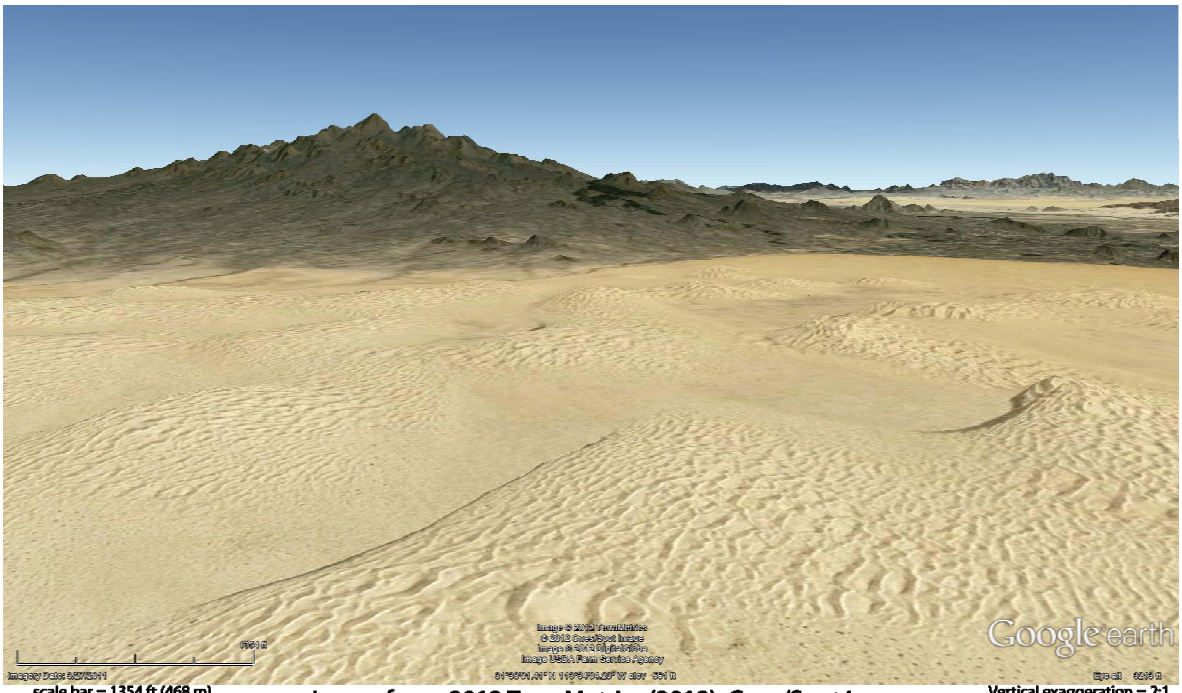

Figure 51: Google Earth 3D image of dunes migrating onto base of slope of a local high in Gran Desierto, Mexico. Eolian deposits near the updip limit of the Norphlet in the TE may have a similar relationship where dunes nearly reach exposed basement on the slopes.

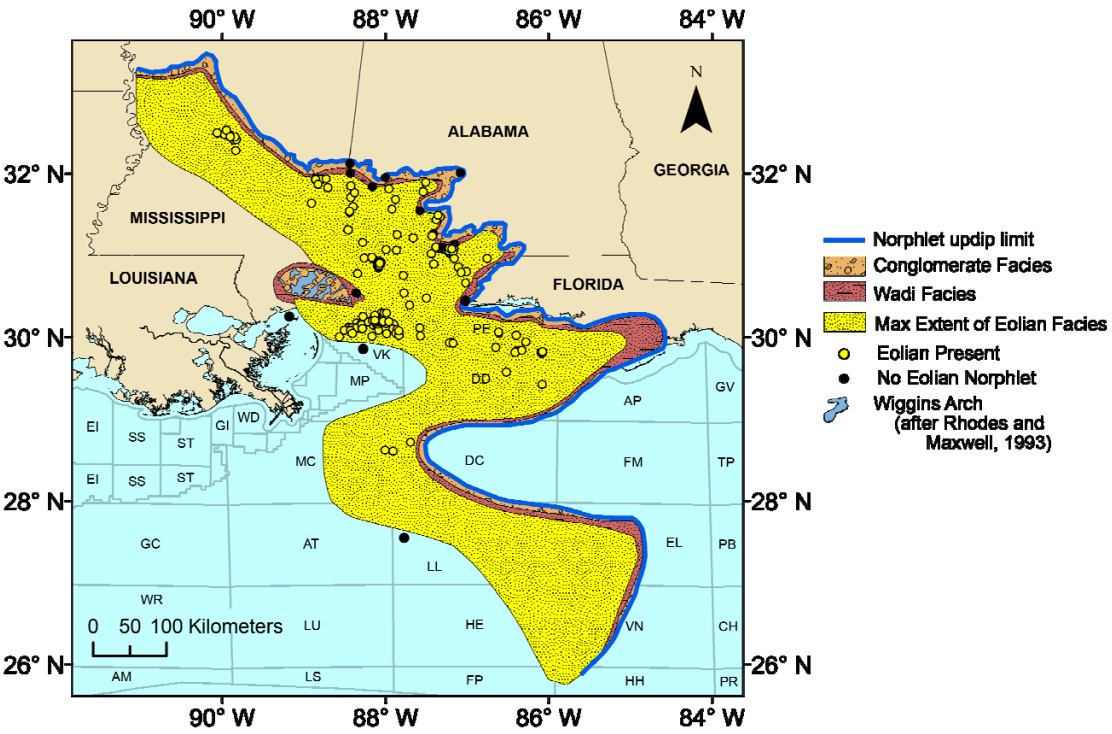

Figure 52: Interpreted maximum extent of Norphlet eolian facies.

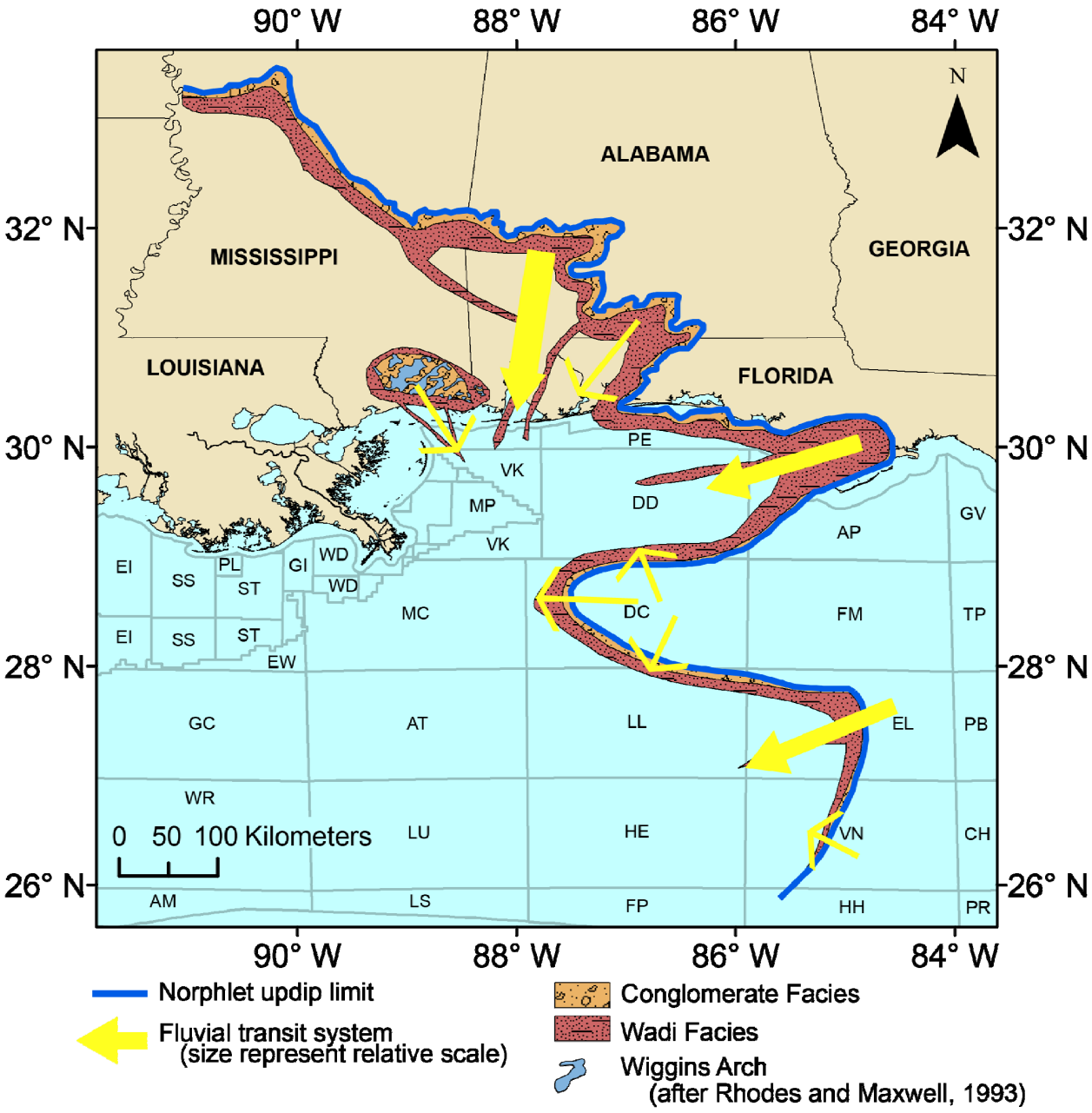

Figure 53: Waterborne sediment transport systems in the Gulf of Mexico. These systems were likely the primary drivers of Norphlet provenance patterns in the EGOM. Wadi and alluvial facies systems flowed off of the highs bringing sediments into the basins which were then reworked by winds into dunes with regionally distinct provenances. These systems also enable prediction of the full extent of the Norphlet in the offshore by highlighting source areas.

6.3 Tectonic Influences

Analysis of the provenance and transport system of the Norphlet Formation shows that basins as sediment funnels is an important aspect of Norphlet distribution. The gradient between the paleoflows and the adjacent highs affects their potential as sediment sources. MGA is a major source for the sand in the offshore as it is onlapped by the Norphlet, Smackover, and the lower section of the Haynesville formations (Figure 23). The obvious erosion on MGA as well as a small graben in the middle of the arch likely funneled sediment from the arch into the Norphlet erg (Figure 25).

MacRae and Watkins (1993) interpret two areas where subsalt reflectors dipped toward each other in the DCSB, which is consistent with the interpretation of Dobson and Buffler (1991) of a syncline with a NW trending axis. In other parts of the DCSB, both studies noted a significant number of subsalt reflectors with apparent dips to the SW (Figure 45). These same reflectors are present on the seismic data but extend farther SW than previously interpreted (Figures 27 and 45). These dipping structures form a series of half grabens roughly perpendicular to the NW trending syncline axis interpreted by Dobson and Buffler (1991). The fill in these grabens is Triassic in age, revealed by drilling in the adjacent South Georgia Graben system (McBride et al., 1987b; Scott, 1991). While the seismic grid in this area is not sufficient to resolve the development of the DCSB, Figure 55 shows a schematic development of one of these half grabens through Oxfordian time. Two major stages of pre-salt extension are followed by a minor later stage of extension, offsetting the base of salt (Figure 55 B-D). The faults cutting the base of the salt do not appear to affect the stratigraphy overlying the salt, and thus formed before or during Callovian time (Figure 55 E). If these faults had even minor offset after Callovian time, the faults would have altered the topography and focused the wadis entering the

GOM (e.g. Permian Upper Rotliegend; Sweet, 1999). During Oxfordian time, minor growth faulting occurred during Smackover deposition and large Norphlet dunes sank into the salt (Figure 55 F; Martens, 1993). The Destin Dome salt anticline developed from sediment loading during Lower Cretaceous through Early Cenozoic time (MacRae and Watkins, 1992).

Norphlet deposition ended with the transgression of a sea over the Norphlet Formation preserving eolian topography of up to 600 ft (183 m) mapped on seismic data at this contact in DD and south of Mobile Bay in the offshore (Martens, 1993; Story, 1998; Ajdukiewicz et al., 2010). To preserve hundreds of feet of Norphlet topography, a low energy, geologically instantaneous, high amplitude,flooding of the dunes must occur (Ahmed Benan and Kocurek, 2000).. While it is not necessary to flood the entire dune (Ahmed Benan and Kocurek, 2000), it would still be beyond the scale of tectonic subsidence or eustatic sea level rise. The lack of bioturbation and thin reworked marine section also supports the concept of a flood, as does the relatively sharp transition from eolian Norphlet sands to Smackover mudstone (Mancini et al., 1985; Markham, 1991). Examples of preserved eolian topography in such a system include: the Entrada Formation being flooded catastrophically in the Todilto Basin (Ahmed Benan and Kocurek, 2000), catastrophic flooding of the Upper Rotliegend by the Zechstein Sea preserved up to 280 ft (85 m) of eolian topography (Strombach and Howell, 2002), and Etendeka flood basalts preserving dunes of the Cretaceous Etjo Formation (Mountney et al., 1999).

In order for a flood of such high amplitude to occur, it would require the GOM to be completely cut off from marine influences similar to how the Entrada and Upper Rotliegend formations were prior to flooding. Data from the Deep Sea Drilling Program Leg 77 show that the Caribbean was an open marine environment by Oxfordian time (Schlager et al., 1984; Pindell, 1985). If the Caribbean was open marine, the Smackover flood may have been a

catastrophic flood as the Caribbean/Atlantic Ocean first entered into the GOM. Oxfordian aged ammonites in the Mexican western GOM correlate with those in Cuba and the North Atlantic (Angeles-Aquino and Cantú-Chapa, 2002), and Western Cuba has some Oxfordian aged ammonites in common with the Smackover Formation (Myczynski, 1994). While these reports support the concept of an Atlantic flood of the GOM, Salvador (1991) reports that ammonites from the Oxfordian GOM are more consistent with Pacific assemblages. The origin of the GOM flood may be uncertain, but the preservation of Norphlet topography in DD and Mobile Bay requires that at least the initial Smackover flood be geologically instantaneous. Because the literature does not have reports of preserved dune topography in updip Norphlet regions, it is possible that once the water in the GOM rose to a level high enough to preserve the dunes in DD and MO it continued transgressing at a rate more consistent with tectonic and eustatic processes.

If the GOM was cut off from the oceans during the deposition of the Norphlet, then there could be no marine equivalent Norphlet. If present, the down dip equivalent may be lithologically similar to Norphlet deposits in south Texas characterized by grey shale, fine-grained micaceous sandstone and red sandy shale (Budd and Louck, 1981). These sediment starved areas are distal from source terranes, and are interpreted wadi, coastal plain, and tidal flat deposits. If the down dip areas were filled with water, they may contain Louann type evaporites or the lacustrine style deposits described by Godo et al. (2011) in the Vicksburg well in western DC. This environment would make the GOM during Oxfordian time like a larger, more symmetrical version of the Simpson Desert where the lowest portions of the basin are filled by the ephemeral Lake Eyre whose depositional facies, while varied, are similar to those seen in the non-eolian down dip Norphlet deposits (Magee et al., 1995; Alley, 1998).

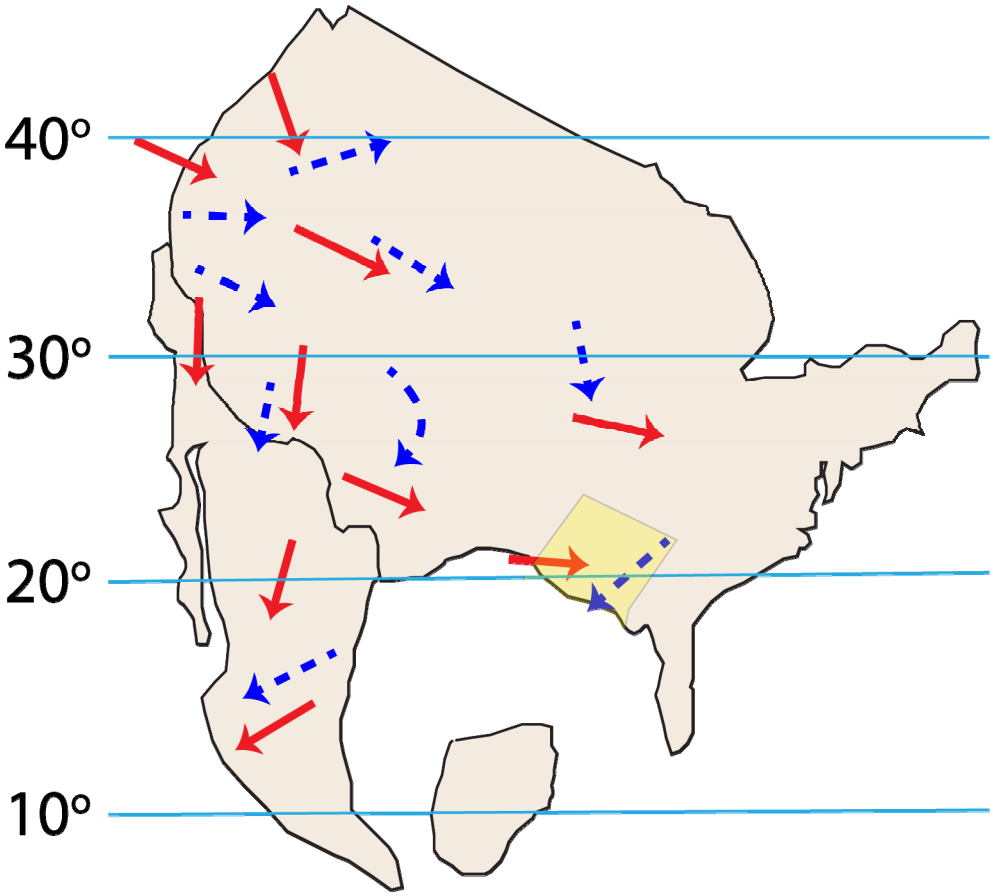

Figure 54: Late Cretaceous (Tithonian) Winds (after Parrish and Peterson, 1988). The red solid lines are prevailing winds and blue dashed lines are winter winds. The prevailing winds in the area of interest (yellow box) are to the present day east/northeast while the winter winds are to the present south.

Figure 55: Half graben schematic evolution. (next page)
A: E-W seismic line through Destin Dome showing the dipping subsalt reflectors. For interpreted line, see appendix 3.
B: Basement is pre-Mesozoic.
C: An initial stage of half graben formation occurred during Early Triassic (?) time. The fill of these basins is likely the Eagle Mills Formation (Scott, 1991; McBride et al., 1987b) with the dipping beds faulted antithetic to the main fault.
D: During Late Triassic (?) time, a later period of extension further rotated the subsalt reflections. Clastic or volcanic rocks with gradually flatter dips filled in the accommodation space as the period of primary extension drew to a close.
E: During Callovian time, deposition of the Louann Salt (pink) occurred and a final period of minor extension created faults which offset the base of salt.
F: The Norphlet and Smackover (Oxfordian) Formations were deposited post extension, but early salt tectonics caused displacement of Norphlet dunes and growth sections in the Smackover Formation.

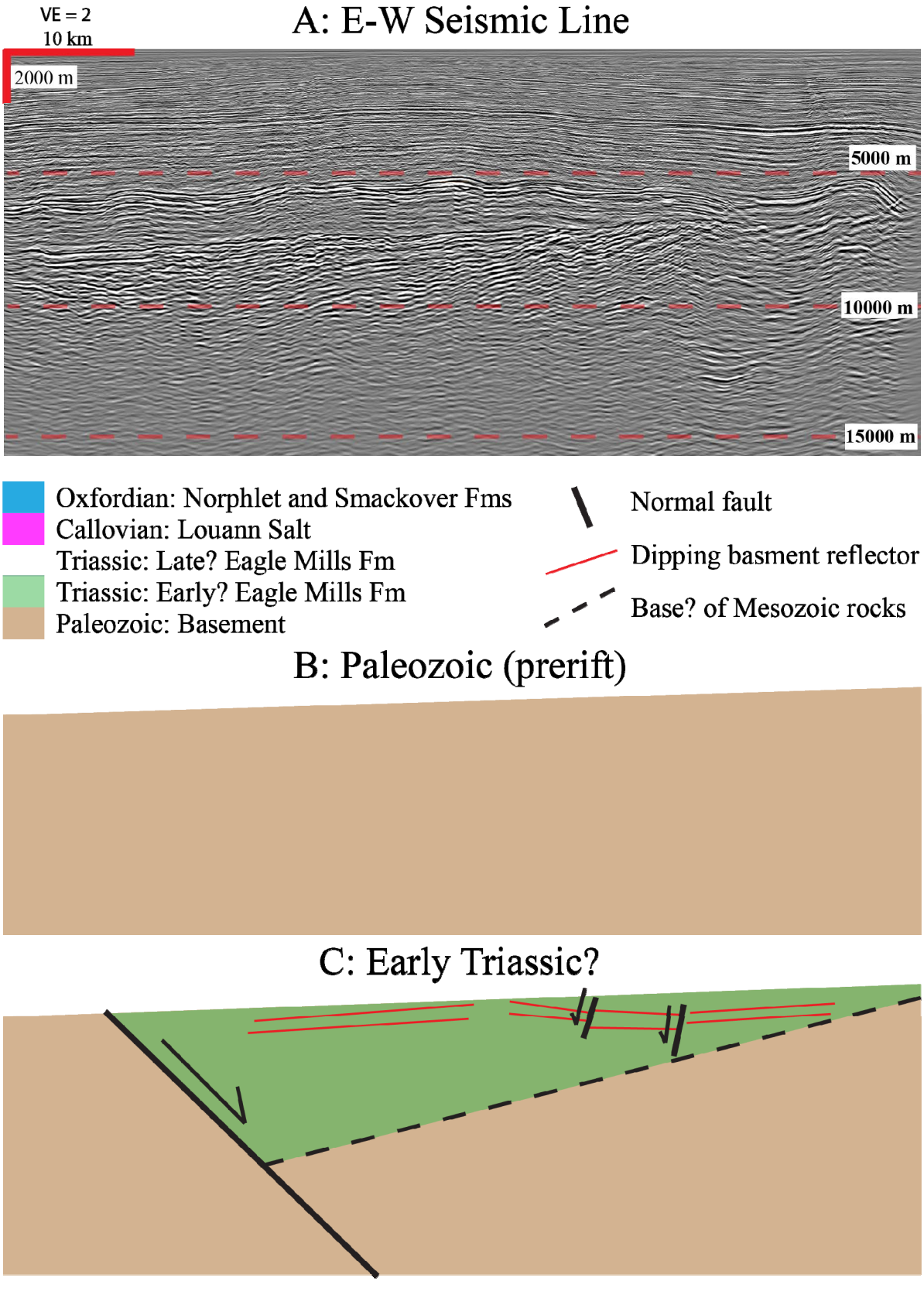
A: E-W Seismic Line
VE = 2
10 km
2000 m
5000 m
10000 m
15000 m
Oxfordian: Norphlet and Smackover Fms
Callovian: Louann Salt
Triassic: Late? Eagle Mills Fm
Triassic: Early? Eagle Mills Fm
Paleozoic: Basement
Normal fault
Dipping basment reflector
Base? of Mesozoic rocks
B: Paleozoic (prerift)
C: Early Triassic?

D: Late Triassic?

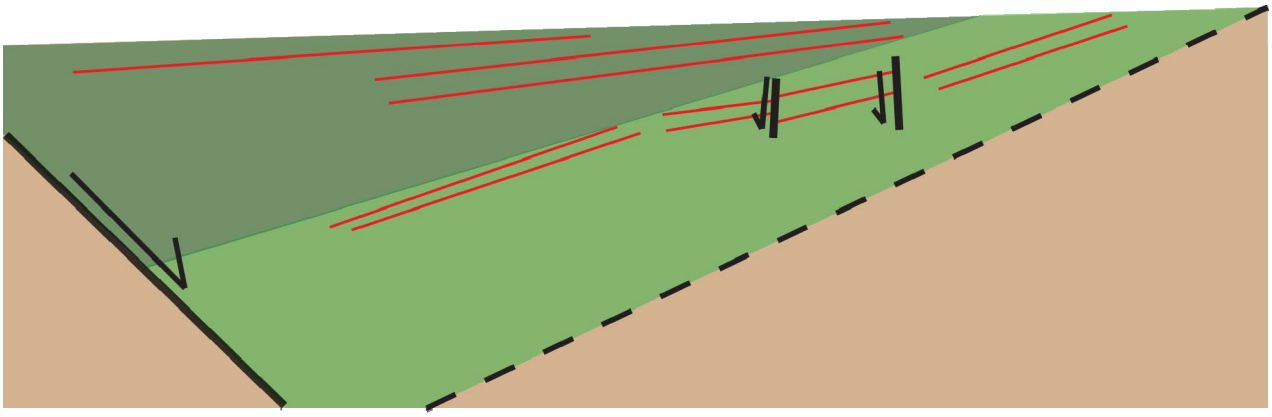

E: Middle Jurassic (Callovian)

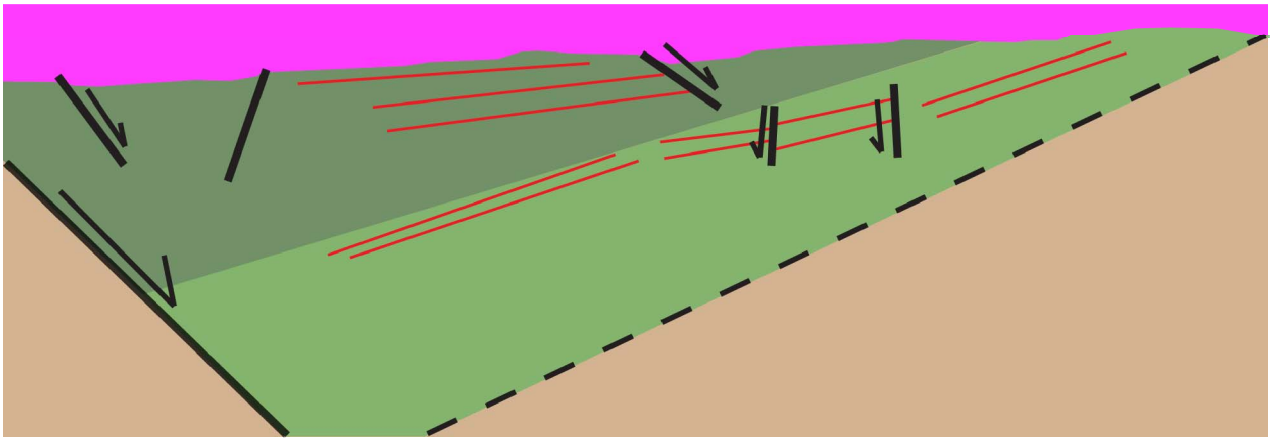

F: Middle Jurassic (Oxfordian)

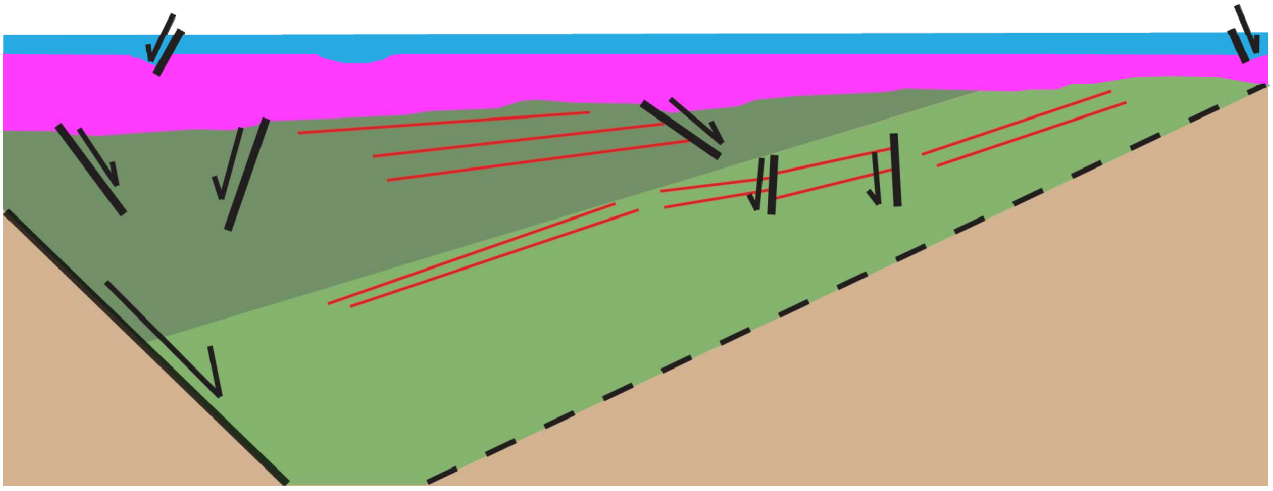

7. CONCLUSIONS

1. The Norphlet Formation has significant wadi facies in the up dip regions with decreasing fluvial influence down depositional dip. These waterborne transit systems are controlled by local structural highs and lows that determine the sediment distribution.

2. Mesozoic aged graben systems compartmentalized the sediment delivery systems for the Norphlet Formation and thus, parts of the Norphlet Formation are sourced from different terranes. The wadi systems into these grabens and eolian transport directions within them support the provenance trends derived from Norphlet detrital zircons.

3. Paleotransport directions calculated from dipmeters show that eolian transport directions are southward in onshore Alabama and southeastward in offshore Alabama. In DD and PE, eolian transport directions are northward to northwestward.

3. Haynesville detrital zircons indicate that sediment distribution patterns were persistent through Late Jurassic time and indicate that the main controlling factor for Norphlet provenance was the wadi systems because the wind driven Norphlet provenance trends could not be matched by waterborne Haynesville deposits.

4. The presence of multiple sediment delivery systems in the areas of previous Norphlet exploration implies that the areas south of Destin Dome will also have unique delivery systems, which extends the Norphlet depositional trend south and into the Tampa Embayment.

5. Seismic reflection data show that the Norphlet Formation onlaps the Middle Ground Arch and contemporaneous erosive surfaces on the arch imply that it was a sediment source for Norphlet deposition in the deep water.

6. The Norphlet Formation, including eolian facies, was pervasive in the Eastern Gulf of Mexico. Seismic reflections similar to those representing the Norphlet, in areas of confirmed Norphlet presence, off the coasts of Alabama and Florida as well as the deep water west of the Middle Ground Arch, are present south of the Middle Ground Arch indicating Norphlet presence is extensive.

7. Preserved eolian topography in geographically distinct locations along with facies distribution trends indicate the Smackover flood may have been a rapid oceanic incursion into a previously close and largely dry basin.

References

Ahmed Benan, C. A. and G. Kocurek, 2000, Catastrophic flooding of an aeolian dune field: Jurassic Entrada and Todilto Formations, Ghost Ranch, New Mexico, USA, Sedimentology, vol. 47, no. 6, p. 1069-1080.

Ajdukiewicz, J., P. Nicholson, and W. Esch, 2010, Prediction of deep reservoir quality using early diagenetic process models in the Jurassic Norphlet Formation, Gulf of Mexico, AAPG Bulletin, vol. 94, no. 8, p. 1189-1227.

Alley, N. F., 1998, Cainozoic stratigraphy, palaeoenvironments and geological evolution of the Lake Eyre Basin, Palaeogeography, Palaeoclimatology, Palaeoecology, vol. 144, no. 3, p. 239-263.

Angeles-Aquino, F. and A. Cantú-Chapa, 2001, Subsurface Upper Jurassic Stratigraphy in the Campeche Shelf, Gulf of Mexico, *in* C. Bartolini, R. T. Buffler, A. Cantú-Chapa, eds., Western Gulf of Mexico Basin: Tectonics, Sedimentary Basins, and Petroleum Systems: AAPG Memoirs, p. 343-352.

Badon, C., 1975, Stratigraphy and Petrology of Jurassic Norphlet Formation, Clarke County, Mississippi, AAPG Bulletin, vol. 59, no. 3, p. 377-392.

Bearden, B. L., 1987, Seismic expression of structural style and hydrocarbon traps in the Norphlet Formation, offshore Alabama: State Oil and Gas Board of Alabama Oil and Gas Report 14, 28 p.

Bird, D. E., K. Burke, S. A. Hall, and J. F. Casey, 2005, Gulf of Mexico tectonic history: Hotspot tracks, crustal boundaries, and early salt distribution, AAPG Bulletin, vol. 89, no. 3, p. 311-328.

Bishop, W. F., 1967, Age of Pre-Smackover Formations, North Louisiana and South Arkansas: GEOLOGICAL NOTES, AAPG Bulletin, vol. 51, p. 244-249.

Black, L., S. Kamo, C. Allen, D. Davis, J. Aleinikoff, J. Valley. R., Mundil, I. Campbell, R. Korsch, I. Williams, and C. Foudoulis, 2004, Improved 206Pb/238U microprobe geochronology by the monitoring of a trace‐element‐related matrix effect; SHRIMP, 8 ID–TIMS, ELA–ICP–MS and oxygen isotope documentation for a series of zirconstandards: Chemical Geology, vol. 205, p. 115-140.

Bureau of Ocean Energy Management, Regulation and Enforcement, 2010, Eastern Gulf of Mexico Milestones,

<http://www.gomr.boemre.gov/homepg/offshore/egom/egomfax.html>, Accessed June, 28, 2011.

Budd, D. and R. Loucks, 1981, Smackover and lower Buckner formations, south Texas: depositional systems on a Jurassic carbonate ramp: Texas Bureau of Economic Geology, Report of Investigations, vol. 112, p. 38.

Craddock, R. A., M. Hutchinson, and J. Stein, 2010, Topographic data reveal a buried fluvial landscape in the Simpson Desert, Australia, Australian Journal of Earth Sciences, vol. 57, no. 1, p. 141-149.

Curray, J. R., 1956, The analysis of two-dimensional orientation data, The Journal of Geology, vol. 64, no. 2, p. 117-131.

Dickinson, W. R. and G. E. Gehrels, 2008, U-Pb ages of detrital zircons in relation to paleogeography: Triassic paleodrainage networks and sediment dispersal across southwest Laurentia, Journal of Sedimentary Research, vol. 78, no. 12, p. 745-764.

Dixon, S., D. Summers, and R. Surdam, 1989, Diagenesis and preservation of porosity in Norphlet Formation (Upper Jurassic), southern Alabama, AAPG Bulletin, vol. 73, no. 6, p. 707-728.

Dobson, L. M. and R. T. Buffler, 1991, Basement rocks and structure, northeast Gulf of Mexico, Gulf Coast Association of Geological Societies Transactions, vol. 41, p. 191-206.

Douglas, S. W., 2010, The Jurassic Norphlet Formation of the deep-water Eastern Gulf of Mexico: a sedimentologic investigation of aeolian facies, their reservoir characteristics, and their depositional history (abs.), Master's thesis, Baylor University, Waco, Texas.

Ewing, T. E., 2001, Review of Late Jurassic Depositional Systems and Potential Hydrocarbon Plays, Northern Gulf of Mexico Basin, Gulf Coast Association of Geological Societies Transactions, vol. 51, p. 85-96.

Fedo, C. M., K. N. Sircombe, and R. H. Rainbird, 2003, Detrital zircon analysis of the sedimentary record, Reviews in Mineralogy and Geochemistry, vol. 53, no. 1, p. 277-303.

Fryberger, S. G. and G. Dean, 1979, Dune forms and wind regime, *in* McKee, E. D., ed, A study of global sand seas: Geological Survey Professional Paper 1052, Washington, D. C., U.S. Government Printing Office, p. 137-169.

Gehrels, G.E., V. Valencia, and J. Ruiz, 2008, Enhanced precision, accuracy, efficiency, and spatial resolution of U‐Pb ages by laser ablation–multicollector–inductively coupled 17, plasma–mass spectrometry: Geochemistry, Geophysics, Geosystems, vol. 9, Q03017, doi:10.1029/2007GC001805.

Gehrels, G. 2010, U-Th-Pb analytical methods (Arizona LaserChron Center, University of Arizona), < https://sites.google.com/a/laserchron.org/laserchron/home>

Gehrels, G. 2010, U-Th-Pb analytical methods for Zircon (Arizona LaserChron Center, University of Arizona), < https://sites.google.com/a/laserchron.org/laserchron/home>

Glennie, K. W., 1972, Permian Rotliegendes of northwest Europe interpreted in light of modern desert sedimentation studies, AAPG Bulletin, vol. 56, no. 6, p. 1048-1071.

Godo, T. J., J. Grimbergen, T. Walker, J. Wagner, S. Gabay, and L. Gaarenstroom, 2006, Norphlet Aeolian dunes in the deepwater Gulf of Mexico (abs.), AAPG Search and Discovery Article #90052, <http://www.searchanddiscovery.com/documents/2006/06088houston_abs/abstracts/godo.htm?q=%2BtitleStrip%3Anorphlet>, Accessed April 5, 2012.

Godo, T. J., E. Chuparova, and D. E. McKinney, 2011, Norphlet aeolian sand fairway established in the deep water Gulf of Mexico (abs.), AAPG Search and Discovery Article #90124, <http://www.searchanddiscovery.com/abstracts/html/2011/annual/abstracts/Godo.html?q=%2BtextStrip%3Anorphlet+%2ByearSort%3A[2010+TO+2011]>, Accessed April 5, 2012.

Goetz, J., 1966, Applications of the Continuous Dipmeter in Western Canada, Journal of Canadian Petroleum Technology, vol. 5, no. 1, p. 24-28.

Gupta, R. and H. D. Johnson, 2001, Characterization of heterolithic deposits using electrofacies analysis in the tide-dominated Lower Jurassic Cook Formation (Gullfaks Field, offshore Norway), Petroleum Geoscience, vol. 7, no. 3, p. 321-330.

Guzman-Vega, M. and M. Mello, 1999, Origin of oil in the Sureste Basin, Mexico, AAPG Bulletin, vol. 83, p. 1068-1095.

Hall, S. A. and I. J. Najmuddin, 1994, Constraints on the tectonic development of the eastern Gulf of Mexico provided by magnetic anomaly data, Journal of Geophysical Research, vol. 99, no. B4, p. 7161-7175.

Halverson, J. R., 1988, The Seismic Expression Of The Jurassic Norphlet Pinchout, Wiggins Arch, Southwest Alabama, USA, Offshore Technology Conference, vol. 20, p. 301-306.

Hartwick, E. E., 2010, Eolian Architecture of Sandstone Reservoirs in the Covenant Field, Sevier County, Utah, AAPG Search and Discovery Article #20091, <http://www.searchanddiscovery.com/documents/2010/20091hartwick/ndx_hartwick.pdf>, Accessed January 17, 2011.

Hoar, R., C. Taylor, K. Story, E. Weise, C. Sharp, and W. Von Herneberg, 1990, Origin and Exploration Significance of Lensing in the Norphlet Formation, Offshore Mafla (abs.), AAPG Search and Discovery Article #91003, <http://www.searchanddiscovery.com/abstracts/html/1990/annual/abstracts/0676a.htm>, Accessed April 5, 2012.

Hocker, C., K. Eastwood, J. Herweijer, and J. Adams, 1990, Use of dipmeter data in clastic sedimentological studies, AAPG Bulletin, vol. 74, no. 2, p. 105-118.

Kocurek, G., 1981, Significance of interdune deposits and bounding surfaces in aeolian dune sands, Sedimentology, vol. 28, no. 6, p. 753-780.

Kocurek, G. and N. Lancaster, 1999, Aeolian system sediment state: theory and Mojave Desert Kelso dune field example, Sedimentology, vol. 46, no. 3, p. 505-515.

Kocurek, G., N. Robinson, and J. Sharp, 2001, The response of the water table in coastal aeolian systems to changes in sea level, Sedimentary Geology, vol. 139, no. 1, p. 1-13.

Lovell, T. and A. Weislogel, 2010, Detrital Zircon U-Pb Age Constraints on the Provenance of the Upper Jurassic Norphlet Formation, Eastern Gulf of Mexico: Implications for Paleogeography, Gulf Coast Association of Geological Societies Transactions, vol. 60, p. 443-460.

Ludwig, K., 2008. Isoplot 3.70, a Geochronological Toolkit for Microsoft Excel: Berkeley Geochronology Center Special Publication 4, Rev. August, 26, p. 77.

MacRae, G. and J. S. Watkins, 1992, Evolution of the Destin Dome, offshore Florida, north-eastern Gulf of Mexico, Marine and Petroleum Geology, vol. 9, no. 5, p. 501--509.

MacRae, G. and J. S. Watkins, 1993, Basin architecture, salt tectonics, and Upper Jurassic structural styles, DeSoto Canyon salt basin, northeastern Gulf of Mexico, AAPG Bulletin, vol. 77, p. 1809-1824.

MacRae, G. and J. Watkins, 1996, Desoto Canyon Salt Basin: tectonic evolution and salt structural styles, Structural framework of the northern Gulf of Mexico: Gulf Coast Association of Geological Societies Special Publication, p. 53-61.

Magee, J., J. Bowler, G. Miller, and D. Williams, 1995, Stratigraphy, sedimentology, chronology and palaeohydrology of Quaternary lacustrine deposits at Madigan Gulf, Lake Eyre, South Australia, Palaeogeography, Palaeoclimatology, Palaeoecology, vol. 113, no. 1, p. 3-42.

Mancini, E. A., R. M. Mink, and B. L. Bearden, 1984, Paleoenvironments and Hydrocarbon Potential of the Upper Jurassic Norphlet Formation of Southwestern and Offshore Alabama, Gulf Coast Association of Geological Societies Transaction, vol. 34 p. 131-135.

Mancini, E. A., T. M. Puckett, W. C. Purcell, B. J. Panetta, 1999, Basin analysis of the Mississippi interior salt basin and petroleum system modeling of the Jurassic Smackover Formation, eastern gulf coastal plain: Topical Reports 1 and 2, Center for Sedimentary Basin Studies, University of Alabama, for U.S. D.O.E., 344p.

Mancini, E. A., R. M. Mink, B. L. Bearden, and R. P. Wilkerson, 1985, Norphlet Formation (Upper Jurassic) of southwestern and offshore Alabama: environments of deposition and petroleum geology, AAPG Bulletin, vol. 69, no. 6, p. 881-898.

Mancini, E. A., Badali, M., Puckett, T. M., Parcell, W. C., and J. C. Llinas, 2001, Mesozoic carbonate petroleum systems in the northeastern Gulf of Mexico: GCSSEPM Foundation 21st Annual Research Conference Proceedings, p. 423-451.

Markham, D. B., 1991, Depositional and diagenetic controls on porosity distribution and development, Norphlet formation, offshore Alabama region, Master's thesis, The University of Alabama, Tuscaloosa, Alabama, 290.

Martens, D. O., 1993, Stratigraphic study of an upper Jurassic Norphlet sand sea in Pensacola and Destin Dome Areas, offshore Florida, Master's thesis, University of Houston, Houston, Texas, 114 p.

Marton G., R. T. Buffler, 1993, Application of simple-shear model to the evolution of passive continental margins of the Gulf of Mexico basin, Geology, vol. 21, no. 6, p. 495-498.

Marton, G. and R. T. Buffler, 1994, Jurassic reconstruction of the Gulf of Mexico Basin, International Geology Review, vol. 36, no. 6, p. 545-586.

Marton, G. L. and R. T. Buffler, 1999, Jurassic—Early Cretaceous tectono-paleogeographic evolution of the southeastern gulf of Mexico basin, Sedimentary Basins of the World, vol. 4, p. 63-91.

Marzano, M. S., G. M. Pense, and P. Andronaco, 1988, A comparison of the Jurassic Norphlet Formation in Mary Ann field, Mobile Bay, Alabama to onshore regional Norphlet trends, Gulf Coast Association of Geological Societies Transactions, vol. 38, p. 85-100.

McBride, E. F., L. Land, and L. Mack, 1987, Diagenesis of eolian and fluvial feldspathic sandstones, Norphlet Formation (Upper Jurassic), Rankin County, Mississippi, and Mobile County, Alabama, American Association of Petroleum Geologists Bulletin, vol. 71, p. 1019-1034.

McBride, J., K. Nelson, and L. Brown, 1987, Early Mesozoic basin structure and tectonics of the Southeastern United States as revealed from COCORP reflection data and the relation to Atlantic rifting, Canadian Society of Petroleum Geologists, Memoir, vol. 12, p. 173-184.

Miller, J. A., 1982, Structural control of Jurassic sedimentation in Alabama and Florida, AAPG Bulletin, vol. 66, no. 9, p. 1289-1301.

Mink, R. M., B. L. Bearden, and E. A. Mancini, 1988, Regional geologic framework of the Norphlet Formation of the onshore and offshore Mississippi, Alabama, and Florida area, OCEANS '88. 'A Partnership of Marine Interests'. Proceedings, p. 762-767.

Montgomery, S., T. H. Walker, G. P. Wahlman, R. C. Tobin, and D. Ziegler, 1999, Upper Jurassic" Reef' Play, East Texas Basin: An Updated Overview: Part 1-Background and Outboard Trend, AAPG Bulletin, vol. 83, p. 707-726.

Mountney, N., J. Howell, S. Flint, and D. Jerram, 1999, Relating eolian bounding-surface geometries to the bed forms that generated them: Etjo Formation, Cretaceous, Namibia, Geology, vol. 27, no. 2, p. 159-162.

Myczynski, R., 1994, Caribbean ammonite assemblages from Upper Jurassic–Lower Cretaceous sequences of Cuba, Studia Geologica Polonica, vol. 105, p. 91-108.

Nagihara, S. and K. O. Jones, 2005, Geothermal heat flow in the northeast margin of the Gulf of Mexico, AAPG Bulletin, vol. 89, no. 6, p. 821-831.

Nurmi, R., 1985, Eolian Sandstone Reservoirs: Bedding Facies and Production Geology Modeling, Society of Petroleum Engineers Annual Technical Conference and Exhibition, vol. 60, 8 p.

Obid, J. A., 2006, Sequence and seismic stratigraphy of the Jurassic strata in northeastern Gulf of Mexico, PhD dissertation, The University of Alabama, Tuscaloosa, Alabama, 253 p.

Odum, M., 2010, Royal Dutch Shell PLC North America Investor Visit: Upstream Americas: profitable growth in Shell heartland, < http://www-static.shell.com/static/investor/downloads/presentations/2010/na_visit/marvin_odum_na_visit_presentation_28092010.pdf >, Accessed October 10, 2011.

Ogg, G., 2010, International stratigraphic chart, International Commission on Stratigraphy, 1 p.

Opdyke, N. D. and S. Runcorn, 1960, Wind direction in the western United States in the late Paleozoic, Geological Society of America Bulletin, vol. 71, no. 7, p. 959-972. Parrish, J. T. and F. Peterson, 1988, Wind directions predicted from global circulation models and wind directions determined from eolian sandstones of the western United States—A comparison, Sedimentary Geology, vol. 56, no. 1, p. 261-282.

Parrish, J.T., and F. Peterson, 1988, Wind directions predicted from global circulation models and wind directions determined from eolian sandstones of the western United States – a comparison, Sedimentary Geology, vol. 56, p. 261-282.

Pepper, F., 1982, Depositional Environments of the Norphlet Formation (Jurassic) for Southwestern Alambama (abs.), Gulf Coast Association of Geological Societies Transactions, vol. 32, p. 17.

Peterson, F., 1988, Pennsylvanian to Jurassic eolian transportation systems in the western United States, Sedimentary Geology, vol. 56, no. 1-4, p. 207-260.

Petty, A. J., S. Thieling, and T. Friedmann, 1994, Mesozoic Stratigraphy of Near Shelf-Edge Deposits, Southern Mississippi, Adjacent State and Federal Waters (abs.), Gulf Coast Association of Geological Societies Transactions, vol. 44, p. 583.

Pindell, J. L., 1985, Alleghenian reconstruction and subsequent evolution of the Gulf of Mexico, Bahamas, and Proto-Caribbean, Tectonics, vol. 4, no. 1, p. 1-39.Pindell, J. L. and L. Kennan, 2009, Tectonic evolution of the Gulf of Mexico, Caribbean and northern South America in the mantle reference frame: an update, Geological Society, London, Special Publications, vol. 328, no. 1, p. 1-55.

Pindell, J. L. and L. Kennan, 2009, Tectonic evolution of the Gulf of Mexico, Caribbean and northern South America in the mantle reference frame: an update, Geological Society, London, Special Publications, vol. 328, no. 1, p. 1-55.

Pindell, J. and L. Kennan, 2001, Kinematic evolution of the Gulf of Mexico and Caribbean, Gulf Coast Section SEPM Transaction, vol. 21, p. 193-220.

Reiche, P., 1938, An analysis of cross-lamination the Coconino Sandstone, The Journal of geology, p. 905-932.

Rhodes, J. A. and G. B. Maxwell, 1993, Jurassic stratigraphy of the Wiggins arch, Mississippi, Gulf Coast Association of Geological Societies Transactions, vol. 43, p. 333-344.

Ridgway, J. G., 2010, Upper Jurassic (Oxfordian) Smackover Facies characterization at Little Cedar Creek Field, Conecuh County, Alabama, Master's thesis, The University of Alabama, Tuscaloosa, Alabama, 128 p.

Rosenfeld, J., 2002, El potencial económico del Bloque de Yucatán en México, Guatemala y Belice, Boletín de la Sociedad Geológica Mexicana, vol. 55, no. 1, p. 30-37.

Salvador, A., 1991, Origin and development of the Gulf of Mexico basin, *in* A. Salvador (ed.), The Gulf of Mexico Basin: The geology of North America, vol. 71, p. 389–443.

Schlager, W., R. T. Buffler, D. Angstadt, J. A. Y. L. Bowdler, P. H. Cotillon, R. D. Dallmeyer, R. B. Halley, H. Kinoshita, L. B. Magoon III, and C. L. McNulty, 1984, Deep sea drilling project, leg 77, southeastern Gulf of Mexico, Geological Society of America Bulletin, vol. 95, no. 2, p. 226-236.

Scott, G. W., 1991, Petrology and provenance of the Norphlet Formation, Panhandle, Florida, Florida Geological Survey Information Circular no. 107, p. 83-120.

Sneh, A., 1983, Desert stream sequences in the Sinai Peninsula, Journal of Sedimentary Research, vol. 53, no. 4, p. 1271-1279.

Stinco, L. P., 2006, Core and log data integration; the key for determining electrofacies, Society of Petrophysicists and Well Log Analysists Symposium Transactions, vol. 47, p. 149-155.

Story, C., 1998, Norphlet geology and 3-D geophysics: Fairway Field, Mobile Bay, Alabama, The Leading Edge, vol. 17, p. 243-248.

Strömbäck, A. C. and J. A. Howell, 2002, Predicting distribution of remobilized aeolian facies using sub-surface data: the Weissliegend of the UK Southern North Sea, Petroleum Geoscience, vol. 8, no. 3, p. 237-249.

Svendsen, J., H. Stollhofen, C. B. E. Krapf, and I. G. Stanistreet, 2003, Mass and hyperconcentrated flow deposits record dune damming and catastrophic breakthrough of ephemeral rivers, Skeleton Coast Erg, Namibia, Sedimentary Geology, vol. 160, no. 1-3, p. 7-31.

Sweet, M., 1999, Interaction between aeolian, fluvial and playa environments in the Permian Upper Rotliegend Group, UK southern North Sea, Sedimentology, vol. 46, no. 1, p. 171-188.

Tew, B. H., R. M. Mink, S. D. Mann, B. L. Bearden, and E. A. Mancini, 1991, Geologic framework of Norphlet and pre-Norphlet strata of the onshore and offshore eastern Gulf of Mexico area, Transactions Gulf Coast Association Geological Societies, vol. 41, p. 590-600.

Tolson, J., C. Copeland, and B. Bearden, 1983, Stratigraphic profiles of Jurassic strata in the western part of the Alabama coastal plain, Geological Survey of Alabama Bulletin, vol. 122, 425 p.

Tyrrell Jr, W. W., 1972, Denkman sandstone member-an important Jurassic reservoir in Mississippi, Alabama, And Florida, Gulf Coast Association of Geological Societies Transactions (abs.), vol. 22, p. 32.

Welch III, W. M., 2003, Clay identification and diagenesis in the updip section of the Norphlet Formation in Alabama, Mississippi State University, Starkville, Mississippi, 88 p.

Wilkerson, R. P., 1981, Environments of deposition of the Norphlet Formation (Jurassic) in South Alabama, Master's thesis, The University of Alabama, Tuscaloosa, Alabama, 141 p.

Wilson, K. L. 2011, The origin and development of the Tampa Embayment: implications for the tectonic evolution of the Eastern Gulf of Mexico, Master's thesis, The University of Alabama, Tuscaloosa, Alabama, 57 p.

APPENDICES

Appendix 1: Well Facies

Appendix 1A. Facies inferred from Wilkerson (1981)

Permit	Shale	Conglomerate	Wadi	Eolian	Permit	Shale	Conglomerate	Wadi	Eolian
836		x			1978				x
1264a				x	1986				x
1352		x			2042				x
1438				x	2082				x
1460	x			x	2085				x
1489	x		x		2094				x
1534	x		x		2207				x
1552				x	2208				x
1572			x	x	2218				x
1652				x	2250				x
1659				x	2258				x
1669			x		2280		x		
1742				x	2325				x
1766			x		2339				x
1902	x		x	x					

Appendix 1B. Facies from Welsh (2003)

Permit	Shale	Conglomerate	Wadi	Eolian
1352		x		
9923		x	x	
10488		x	x	x
7590		x	?	?
10928			x	
5101			x	x
6805				x

Appendix 1C. Facies from Ridgway (2010)

Permit	Eolian	Wadi	Shale	Conglomerate
13472				x
14708				x
15068b				x
15263b				x

Appendix 1D: Log facies interpretations in Alabama

Well	Shale	Conglomerate	Wadi	Eolian	Well	Shale	Conglomerate	Wadi	Eolian
836		X			3476	x			x
1429	x		x	X	3548				x
1460	x			X	3605				x
1469			x	X	3632				x
1469			x	X	3697				x
1486				X	3714				x
1489	x		x		3802				x
1493			?		3840				x
1508			x	X	3895			x	?
1512		X			3963			?	
1517	x			?	4060			x	
1523			x		4068				x
1530			?		4131				x
1542			?		4183			x	x
1548			?		4183			x	x
1561	x		x		4183				x
1601				?	4266				x
1617			?		4335	x		x	
1652			x	X	4347				x
1659				X	4395			x	x
1709			x	X	4436				x
1740	x		x	X	4477				x
1747		X			4543	x		x	
1766				X	4557			?	
1768			x		4557			x	x
1819		X			4647	x		x	x
1840				X	4693				x
1840				X	4705				x
1862				X	4723				x
1874				X	4894			x	?
1902	x		x	X	4895				x
1906				X	4975			x	
1910				X	5052				x
1949			x	X	5053			?	
1974			?		5210				x
1978				X	5315				x
1986				X	5474				x
2042				X	6109				x

Well	Shale	Conglomerate	Wadi	Eolian	Well	Shale	Conglomerate	Wadi	Eolian
2043				X	6846			x	?
2049				X	7080				x
2069					7697				x
2073				X	8889				x
2075				X	8943				x
2082				X	9477				x
2085				X	9540				x
2094				X	9597				x
2126				X	9597				x
2149			x	X	9863				x
2207				X	9934				x
2208				X	9962				x
2218				X	9985				x
2232			x	?	10121				x
2232			x	?	10211				x
2250				X	10361				x
2258				X	10444				?
2261				X	10444			x	x
2280		X			10599				x
2325				X	10626				x
2339				X	10669				x
2454			x	X	10702				x
2484				X	11007				x
2543				X	11009				x
2545				X	11062				x
2587				X	11118				x
2629				X	11180				x
2645				X	11290		x		x
2735				X	11409				x
2740				X	11434				x
2746				X	11825				x
2816			x		12005				x
2961				X	12155				x
2991	x		?		12309				x
3036				X	12393				x
3039				X	13589			x	x
3039				X	13589			x	x
3127				X	15069				x
3135				X	15847			x	?
3213				X	16003				x

Well	Shale	Conglomerate	Wadi	Eolian	Well	Shale	Conglomerate	Wadi	Eolian
3226		X			16014		x		x
3247				X	16116				x
3277				X	16152	x		x	x
3451				X					

Appendix 1E: Log facies interpretations in Mississippi

Name	Shale	Wadi	Eolian	Name	Shale	Wadi	Eolian
A. Foote Estate #1		x	?	MASONITE 15-15 2			x
Atchley 13-4 # 1			x	MASONITE 25-14 1			x
BAKER 8-5 1			x	Masonite Corp. 17-12 1			x
BARKSDALE 5-9 1			x	MASONITE ETAL UNIT 15-14			x
BARKSDALE 6-3 1			x	MASONITE UNIT 15-11 1		x	x
BISHOP-COOLEY ETAL 1			?	MASONITE-FLB 15-10 1			x
BOARD OF SUPERVISORS 1		x	x	McKAY ET AL UNIT 1ST		x	x
Brewer-Garner 11-13 1			x	PARAMOUNT-JOHNSTON 1		x	x
D R YANDELL 1			?	PEARL RIVER 13-7 1			x
Denkman 1		x	x	PEARL RIVER 1-4 1			x
HAROLD KARGES 18-3 1		x	x	PEARL RIVER 2-11 1			x
HAUBERG # 1			?	PEARL RIVER 2-4 1			x
HAUBERG ET AL UNIT 1	x		x	PEARL RIVER 2-5 1			x
HAUBERG ETAL UNIT 5			?	PEARL RIVER 3-2 1			x
Hunter-Mason 11-5 1		x	x	PEARL RIVER 34-16 1			x
IP 15-4 1		x	x	PEARL RIVER 35-14 1			x
J O COX ETAL 1			x	PEARL RIVER 3-8 1			x
Jessie Allen 17-14 1S			x	P.R.V.A. 13-10 1			x
Jessie Allen 20-3 1			x	P.R.V.A. 13-16 1			x
LUCAS ET AL SWDW # 1		x	x	RANKN CTY BD OF SUP 2			x
LUCAS R 1-R			x	SCARBOROUGH 13-3 SWDW		x	x
M. M. Hughes 2			x	YANDELL 35-8 2			x
M. M. HUGHES SWDW # 1			x				

Appendix 1F: Log facies interpretations in OCS wells

Well	API	Shale	Wadi	Eolian	Well	API	Shale	Wadi	Eolian
DD 111	608224003400		x	x	MO 867	608154001100		x	x
DD 160-1	608224001900	x		x	MO 868	608154002600			x
DD 160-2	608224002100	x	x	x	MO 869-1	608154005600			x
DD 162-3	608224001400		x	x	MO 869-2	608154008200			x
DD 166	608224000600				MO 872	608154005200			x
DD 167	608224003800		x		MO 904-1	608154004100			x
DD 31	608224001600	x	x	x	MO 904-2	608154009800			x
DD 422	608224002000		x	?	MO 906-2	608154007400			x
DD 56-1	608224003500			x	MO 908-3	608154008000			x
DD 56-2	608224003900			x	MO 909	608154000400	x		x
DD 563	608224001800			x	MO 913	608154001400			?
DD 57	608224004100		x	x	MO 916-A2	608154007100			x
MO 1006	608154001700			x	MO 916-B3	608154007900		x	x
MO 819	608154010100			x	MO 917-A2	608154007500			x
MO 820	608154008800			x	MO 950	608154007000			x
MO 821	608154002800			x	MO 958-2	608154009700			x
MO 822-1	608154001600			x	MO 961-2	608154008600			x
MO 822-2	608154003900			x	MO 991-2	608154003400		x	x
MO 823-A1	608154000700			x	MO 999	608154003700		?	?
MO 823-A2	608154005400			x	MO 1005	608154011600			x
MO 823-A3	608154006300		x	x	MO 918-1	608154010700		?	x
MO 823-A4	608154006600			x	PE 948-1	608214000100		x	x
MO 823-A5	608154010500			x	PE 948-2	608214000200			x
MO 826	608154000900			x	PE 973	608214000000		x	x
MO 827	608154003000			x	PE 996	608214000300	x	x	x
MO 861-1	608154001500			x	DC 353	608234001400	x	x	x
MO 861-8	608154007200			x	DC 269	608234000600			x
MO 862	608154002900		x	x	MC392	608174117200	?	?	x
MO 863-3	608154008100		x	x	LL399	608244000301			
MO 864-3	608154008300			x	VK 117	608164009300	?		
MO 864-4	608154010300			x					

Appendix 2: Dipmeter Resultants

Well	n (dipping surfaces)	Resultant Vector (˚)	Correlation Coefficient	Well	n (dipping surfaces)	Resultant Vector (˚)	Correlation Coefficient
AL-10669	139	166	0.41	AL-4647B	78	192	0.30
AL-11007	135	209	0.72	AL-4895	121	209	0.91
AL-11290	40	172	0.80	AL-4975	27	338	0.65
AL-1508	55	165	0.56	AL-7697	78	121	0.55
AL-1652	103	185	0.25	AL-8943	25	264	0.58
AL-1840	17	256	0.49	AL-9597	132	119	0.72
AL-1902	23	84	0.56	AL-9985	85	134	0.19
AL-1906	153	204	0.09	DD-160-1	432	333	0.77
AL-1910	145	201	0.52	DD-160-2	99	3	0.74
AL-1978	61	191	0.72	DD-31	307	350	0.74
AL-2049	22	182	0.62	DD-422	9	303	0.87
AL-2094	11	51	0.08	DD-563	73	265	0.52
AL-2454	41	129	0.27	MO-820	316	211	0.19
AL-2484	30	190	0.84	MO-823-A2	301	165	0.67
AL-3548	43	131	0.79	MO-867	120	158	0.62
AL-3632	169	159	0.51	MO-872	32	101	0.86
AL-3802	85	152	0.72	MO-827	36	115	0.48
AL-3895	16	26	0.95	MO-869-1	65	182	0.56
AL-4060	9	244	0.65	MS-A-Foote1	32	255	0.35
AL-4183	82	149	0.75	MS-Masonite-25-14	37	173	0.75
AL-4266	13	108	0.35	MS-Scarborough-13-3	58	245	0.52
AL-4347	23	9	0.61	PE-948-1	142	305	0.39
AL-4543	36	109	0.56	PE973	293	94	0.61

Appendix 3: Interpreted east-west line